SEASONAL DYNAMICS IN BETHIC METABOLISM IN A SUBARCTIC FJORD

Master Thesis by
Heidi L. Sørensen

Supervisors

Prof. Ronnie N. Glud

Prof. Bo Thamdrup

Prof. Søren Rysgaard

May 2012

University of Southern Denmark
Institute of Biology
Campusvej 55
5230 Odense M
Denmark

Greenland Climate Research Centre
Kivioq 2
Box 570
3900 Nuuk
Greenland

Acknowledgments

During the last year I have worked on my master project with Professors' Ronnie N. Glud and Bo Thamdrup at the Institute of Biology at the University of Southern Denmark (SDU) and Professor Søren Rysgaard at Greenland Climate Research Centre (GCRC). I would like express my gratitude for their help and support throughout my work. On this note, I would also like to thank Anni Glud for all her help and for always stepping up when help was needed!

During my master project I was so fortunate as to get the opportunity the work in collaboration with GCRC in Nuuk, Greenland. This was has been an amazing experience and everybody at GCRC are truly missed now that I am back in Denmark. I would like to thank Thomas Juul-Pedersen, Martin E. Blicher, Kristine Arendt, Dorte Haubjerg Søgaard, John Mortensen, Peter Schmidt Mikkelsen, Kunuk Lennert, Ivali Lennert, Louise Mølgaard, and Rebecca Scheuerlein for always helping and guiding me in my work at GCRC. Naturally I would also like to thank Thomas Krogh for allowing me to be an annoying student! A special thanks goes to Lorenz Meire and Karl Attard for being excellent work buddies as well as friends and in general for putting up with me. And of course impossible to forget - Maia for keeping up my spirit whenever it was needed!

At SDU I would very like to thank Heidi Grøn Jensen, Charlotte Wiking Antivaki, Zeinab Lulu El-Ahmad and Karen Elmquist for all their help with analyzing samples and in general helping when they could. A special thanks goes to my fellow student and especially Diego Giao Garcia for tweaking my thesis and Helene Schmidt and Signe Friis Nielsen for supporting, helping and supplying me with all you can eat candy, chocolate, cookies, chips during the last couples of days in my writing phase!

A thousand thank you's goes to my dear family for always supporting me (and putting up with me in general). Last but not least, thanks to my closest friends Maria Storm Mollerup, Pernille Sine Lassen and Sheila Lefoli Maibom-Thomsen for being my all time favourite dumplings.

Table of contents

1. Abstract

1.1 English Abstract

Sediments play a key role in the marine carbon cycle through carbon oxidation and retention of the organic material reaching the seabed. The benthic metabolism is mainly controlled by the amount and condition of the organic material transferred to the seabed (Westrich and Berner 1984). Consequently the strong seasonal pattern in organic material transfer influences the benthic dynamics (Therkildsen and Lomstein 1993). In the Higharctic regions, sea ice cover restricts the transfer of organic material to the seabed to a few months during the summer (Subba Rao and Platt 1984). In subarctic regions however, the transfer of organic material is less restricted. Thus, the benthic metabolisms patterns was expected to vary significantly at different longitudes.

This study aims to evaluate the seasonal dynamics in a benthic subarctic system and to study to what extent the variation in productivity and sedimentation is reflected in the degradation pathways and the overall degradation efficiency. Through this, one can be provided with an estimate of how conditions in the Higharctic may transform provided predicted climate changes for the region.

Results indicated a relative seasonal variation in benthic metabolism. A peak in pelagic primary production was observed in both May and August. Increased sedimentation rates followed increased primary production. A slight variation in the oxygen uptake was observed following the increased sedimentation of organic material (range of mean ± SD; 6.3 ± 0.9 - 11.9 ± 0.6 mmol m^{-2} d^{1-}). A delayed response to the increased sedimentation rates was furthermore observed in both the denitrification- (range of mean ± SD; 0.6 ± 0.001 - 1.34 ± 0.4 mmol m^{-2} d^{1-}) and the sulfate reduction rates (range of mean ± SD; 0.4 ± 0.2 - 2.4 ± 0.7 mmol m^{-2} d^{1-}). To recap, benthic mineralisation rates increased on two occasions following the increased primary production rates.

Considering the total carbon oxidation rates, Kobbefjord resembled an intermediate between temperate and the higharctic fjord systems. However, the relative importance of the different electron acceptors at Kobbefjord resembled those at Young Sound, despite the large difference in sedimentation material. Provided that benthic variation in Young Sound in time should resemble those in Kobbefjord, an increase in both carbon oxidation and retention rates would therefore be expected.

1.2 Danish Abstract

Havsedimenter spiller en central rolle for den marine karboncyklus gennem både oxidation og Tilbageholdelse af karbon i organisk materiale som ender på havbunden. Den bentiske metabolisme er hovedsageligt kontrolleret af mængden samt tilstandsformen af det organiske materiale, der når havbunden (Westrich and Berner 1984). Af denne årsag ses en tydelig ændring i den bentiske metabolisme ved skiftende årstider (Therkildsen and Lomstein 1993). I højarktiske områder begrænser havis mængden af organisk materiale som når bundet, til få måneder i sommerperioden. (Subba Rao and Platt 1984). I subarktiske områder vil mængden af tilgængeligt organisk materiale til gengæld være mindre begrænset. Af denne grund, er det forventet at den biogeokemiske metabolisme vil variere signifikant ved forskellige længdegrader.

Dette studie har til formål at belyse sæson variationen for et subarktisk bentisk system, samt undersøge til hvilken grad variation i produktivitet og sedimentering afspejles i nedbrydningsprocesserne og den overordnede nedbrydnings effektivitet. Herigennem ville det således kunne estimeres, hvorledes forholdene i højarktiske områder vil kunne ændre sig under forudsætning af at fremsatte prognoser for klimaændringer for området er gældende.

Resultaterne i dette studie indikerede en årstidsrelateret ændring i den bentiske metabolisme. I både maj og august måned blev øget pelagisk primærproduktion observeret. Øgede sedimentationsrater af organisk materiale fulgte den øgede primærproduktion, og ilt optaget steg i takt med dette (middelværdien ± SD variation; 6.3 ± 0.9 - 11.9 ± 0.6 mmol m^{-2} d^{1-}). En forsinket respons til denne øgede sedimentationsrate kunne dernæst observeres i både denitrifikation- (middelværdien ± SD variation; 0.6 ± 0.001 - 1.34 ± 0.4 mmol m^{-2} d^{1-}) og sulfat reduktionsrater/hastigheder (middelværdien ± SD variation; 0.4 ± 0.2 - 2.4 ± 0.7 mmol m^{-2} d^{1-}). Der blev således, på to tidspunkter i løbet af studiet, observeret en stigning i de bentiske mineraliseringsprocesser grundet den øgede primærproduktion.

Med hensyn til de totale karbonoxidations rater; kunne Kobbefjord tilnærmelsesvis anses som et intermediat mellem tempererede og højarktiske fjordsystemer. Den relative betydning af de forskellige elektronacceptorer i Kobbefjord mindede dog om hvorledes fordelingen var i Young Sound, på trods af store forskelle i sedimentationsrater. Givet at de bentiske forhold i Young Sound med tiden vil ligne Kobbefjords, må en stigning i både karbonoxidation og -retention være forventet.

2. Introduction

2.1 Climate Changes and the Arctic Marine Carbon Cycle

During the past decades the temperature has increased significantly in the Arctic. This has reduced the extent of the sea ice cover by approximately 29% since 1980 (Figure 1) (Semiletov et al 2004, Stein 2008; IPCC). In fact, in 2007 a record low minimum sea ice cover was measured, which accounts for a 40% decrease in sea ice extent since 1979 (Stein 2008). Loss of multiyear sea ice and decreased thickness in sea ice has likewise been observed (Stein 2008). As a consequence, the duration of open water has increased, thus leading to enhanced light availability in the surface waters. Increasing precipitation and enhanced run-off from glacier melt, has most likely increased stratification of the water column. Furthermore, as surface water is less saline it is easily warmed up, which may have intensified the stratification. Upwelling of bottom water can subsequently be stimulated through this stratification (Figure 2) (see section 2.2 for further details). These changes are believed to increase primary production in arctic waters (Rysgaard et al. 1999; Arrigo et al 2008). The fact that sea ice cover efficiently prevents wind-driven upwelling of deep waters, whereby nutrients normally are transferred to the photic zone furthermore supports that primary production is stimulated (Stein 2008). Hence, as the sea ice cover decreases, wind-driven upwelling may be enhanced (Carmack and McLaughlin 2011). Heterotrophic

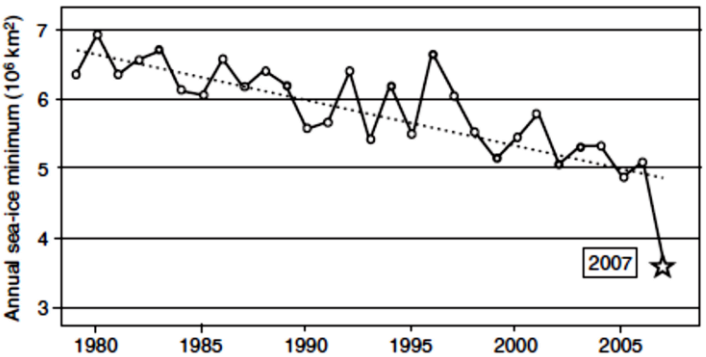

Figure 1. The minimum sea ice extent in the Arctic Ocean has decreased significantly during the last few decades. In 2007 (indicated by a star) a record low extent was observed. Figure from Stein 2008.

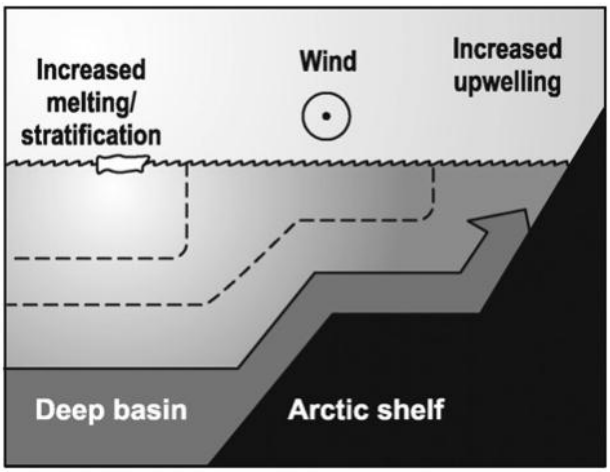

Figure 2. Enhanced fresh water runoff, increase stratification in the ocean, whereby upwelling from nutrient rich bottom water is stimulated. Figure from Carmack and McLaughlin 2011.

bacterial activity may therefore increase, stimulating re-cycling of nutrients (see section 2.2) (Nielsen et al. 2007).

In general it has been hypothesized that increased primary production will increase zooplankton growth and production. Enhanced grazing could lead to increased sedimentation through increased fecal pellet production (Rysgaard and Glud 2007). Hence, sedimentation may increase as well. Furthermore, changes in the zooplankton community can further be stimulated as grazing by larger copepods (the primary grazers at present) is limited to a certain period. As the primary production period is prolonged the importance of protozooplankton may increase (Figure 3). Sedimentation patterns may thus be altered as the grazing community changes. Degradation of the depositing material may change, resulting in altered material reaching the sediment surface. Through degradation of the organic material in the water column, re-cycling of nutrients may hereafter stimulate primary production again. Nevertheless, it is hypothesised that the overall organic material amount transfer to the benthic system will increase due to the climate changes (Rysgaard and Glud 2007).

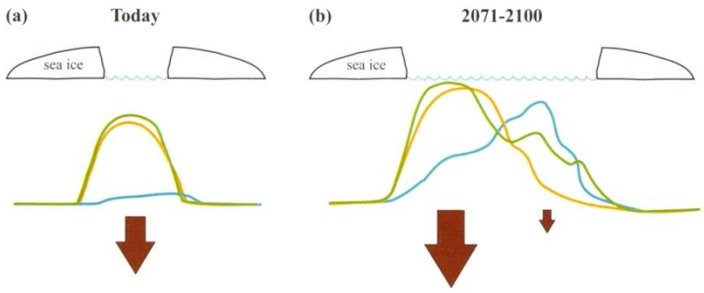

Figure 3. A. the present sea ice extent, primary production (green curve) and grazing by copepods (yellow curve) and protozooplankton (blur curve). B. Predictions on changes in primary production and grazing due to sea ice reduction. Figure from Rysgaard and Glud 2007).

As an increased amount of organic material is transferred to the sediment, degradation rates naturally increase as well. Oxygen is rapidly consumed to degrade the organic material and smaller components become available for anoxic processes (see section 2.3.1). The relative importance of oxic versus anoxic mineralization processes in the sediment may therefore change. Anoxic processes become more prominent in the total benthic mineralization with increasing input of organic material (Thamdrup and Canfield 1996) (see section 2.3.3). Consequently changes may likewise occur in the carbon retention rates, as part of the increased flux of organic material to the sediment is not degraded. Further details in section 2.3.1.

A temperature increase of approximately 3-4 degrees of the Arctic is predicted for the next 50 years (Stein 2008). Thus, the changes mentioned above may quickly be induced. Both the pelagic and benthic system are strongly co-dependent, thus changes in one of systems would surely affect the other (Glud et al 1998; Kostka et al 1999). It is therefore imperative to continue to investigate the Arctic Ocean to evaluate further climate changes.

2.2 Pelagic Systems

The pelagic system is a network of multiple processes occurring at the same time. In the system both primary and secondary production occur, ultimately affecting the carbon cycle (Figure 4). The degree of primary production depends on nutrient and light levels. Photosynthetic organisms (autotrophs) depend on the light intensities in order to stimulate primary production. Light only penetrates the water to a certain depth; this is referred to as the photic or euphotic zone. In shallow waters the photic zone may reach the sediment surface and thus stimulate primary production here. In the photic zone nutrients are rapidly consumed, whereas the nutrient level is high in the water below the photic zone. In the surface water nutrient levels are determined by discharges from rivers and fresh water run-off from land as well as decomposition of particulate and dissolved organic material (DOM, POM) within the water column (Konhauser 2007). Organic material is supplied from runoff from land and can stimulate primary production. At sallow water depths, organic material is not degraded to a large extend due to time limitation before the organic material reaches the seabed. Therefore more organic material reaches the seabed. Due to this primary production is stimulated more at shallow waters.

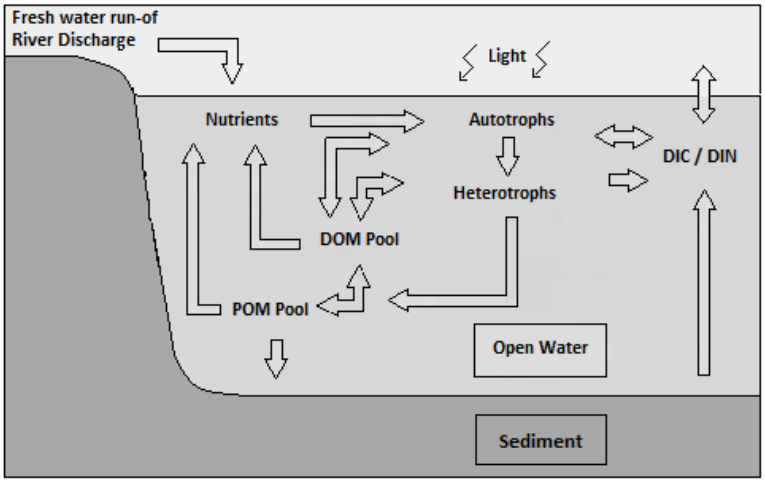

Figure 4. Organic matter cycle in the ocean. Nutrients enter the marine system through freshwater run-off/river discharge or are produced within either the pelagic or the benthic system. Photosynthetic organisms (autotrophs) use the nutrients and light to produce biomass. Autotrophs are consumed by herotrophs, entering the pelagic food chain. All organisms contribute to the POM pool through death and/or fecal contribution. Parts of the POM pool becomes part of the DOM pool, which is then decomposed into nutrients. The remaining part of the POM pool sediments. Nutrient produced in the sediment is released to the bottom water. Following upwelling, these nutrients may be transferred to the photic zone, where they are utilized by the autotrophs. Figure modified from Konhauser (2007).

Generally, primary production is divided into new and regenerated production depending on the nutrient source (Figure 5). Even though phosphorous and nitrogen can limit primary production simultaneously, nitrogen is believed to the be main limiting nutrient in the sea (Howarth 1988). Due to this nitrogen is the main focus when referring to new and regenerated production. New production is fueled by nutrients from sources outside the photic zone such as diffusion and upwelling of nutrient from deeper waters and/or

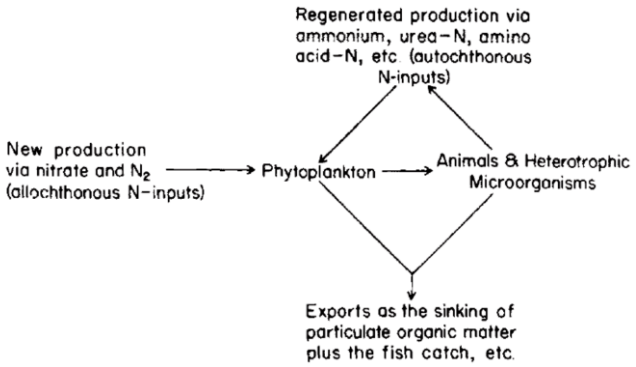

Figure 5. Primary Production is driven by nutrients (nitrogen source) from either within the photic zone or outside it. Whereas regenerated Primary Production is driven by nutrients recycled in the photic zone, new production is driven by nutrient supplied mainly from the nutrient rich bottom water. Figure from Eppley and Peterson 1979.

runoff from land. Furthermore, deposition from the atmosphere may also supply minimal fraction of organic material/nutrient. Regenerated production on the other hand, is fueled by nutrients regenerated by heterotrophic organisms within the photic zone (Eppley and Peterson 1979; Dugdale and Goering 1967; Bury et al 2012). The nitrogen source for new production is mainly NO_3^- and N_2, whereas NH_4^+ is the main nitrogen source in regenerated production (Dugdale and Goering 1967). However, high rates of nitrification may generate high concentrations of NO_3^- from the recycled NH_4^+ in the mixed layer of the water column (Domine et al. 2010). Naturally, the degree of new production is highly dependent on nutrient being transported into the photic zone – thus at coastal areas especially upwelling plays a major role (see later in this section) (Bury et al. 2012).

The fate of primary producers is to either undergo grazing or to contribute to sedimentation through dead matter. Within the photic zone, heterothrophs such as zooplankton efficiently consume primary producers, thereby keeping parts of the produced organic material in the zone. Below the photic zone, heterothrophs continue to consume the available organic material, thereby releasing nutrients. Grazing occurs on several trophic levels through the water column through the pelagic food chain (Canfield et al 2005). Heterotrophic decomposition results in the production of fecal pellets, which contribute significantly to the particulate matter sinking towards the seabed. Parts of the fecal pellets are decomposed by heterothrophs through the water column again. Furthermore, enzymes from microflora in the gut of heterothrophs may remain attached to the fecal pellets, thus degrading the particles outside the organism (Wakeham and Lee 1988).

All dead organisms and fecal pellets are a part of the particulate organic carbon (POC) pool. A part of this POC pool is converted into dissolved organic carbon (DOC) through hydrolysis/fermentation catalyzed mainly by heterotrophic bacteria (Canfield et al. 2005). In fact, in some regions nearly 100% of the POC pool within the pelagic system is converted by heterotrophic bacteria (Middelboe et al - in press). The higher the water column, the more of the POC is recycled in the pelagic system (Canfield et al 2005; Konhauser 2007). The remainder of the POC pool sediments to the seafloor (Konhauser 2007). Nevertheless, sedimentation may be increased by larger organisms, e.g., large copepods producing dense fecal pellets (Juul-Pedersen el at 2006). The sinking particles (~20- 200 µM) reaching the sediment surface, are often referred to as marine

snow (Konhauser 2007; Turner 2002). In general, the composition of the particles reaching the seabed is highly dependent on the organisms reworking the organic material in the water column (Wakeham and Lee 1988). The sedimentation rate can be measured as material trapped in sediment traps. Of the carbon reaching the seabed, part is mineralized and released to the water column (section 2.3), but the remaining carbon is buried. Not only is carbon buried, but nutrients are likewise preserved in the sediment (Canfield et al 2005). In coastal areas receiving increased amounts of organic material, sediment may in fact be considered as nitrogen and carbon sinks (Glud et al. 1998). Naturally, terrestrial run-off may supply additional organic material and in some areas this may account for all the organic matter transferred to the benthic system.

Estuaries are extremely dynamic systems. Freshwater is transferred to the estuary, where it stimulates stratification through salinity difference as saltwater is denser than freshwater. Furthermore, stratification of the water column can be stimulated by temperature differences between the surface layer and the bottom layer. The interface between the two layers with different density is normally referred to as a pycnocline (Wolanski 2007). Saline water is pressed towards the head of the estuary from beneath, while fresh water is pressed towards the mouth of the estuary. Thereby a seawater front is created at the bottom of the estuarine (Figure 6A). The saline and fresh water is mixed at the boundary layer, creating a circulation, whereby bottom water is transferred to the surface of the water column. This transfer of bottom water to the surface is referred to as estuarine upwelling (Sumich and Morrissey 2004). Naturally, tidal changes affect the stratification of the water column. The bigger tidal change the more the fresh – and salt water is mixed (Wolanski 2007). Fjord systems are normally limited by sills, creating a basin. As freshwater is transferred to the water column, it moves out of the fjord on top of the denser saltwater. By this circulations in the water saltwater is drawn into the fjord (Figure 6B). Surface water is strongly affected by wind that creates turbulence in the water column. The overall effect of this is stimulation of primary

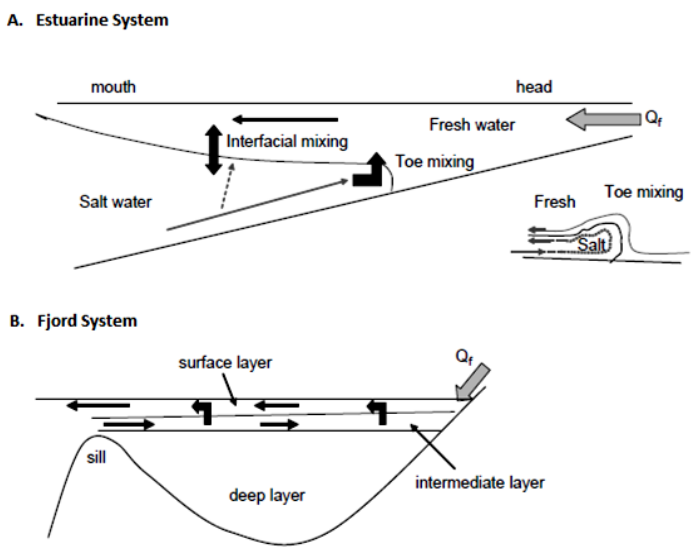

Figure 6. A. Transfer of freshwater to estuaries stimulates stratification of the water column. Two layers of different density are created. B. In a fjord system the transfer of fresh water stimulates a circulation of freshwater going out of the fjord and saltwater going in. Figure from Wolanski 2007.

production. Naturally, the degree of stratification varies according to climate, for instance stratification is more distinctive in tropical areas than polar areas (Sumich and Morrissey 2004).

2.3 Benthic Systems

In the sediment organic matter is degraded through aerobic and anaerobic microbial processes. In the following sections, the degradation through aerobic and anaerobic processes is described. In sediment located in the photic zone, primary production occurs at the sediment surface. In the following section, only sediment located below the photic zone is described.

2.3.1 Degradation of Organic Material (Carbon cycle)

Organic material is composed of carbohydrates, proteins, nucleic acids and lipids. Throughout the sediment the large structures (macromolecules) undergo depolymerisation by bacteria to be fractionated into smaller monomers (Figure 7) (Schulz and Zabel 2006). This depolymerisation by hydrolysis and the following fermentation are performed by fungi and prokaryotes (Canfield et al 2005). The depolymerisation aided by bacteria, is done by either excreting exoenzymes or by having exoenzymes associated with the membrane/cell wall. Water soluble macromolecules are depolymerised/hydrolyzed to monomers without difficulty, whereas molecules with low water solubility, such as lipids are preserved better (Schulz and Zabel 2006). The smaller components (monomers and oligomers) can then be transported across the cell membrane of heterotrophic bacteria, where they are further hydrolysed (Arnosti and Holmer 1999). The produced monomers are rapidly consumed whereas polymers and oligomers occasionally are released from the sediment as DOM. The monomeric compounds such as carbohydrates and amino acids are fermented to small fatty acids (e.g. formate, acetate, propionate and butyrate). Through second fermentation these products can then be converted into H_2 and CO_2 (Schultz and Zabel 2006). Following further degradation through respiration processes in the sediment (Section 2.3.2), nutrients such as NH_4^+, HPO_4^{2-} and CO_2 are released to the water (Schultz and Zabel 2006; Canfield et al 2005; Rysgaard et al. 1993). Some of the structurally complex and aromatic components in the organic material reaching the sediment, cannot be hydrolyzed anaerobic, wherefore aerobic decomposition

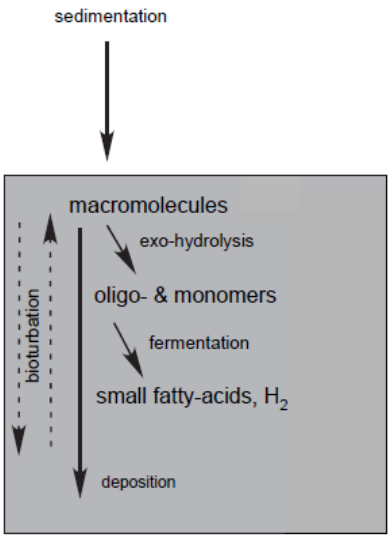

Figure 7. Organic material is degraded in the sediment through hydrolyses and fermentation. Through this substrates are available for bacteria to utilize them. The remainder the organic material is buried. Following respiration processes, nutrients are released to the water. Figure from Glud 2008.

is necessary (Kristensen et al. 1995). However, some of the components in the organic material such as insoluble non-hydrolysable highly aliphatic biopolymers are highly stable in the sediment. Hence, special decomposing methods are needed to degrade them. The result is that some of the organic material is buried (Schulz and Zabel 2006).

2.3.2 Nitrogen Cycle

Along with carbon, nitrogen is an important atom necessary in biomass production. In the ocean, nitrogen tends to be a limiting component in primary production and the cycling of this is therefore important. As mentioned, NH_4^+ is released from the decomposition of organic material. This happens through ammonification. The NH_4^+ can be incorporated in organisms forming organic bound nitrogen (NH_4^+ assimilation). In the presence of oxygen NH_4^+ can also be converted to NO_3^- through nitrification. The NO_3^- can hereafter be incorporated in biomass (organic-N) (NO_x assimilation). At anoxic conditions, NO_3^- can be turned into NH_4^+ through NO_3^- ammonification or converted to N_2 through denitrification (section 2.3.2). The intermediate product NO_2^- from denitrification and nitrification can along with NH_4^+ be converted into N_2 through anammox (Canfield et al 2005). Furthermore, Luther et al (1997) has suggested that production of N_2 may also happen through oxidation of NH_3 and organic-N by MnO_2 in the presence of O_2. The N_2 diffuses out of the ocean, but can be absorbed again trough N_2 fixation. Normally, nitrogen compounds are buried in the form of organic-N or NH_4^+.

2.3.3 Respiration Processes

The bacteria located within the sediment employing different processes to obtain energy. The yield of energy depends on the electron acceptor. This leads to a stratification of processes occurring within the sediment (Figure 8). As oxygen has the highest energy yield, it is rapidly consumed in the top of the sediment. During this aerobic respiration, oxygen is used as an electron acceptor and is reduced to H_2O, while organic carbon oxidized forming CO_2 (Konhauser 2007). However, oxygen is quickly depleted (within a few millimeters) and other less energy yielding processes are promoted (Konhauser 2007). Following oxygen respiration is denitrification. Denitrifiers use the NO_3^- in the sediment and form N_2, which then diffuse out of the sediment. As NO_3^- is depleted from the sediment oxidized manganese (Mn^{4+}) is reduced. However, the reduced manganese (Mn^{2+}) is easily re-oxidized by O_2 and NO_3^-. Following the manganese reduction zone, oxidized iron (Fe^{3+}) is reduced. As with reduced manganese, reduced iron (Fe^{2+}) is quickly re-oxidized by oxidized compounds (e.g. NO_3^-). Next in line of processes occurring in the sediment is sulfate reduction (SR). In coastal areas sulfate reduction has a more dominant role among the anoxic processes being accountable for most of CO_2 production (Canfield et al. 2005). Some of the sulfate reducers are also capable of reducing elemental sulfur, thiosulfate and sulfite (Canfield et al 2005). Through sulfate reduction

hydrogen sulfide (H_2S) is produced. The majority of the H_2S is re-oxidized but a part reacts with Fe^{2+} and form FeS, which eventually turn into pyrite (FeS_2). In areas receiving high amounts of organic material, sulfate reduction rates are increased and more pyrite is formed and buried (Konhauser 2007). In some cases, organic material contribution is so extensive, that H_2S production is elevated so much, that the H_2S reaches the sediment surface and creates an oxygen – sulfide interface near the sediment surface (Konhauser 2007).

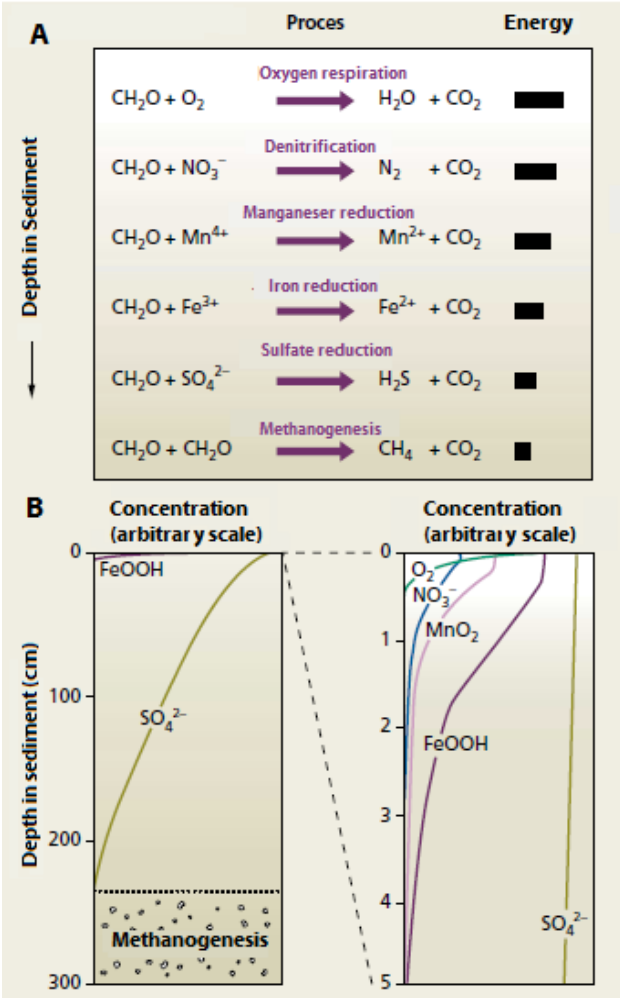

Figure 8. A: Aerobic and anaerobic processes in the sediment according to depth. Reactions and rough ratios of energy yield are shown for each process. B: Distribution of available electron acceptors throughout the sediment. Figure modified from Christensen et al. 2002.

Finally, methane (CH_4) is produced by methanogenesis as sulfate is depleted in the sediment. The CH_4 diffuses upwards and is re-oxidized through either methanotrophy (utilized by aerobic organisms) or possibly by Anaerobic Oxidation of Methane (AOM) (Canfield et al 2005). In AOM CH_4 reacts with SO_4^{2-} producing H_2S and CO_2. The indication of AOM occurring in the sediment was observed from the increased production of H_2S at the bottom of the SR zone. This process occurs between the sulfate reduction zone and the methanogenesis zone (Iversen and Jørgensen 1985). In general, methanogenesis does not account for a significant part of the CO_2 production as it is limited by organic matter. Most of the organic matter is used by sulfate reducers before it reaches the methanogenesis zone. As a result, methanogenesis is regulated by sulfate reduction. However, should the organic material input increase significantly methanogenesis may be induced (Canfield et al 2005). Generally there is a strong competition between sulfate reducers end methanogens fore the substrates/electron donors in marine sediment. In fact, methane production has been shown to be suppressed until sulfate concentrations become very low (< 1 mM) (Martens and Berner 1974).

2.3.4 Carbon Oxidation

The net result of the processes mentioned above contributes to the total carbon oxidation (CO_2 production). The CO_2 produced in the processes depends on the stoichiometry of the specific reaction

(Figure 9). For every respiration reaction, organic material (denoted CH_2O in Figure 9) is converted to CO_2 and H_2O. To do this, bacteria use electron acceptors (O_2, NO_3^-, Mn^{4+} Fe^{3+} and SO_4^{-2}). Nevertheless, several electron acceptors may be required in order to completely oxidize the organic material (CH_2O in this instance). For example, to oxidize CH_2O with Fe^{3+}, $4Fe^{3+}$ are needed. As indicated by arrows in (Figure 9) some of the reduced equivalents are not re-oxidized; Fe^{-2} and H_2S precipitates (eventually forming FeS_2) and CH_4 and N_2 diffuse towards the sediment surface.

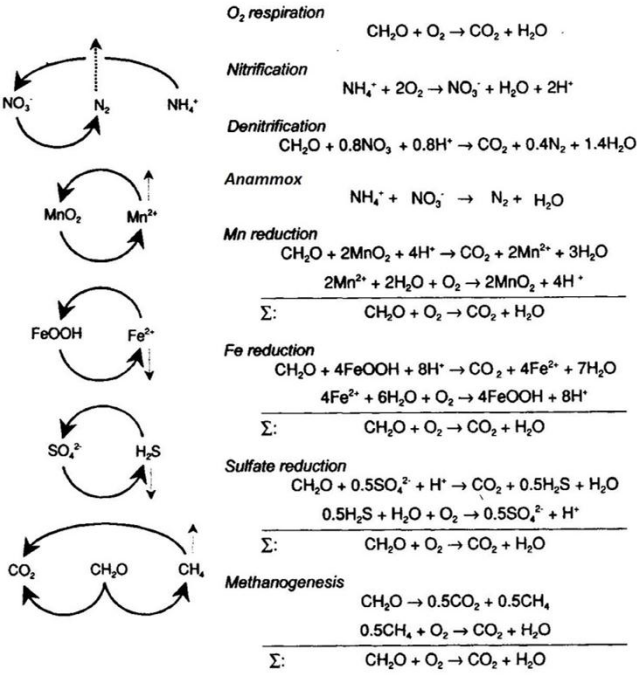

Figure 9. Benthic processes including net production of CO_2 and coupled re-oxidation. The stoichiometry is indicated by the number of electron acceptors used in the production of one CO_2. Figure modified from Canfield et al. 2005.

Oxygen is not only used in oxygen respiration, but also for re-oxidizing reduced equivalents from the anoxic processes. Even though oxygen may not be the actual oxidant deep in the sediment, the compounds that have been oxidized by oxygen are oxidants instead. Hence, oxygen is the terminal oxidant in the sediment. This re-oxidation throughout the sediment is called the redox-cascade (Figure 10). According to the stoichiometry CO_2 is equivalent to O_2, meaning that for every O_2 used, one CO_2 is produced. The total oxygen uptake (TOU) can therefore be used as a proxy for the total carbon oxidation in the sediment, integrating both the oxic and anoxic oxidation. In this assumption however, minor contribution from N_2 release and Fes/FeS_2 burial are not accounted for. The TOU can be measured as the consumption of oxygen over time. In sediments, oxygen uptake is normally limited by diffusion into the sediment. As a result of this, diffusive oxygen uptake (DOU) is a measurement of the oxygen consumption in the sediment,

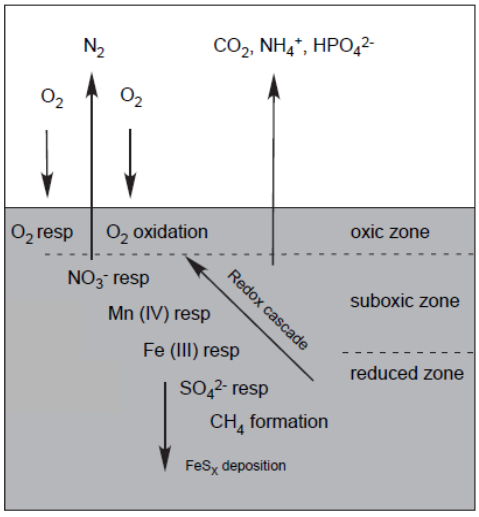

Figure 10. Reduced equivalents in the sediment are re-oxidized through the Redox cascade. Oxygen is consumed in the sediment for both oxygen respiration and re-oxidation and therefore serves as a proxy of the total carbon oxidation. CO_2, N_2, NH_4^+ and HPO_4^{2-} are released from the sediment following the degradation of organic material and respiration. Figure from Glud 2008.

without disturbance. The DOU is calculated from the concentration gradient within the diffusive boundary layer (DBL) or slightly below. As the TOU may exceed the DOU, the remainder of the oxygen uptake is believed to be mediated by benthic fauna (Benthos Mediated Uptake – BMU) (Glud 2008). The effect of bioturbation by benthic macro organisms is described below.

2.3.5 Variation in Benthic metabolism

Carbon oxidation rates and pathways vary according to location and the physical/biological parameters affecting this location. Carbon oxidation tends to be dominated by oxic respiration in the deep-sea. In shallow waters on the other hand, the anoxic carbon oxidation are often more important and may dominate the total carbon oxidation (Figure 12) Near-shore sediments can often be subjected to an increased amount of a certain electron acceptors through run-off from the shore. This type of electron acceptor may therefore dominate the carbon oxidation in that area (Figure 11).

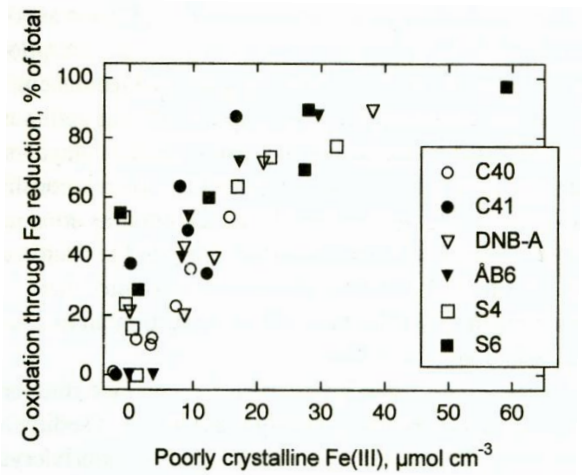

Figure 11. Contribution to total carbon oxidation with iron as electron acceptor according to iron (III) concentration in sediment. Location of stations used: Chile (C40 and C41), NE Greenland Fjord (DNB-A), Aarhus Bay (ÅB6) and Skagerrak (S4 and S6). Graph from Thamdrup 2000.

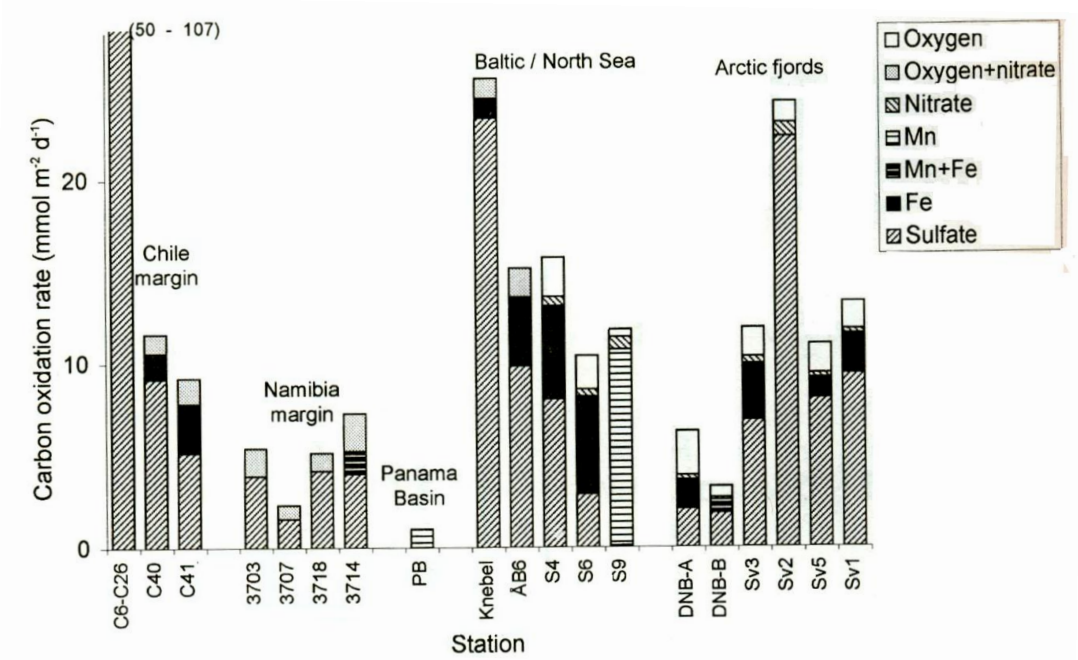

Figure 12. At different locations the relative importance of the different electron acceptors varies. Sulfate reduction seems to be the dominant respiration process, but at some places other electron acceptors dominate (e.g. S9 where carbon oxidation is dominated by manganese reduction). Going from left to right, the water depth increase in each of the groups from the different locations. Hence, the relative importance of other electron donors than SO_4^{2-} increases with increasing water depth. Figure from Thamdrup 2000.

In areas subjected to intensive loading of organic material sulfate reduction accounts for the majority of the total carbon oxidation (Figure 13) (Thamdrup and Canfield 1996), whereas oxygen has a more significant role in areas with less organic material contribution (Canfield et al. 1993). As a rule, if sedimentation increases the anoxic processes become more dominant due to rapid oxygen consumption. Overall, elevated sedimentation is expected to increase the benthic mineralization rate (Figure 13).

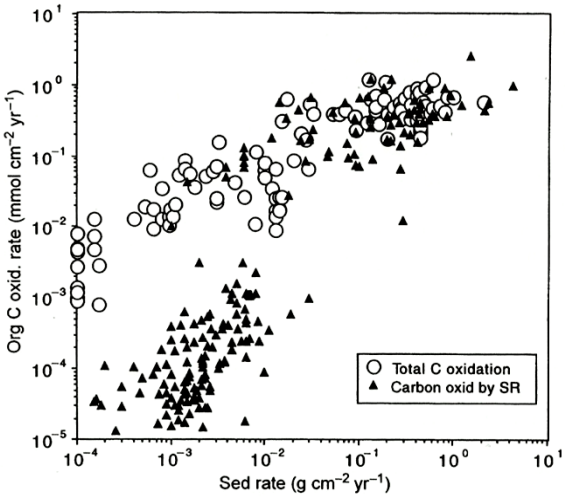

Figure 13. As the sedimentation rate increase, the rate of carbon oxidation increase as well. Moreover, carbon oxidation through sulfate reduction becomes more significant with increased organic matter loading. Graphs from Canfield 2005.

From the total carbon input to the benthic system, the majority is oxidized and released from the system, but a fraction is permanently buried (Glud et al. 1998). The released CO_2 and nutrients from the sediment hereafter stimulates primary production in the water column. Subsequently, nutrient release stimulates pelagic processes, which in return stimulates organic material transfer to the benthic system (Glud et al. 1998; Kostka et al, 1999; Rysgaard et al. 1998).

The degradation of the organic material is affected by several factors. These factors include; type of bottom, substrate availability (both electron acceptors and organic material) and bioturbation. The type of the seabed is important as to how organic material is degraded. The difference between sediment types is mainly the size of the grains, where sediment consisting of small grain size is characterized as muddy (grain diameter below 63 µm). This ultimately affects permeability of the sediment. As sediment is packed closer the permeability decreases. Sandy sediments and hard bottom seabeds are not subjected to large amounts of organic material (Baeyens et al 1991).

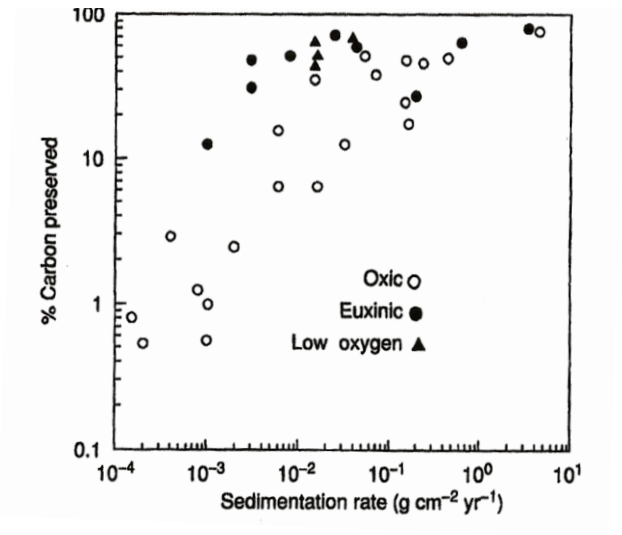

Figure 14. Carbon preservation depends on sedimentation rates, where increased sedimentation leads to increased preservation of carbon. However, the preservation moreover depends on oxygen availability and preservation is higher at oxygen depleted sites where sedimentation rates are low. Figure from Canfield et al 2005.

Sandy sediments are more oxidized, wherefore organic material is efficiently recycled through oxygen respiration (Glud et al 2010). In muddy sediments, however, more organic material is available and both oxic and anoxic processes are involved. As more organic material is transferred to the muddy sediment and it is packed closer together, the anoxic layer is more prominent. Due to this, the sediment becomes more reduced and e.g. metal-sulfide formation increase in sandy sediments (Baeyens et al 1991).

Bioturbation is a major parameter to be considered. Through bioturbation sediment is mixed additionally by organisms (Thamdrup et al. 2007). By this, oxygen penetrates deeper into the sediment through burrows. Through irrigation oxygen is available to degrade relatively refractory organic compounds buried in the sediment (Andersen and Kristensen 1992). More organic material is henceforth available for anaerobic mineralization. However, the main controlling factor on benthic metabolism is the amount and lability of the organic material. As more organic material is transferred to the sediment, carbon oxidation increases (Figure 13), but preservation of carbon increase as well (Figure 14). At places where sedimentation rates are low, preservation of carbon depends on oxygen availability and as sedimentation increase preservation increase as well. On the contrary, places subjected to high sedimentation rates (above 10^{-1} g m^{-2} y^{-1}) at least half of the carbon is preserved regardless of the oxygen availability (Canfield et al. 2005).

2.4 Seasonal Variation

Blooms of algae/photosynthetic organisms normally occur during the spring when light intensities increase and nutrients are abundant in the well mixed water column. As nutrients are depleted, the number of photosynthetic organisms decreases. The primary production pattern however is very different depending on the geographical location (Figure 15).

Primary production ultimately triggers an increase in particle flux downwards (Wakeham and Lee 1988). Thus, more organic material is transferred to the seabed following blooms of primary production. The transportation of this organic material to the seabed depends strongly on both vertical and lateral carbon transport, surface area with primary production and the sedimentation rate (Glud 2008). Following a spring bloom, oxygen consumption is more prominent in the top of the sediment as organic material is degraded. As a result the oxygen penetration depth decreases as oxygen is used rapidly in the sediment (Thamdrup et al. 2007). Not only is oxygen respiration affected, but organic material for the anoxic respiration processes is likewise enhanced. Siem-Jørgensen et al. (2008) showed that viral and bacterial activity clearly increased following a summer spring. Thus, benthic metabolism is highly dependent on seasonal variation.

As mentioned, oxygen is rapidly consumed following a spring bloom and reduced equivalents for anoxic processes may accumulate, creating an oxygen debt. Typically, an oxygen debt is created during the summer and then "repaid" during the winter by increased oxygen uptake. Due to this, oxygen consumption may appear relatively constant during the year. Though, by comparing oxygen uptake with CO_2 release, the potential debt can be assessed. The production of CO_2 is a measurement of the actual organic carbon oxidation, whereas the re-oxidation of reduced equivalent is included in the oxygen uptake, thus the difference must be attributed to the oxygen debt. Both CO_2 production and O_2 varies according to the supply of organic material, which is mainly controlled by seasonality changes (Figure 16A). The ratio between produced CO_2 and oxygen uptake is referred to as the respiration quotient (RQ) and is normally between 0.8 and 1.2 (Figure 16B) (Glud 2008). The RQ values change during the year. Following a spring bloom the RQ value increase as organic material is transferred to the sediment, where it is degraded releasing CO_2. If the value exceeds 1, re-oxidation of the reduced equivalent is incomplete. Thus the reduced electron acceptors may accumulate in the sediment. When the RQ value is lower than 1, oxygen is most likely being used to re-oxidize the reduced electron acceptors. This re-oxidation may be stimulated through bioturbation, where the reduced compounds are easily exposed to the oxygen (Therkildsen and Lomstein 1993). On an annual basis, the produced CO_2 should be equal to the O_2 uptake. However, if the annual value is lower it would correspond to extensive re-oxidation of reduced equivalents.

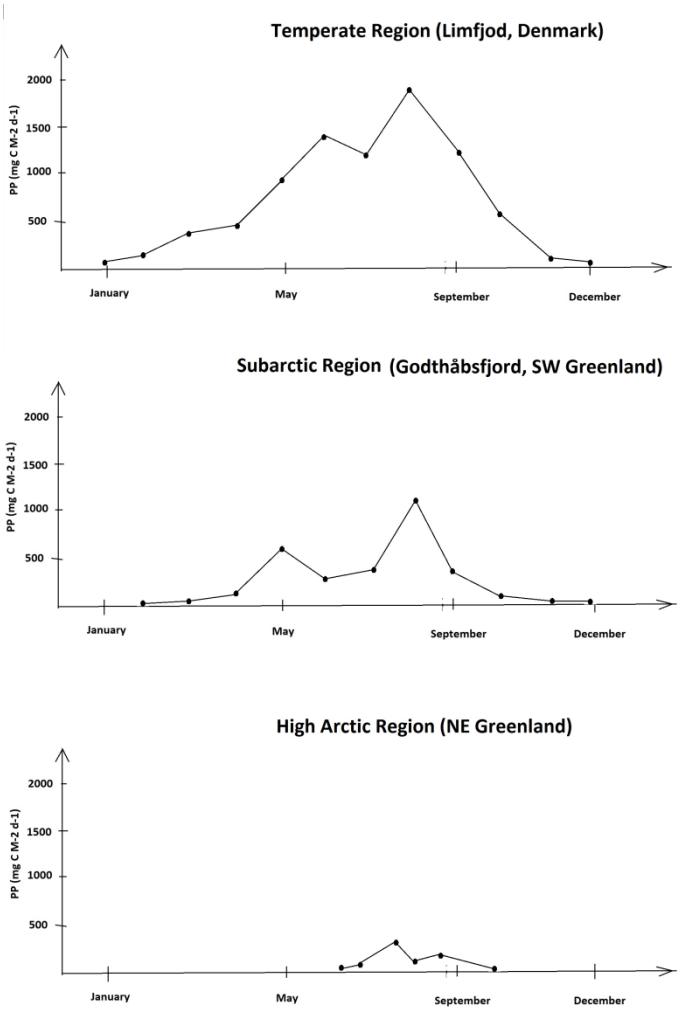

Figure 15. Comparison of Primary production at different geographis regions; Temperate, Subarctic and Higharctic. All values are in mg C m^{-2} d^{-1}. Graph from temperate region is redrawn from data of Limfjord between 1997 and 2007 (Krause-Jensen et al 2012). Graph from the subarctic region is redrawn the trend seen Godthåbsfjord in the NERO annual reports (2nd and 4th). The graph from the Higharctic region is redrawn from values recorded at Young Sound in Rysgaard et al. (1999).

It may even suggest that reduced equivalents have accumulated previous years. Furthermore, neither precipitation of CO_3^{2-} through $CaCO_3$ production (Therkildsen and Lomstein 1993) nor CO_2 release from shell dissolution (Doney et al 2009) is accounted for. Thus CO_2 production/release may in fact be relatively different from the measured values.

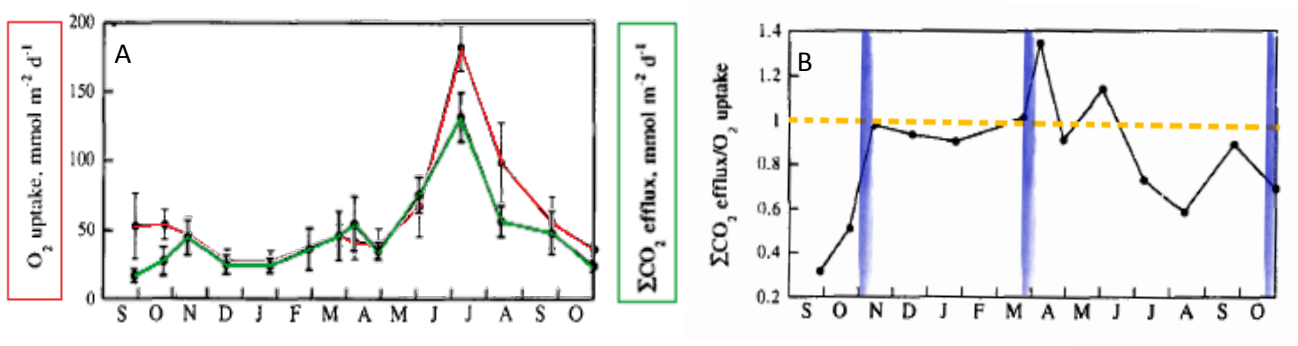

Figure 16. A. O_2 uptake (red line) and CO_2 production (green line) vary according to the season. CO_2production is a measurement of total carbon oxidation, whereas O_2 consumption intergrades both carbon oxidation and re-oxidation of reduced equivalents. B. The ratio CO_2 production/ O_2 consumption, also known as the respiration quotient (RQ), is an indicator of accumulation of reduced compounds in the sediment. If the RQ value is below 1 (RQ = 1 is indicated by a yellow line), additional O_2 is consumed to re-oxidize reduced equivalents. Blue lines indicate blooms of primary production. Graphs from Therkildsen and Lomstein (1993).

2.5 Arctic and Subarctic Systems

2.5.1 Arctic systems

The arctic waters experience strong seasonal variation such as sunlight variation, increased runoff during the spring/summer and ice formation (Stein 2008). As temperature and irradiance decrease, the sea ice cover expands and the arctic waters are covered by ice (Figure 17B). This sea ice cover is present in the entire polar region most of the year and the center is comprised of multiyear sea ice (Stein 2008). As the sea ice is formed, salt concentrations in the surrounding water increase. Expansion of the sea ice results

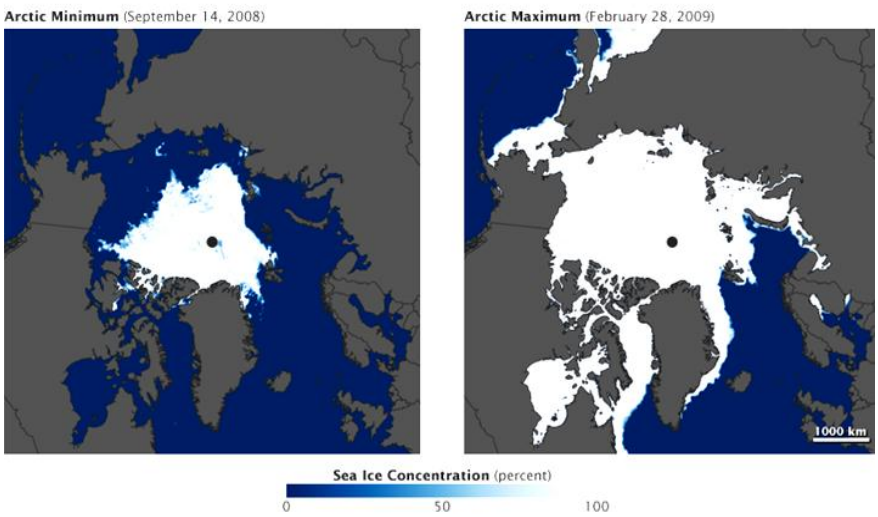

Figure 17. Sea ice extent changes during the season. A. Minimum sea ice extent measured in 2008. B. Maximum sea ice extent measured in 2009. Figure from http://earthobservatory.nasa.gov/Features/Sea ice/page3.php

in the formation of brine pockets and channels (NSIDC). The sea ice itself plays an important role as CO_2 sink through open brine channels (Semiletov et al. 2004). Nutrients and substrates are enclosed in the ice as well as salt and concentration levels may end up exceeding those of the underlying water column. Though light is limited, space reduced and salinity increased, autotrophic and heterotrophic microorganisms enclosed in the sea ice remain active (Søgaard et al 2010). The organisms are challenged by fluctuating nutrient supply and physical parameters (e.g. temperature, salinity and light). As light availability increases autotrophic growth is stimulated. Nevertheless, light penetration may be limited by snow and thereby limit autotrophic growth (Søgaard et al 2010). Nutrient supply becomes a limiting factor as primary production increases. Furthermore, growth efficiency is limited by temperature. In general, sea ice primary production only contributes a small fraction of the total primary production in areas with open water periods. However, in areas with multiyear sea ice, sea ice algae can contribute to more than half of the total primary production (Stein 2008). It is however important the keep in mind, that primary production is very low at these areas.

In Higharctic systems the sea ice normally covers the sea part of the year, being absent only a few months every year. As sea ice cover is intact, most of the light is reflected (Stein 2008). Thus the majority of primary production is limited to open water periods. The open water primary production growth season is approximately 120 days (Subba Rao and Platt 1984). During the summer, light duration lasts most of the day and temperatures increase. Due to this, sea ice melts (Figure 17A) and primary production is greatly stimulated. As ice covers the water, it efficiently isolates the water from wind-driven movement and mixing. In the absence of the ice cover, the hydrography is strongly affected by wind movement and consequently the extent of freshwater runoff.

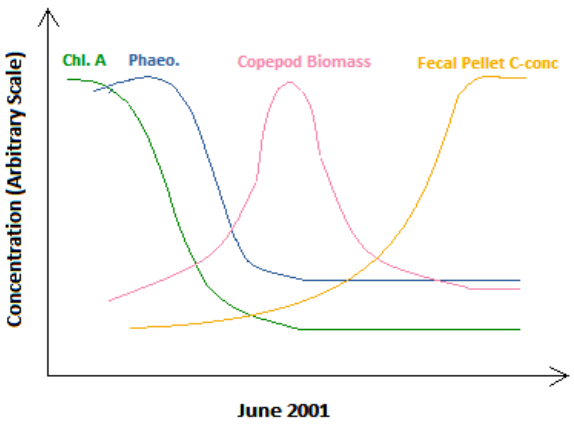

Figure 18. Pelagic coupling in Disco bay June 2001. Open water primary production is limited to short period. Primary production (indicated by Chl.A concentration increase) increase in the beginning of June. This is followed by an increase in Phaeopigment concentration (a degradation product of Chl. A.) as the primary producers are degraded. The copepod number increase (indicated by carbon biomass of *Calanus*) in the water column as primary production increase. Grazing of primary producer by copepods result in increased fecal pellets production. The fecal pellets hereafter sediments towards the seabed. Figure constructed from data from Juul-Petersen et al. 2006.

During the summer unicellular algae quickly increase in numbers (Figure 18 – Chl.A). Because Primary production is limited during the ice cover and nutrients are supplied from the bottom water, this is

new production. The secondary production is tightly coupled to the primary production (Juul-Petersen et al. 2006; Rysgaard et al. 1999). In several arctic areas (e.g. Disco Bay and Young Sound), copepods have been shown to be the dominant grazers of primary producers (Juul-Petersen et al. 2006; Rysgaard et al. 1999). The copepod population increases in the photic zone (Figure 18 – Copepod biomass) and as grazing commences the concentration of the degradation product phaeopigment increases (Figure 18 – Phaeo.). Naturally, as grazing on primary producers occurs, more fecal pellets are produced (Figure 18 – Fecal pellets). As described in section 2.2, fecal pellet undergo re-working in both the photic zone and beneath. Eventually, a part of this produced biomass sediments. Other than transport of organic material from rivers and runoff, this produced biomass (including the re-working of this material) is the main supply of organic material to the benthic system. Compared to this open water primary production sea ice algae rarely contribute significantly to the benthic system (Glud 2008).

In the benthic system organic material is degraded as described in section 2.3. However, rates are believed to be significant lower in arctic sediments. Previously, temperature was believed to be one of the controlling factors on benthic metabolism in the Arctic. However, lately it has been implied that the actual controlling factor is in fact the amount of organic material (Kostka et al. 1999; Sagemann et al. 1998; Thamdrup and Fleisher 1998). Sagemann et al. (1998) and Thamdrup and Fleischer (1998) used sediments from Svalbard (Arctic Ocean) to measure rates of sulfate reduction and oxygen respiration, nitrogen mineralization and nitrification, respectively, at different temperatures. Both investigations showed that low temperatures did not limit mineralization. The arctic mineralization pattern seems similar to those at lower latitudes (Kostka et al. 1999). Nevertheless, difference in the amount and composition of the organic material being transferred to the system vary, as the pelagic systems vary at different latitudes.

2.5.2. Case study: Young Sound

Extensive studies have been made at Young Sound, a Higharctic fjord in Northeast Greenland (e.g. Rysgaard et al 1999; Glud et al 2000; Rysgaard and Glud 2007 and references therein). The fjord has been monitored since 1994 to investigate long-term effects of climate changes. This fjord along with the Nuuk area is still a part of the ongoing monitoring program: Greenland Ecological Monitoring – GEM (http://www2.dmu.dk/gem/).

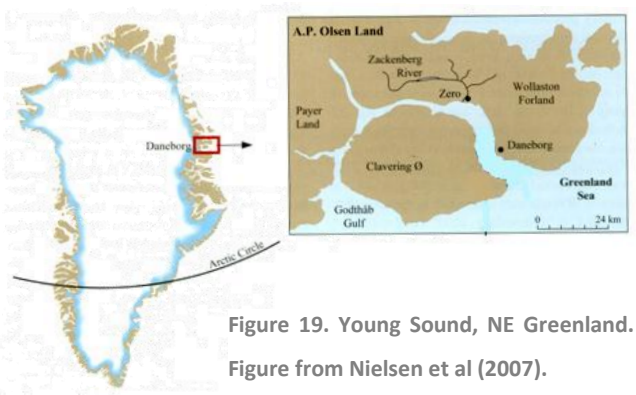

Figure 19. Young Sound, NE Greenland. Figure from Nielsen et al (2007).

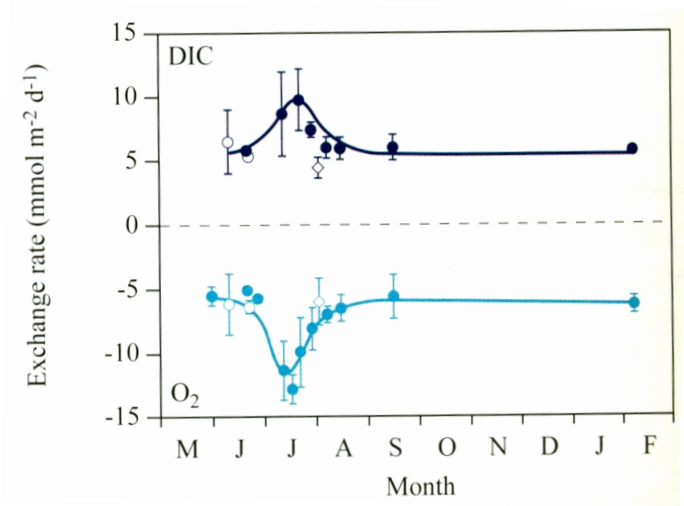

Figure 20. Following the summer bloom benthic exchange rates of $O_2$and CO_2 increase as organic material is transferred to the system. During the presence of sea ice, rates returns to background levels. Figure from Thamdrup et al. 2007).

Young Sound is a classical Higharctic system. The climate in Young Sound (Figure 19) is strongly affected by the cold *East Greenland Current*. Ice and water with low salinity are transferred from the Arctic Sea. Due to this, the area is coved by ice most of the year through a combination of landfast ice and the Pack-ice (Buch 2007). Due to the thick snow cover, sea ice primary production is often limited (Rysgaard and Sejr 2007). As the temperature increase, the sea ice melts and the water is transferred to the fjord. To begin with, runoff is mainly controlled by snow melt from nearby areas. This is later replaced by rainfall and melting of glaciers and snow from higher grounds. This runoff leads to suspension of sediment, but compared to other Arctic places, suspension of sediment at Young Sound is low (Mernild et al 2007). Furthermore, freshwater input to the fjord increases stratification and thereby stimulates estuarine circulation. Thus, nutrients are transferred to the photic zone. Mixing of the water is primarily caused by tidal changes and wind forcing (Bendtsen et al 2007). Open water primary production is stimulated and the organisms quickly increase in numbers (new production). Primary producers are efficiently grazed by copepods and vertically all primary producers are consumed (Nielsen et al 2007). High-density fecal pellets from the copepods descend from the surface and account for approximately 20% of the material reaching the sediment. 40% of the sedimenting material is of terrestrial origin, whereas the remaining 40% is poorly defined detritus (Glud and Rysgaard 2007).

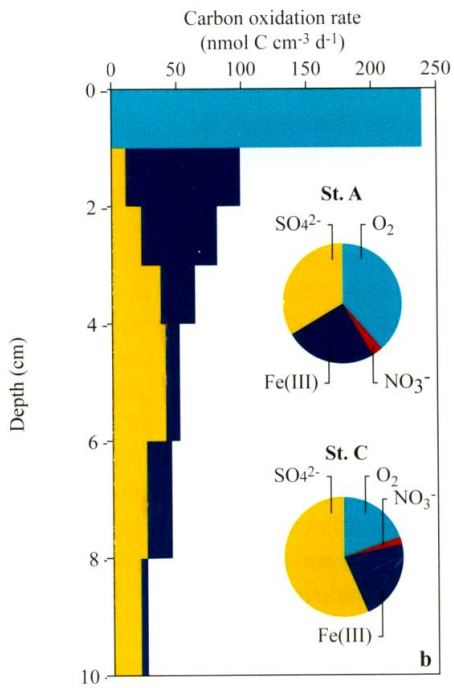

Figure 21. Carbon oxidation at Young Sound using different electron acceptors. The relative distribution of the electron acceptors according to sediment depth (cm) and the percentage distribution of the electron acceptors.

As organic material is transferred to the sediment through either terrestrial sources or by products of primary production, O_2 uptake and CO_2 production rapidly increase (Figure 20). However, within a few weeks the exchange rates decrease again and remain

more or less stable until the next summer bloom. The "baseline" in exchange rates of O_2 and CO_2 (~ 5 mmol m^{-2} d^{-1}) is fueled by accumulated organic material with low reactivity (Thamdrup et al 2007). Of the total carbon oxidation, O_2, Fe^{3+} and SO_4^{2-} are the most important electron acceptors. At stations closest to the shore oxygen respiration seems to be the most important process, whereas SR is more prominent further out, accounting for more than half of the oxidation. Denitrification however, did not contribute with more than 5% and contribution from manganese was undetectable. Iron, on the other hand, contributed to almost 25% of the oxidation (Figure 21). Approximately 70% of all the organic material transferred to the benthic system is mineralized, while 30% is buried (Thamdrup et al. 2007). Of the mineralized part, macrofauna is responsible for around 15 % (Glud and Rysgaard 2007). In general, variation in benthic metabolism at Young Sound is restricted to open water periods.

2.5.3 Comparison between Higharctic and Subarctic systems

Subarctic regions are often characterized by having long and cold winters and a mild summer. In general, the climate is milder than at Higharctic regions. A key factor is the sea ice extent. Compared to Higharctic systems, subarctic sea ice extent is less prominent. Thus, open water production is less constrained. Furthermore, recycling of nutrients in the photic zone is more pronounced thereby fuelling regenerated primary production. Compared to Higharctic areas, where primary production is mainly new production, subarctic primary production consists of both regenerated and new production. Due to a more prominent primary production, sedimentation could be expected to be higher in subarctic areas. However, the sedimentation is highly depended on the secondary producers within the water column. Whereas secondary producers in the Higharctic consist mainly of copepods, protozooplankton are the dominant secondary producers in the subarctic region (Nielsen et al 2007). Grazing by small zooplankton results in production of smaller fecal pellets that sink at a slower velocity compared to larger pellets. However, fecal pellets may be attached to marine snow, whereby size and density increase (Turner 2002). Naturally, bacterial respiration plays a significant role as the total bacterial carbon processing may actually exceed the autotrophic carbon fixation (Giorgio et al 1997). In general, the amount of sedimenting material depends on the amount of produced material in the water. Climate changes are expected to affect both the pelagic and the benthic systems in the Higharctic significantly and by using the natural climate gradient along the Greenlandic coastline, potential changes can be estimated.

In this master project Kobbefjord, SW Greenland was chosen to be the study site. Kobbefjord is a fjord located in a subarctic region. As it is located close to Nuuk (Greenland) and easy to reach, several investigations have been performed here (e.g. Glud et al 2010; Middelboe et al 2012). Furthermore, Kobbefjord is a part of the ongoing monitoring program: Greenland Ecological Monitoring – GEM

(http://www2.dmu.dk/gem/). This subarctic marine system is in general expected to represent an intermediate between temperate and Higharctic systems. The relative importance of all processes is therefore expected to differ according to the geographical location. Within the nitrogen cycle, one example is anammox. Rysgaard et al (2004) proposed that anammox contribution to total N_2 production depend upon water depth and NO_3^- concentrations, where deep waters and high NO_3^- concentration should favor anammox. Furthermore, through experiments the anammox optimum temperature was found to be lower that the optimum temperature for denitrification. Therefore anammox may contribute more to the N_2 production in Kobbefjord compared to e.g. Young Sound as bottom water temperatures may be slightly higher in Kobbefjord (Rysgaard et al. 2004). Ultimately the aim is to characterize the subarctic systems to better understand potential effects of climate changes as models predict that by the year 2070 conditions in Higharctic regions will resemble those of subarctic regions (Rysgaard and Glud 2007).

3. Materials and Methods

3.1 Study site

During this study samples were collected in Kobbefjord, Greenland (N 64°10.479 W 051°31.269). The sampling site is located in a fjord near Nuuk, Greenland (Figure 22). The maximum depth of the fjord varies along its axis between a few meters to 125 meters (NERO 3rd annual report; Mikkelsen et al. 2008). At the deepest parts of the fjord sediment accumulates, creating "sediment pockets". The study site was chosen to be at a depth of approximately 110 m (below the photic zone).

Due to its close location to Nuuk the sample site may be influenced by human activities in the surrounding areas. Freshwater is mainly supplied melt water in runoff from the head of the fjord.

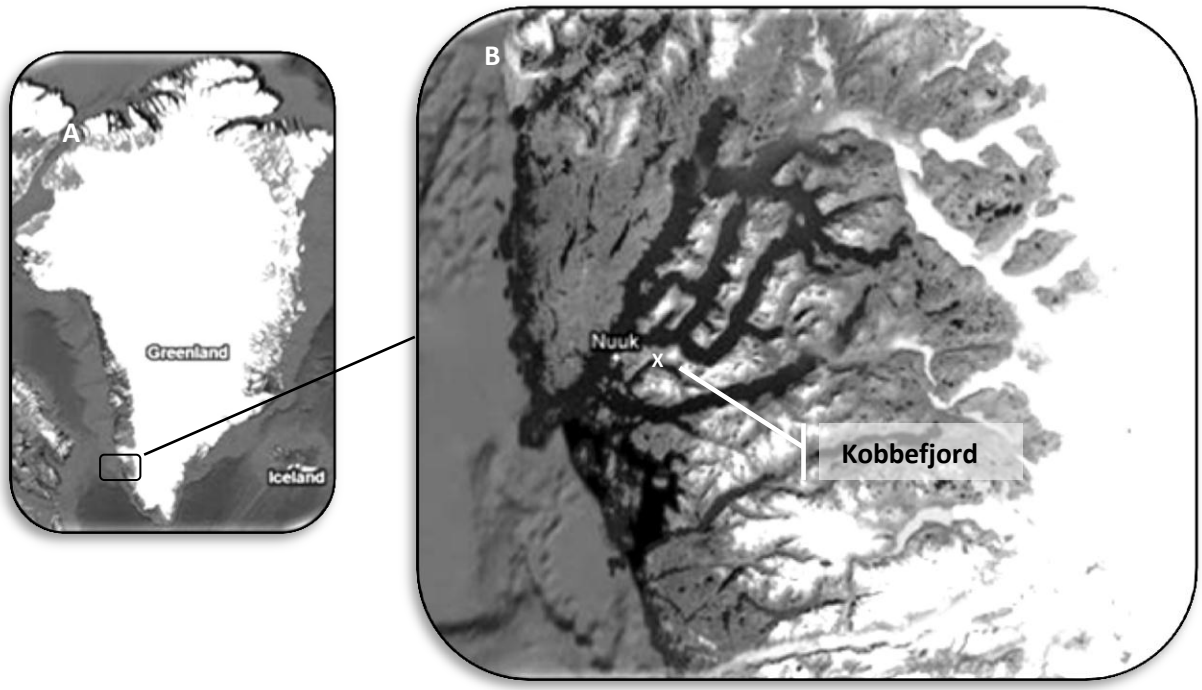

Figure 22: Location of the Study in Kobbefjord (B), Greenland (A). The sample site (N 64°10.479 W 051°31.269) was at the marked on the map with an X. Maps obtained from Google maps.

3.2 Sampling

Monthly sediment cores and bottom water were collected between May 2011 and January 2012. The sediment was retrieved in Plexiglas tubes with a diameter of 5.3 cm and heights between 50 and 30 cm

using a kajak sampler (KC Denmark research Equipment). The number of cores retrieved varied between months depending on which experiments that were preformed (the number of cores retrieved at each sampling session is listed in (Table 1). Water was retrieved using a Niskin bottle (KC Denmark research Equipment). Next to collecting sediment cores, measurements of primary production and sedimentation rates were made and a CTD profile (Seabird Electronics Inc, USA) was obtained.

Water samples from the depths; 5 m, 10 m, 20 m, 30 m and 40 m were retrieved and put into three 118 ml glass bottles with lids per depth (two transparent bottles and one bottle covered with dark tape). 200 µl of $NaH^{14}CO_3$ (20 µCi/ml) was added to each of the bottles and the bottles were sealed. The bottles were lowered into the water and left at the above-mentioned depths using a mooring system, for approximately two hours (time and position was noted). Primary production continues in the two clear bottles where the added C14 is converted to biomass, whereas the dark bottle serves as a background measurement due to repressed primary production. Sedimentation rates were measured by lowering four canisters (diameter: 7.2 cm, height: 50 cm) filled with filtered seawater and additional salt to a depth of 70 m. These were left for at least two hours. Only the top 5 cm of the water in the canisters are mixed with the surrounding water, hence sedimentating particles remain in the canisters. CTD measurements included depth (m), temperature (^{O}C), conductivity (s/m), fluorescence, Par/irradiance, oxygen concentration (µmol/kg), salinity (‰), Density (Kg/m^3), Sound velocity (m/s).

3.3 Experimental Program

On every occasion, exchange rates of oxygen, dissolved inorganic carbon (DIC), ammonia (NH_4^+), nitrate, (NO_3^-) nitrite (NO_2^-) and alkalinity were measured in six cores. The cores were subsequently used for oxygen and pH microprofiles (two cores), direct measurement of denitrification (three cores) and anammox (one core) and porewater profiles of pH, DIC, sulphate, sulphide, iron, nitrate, ammonia and alkalinity (two cores). Three additional cores were used for sulfate reduction rates (SRR) during each sampling campaign. On three occasions sediment characteristics such as water content, porosity and organic content (OC) were measured as well as rates of DIC, NH_4^+ , Iron (Fe^{2+} and Fe^{3+}), manganese (Mn^{2+}) and SRR measured through bag incubations. Once, a lead (^{210}Pb) profile was made and an experiment with organic material added to cores. The program of the sampling campaigns is shown in table 1. Detailed descriptions of the different analyses and experiments are described below.

Table 1. The sampling program of the complete study as well as the numbers of replicas of cores used for each analysis. The first sampling session was the 9th of May 2011 and the last session was the 3rd of January 2012. Some cores were used for several analysis e.g. the cores for exchange rates were later used for microprofiles, porewater profiles, denitrification and anammox. The number of extracted cores for each month is shown in the last row. Exchange rates, microprofiles, porewater profiles, denitrification anammox and sulfate reduction rates were measured each month. Sediment characteristics were measured in June, September and November. In December a lead profile was made. Bagincubations were made in July, October and December.

Sampling		May	June	July	August	September	October	November	December	January
Fluxes										
	Oxygen	6	6	6	6	6	6	6	6	6
	DIC	6	6	6	6	6	6	6	6	6
	NH4+	6	6	6	6	6	6	6	6	6
	Nox	6	6	6	6	6	6	6	6	6
	Alkalinity	6	6	6	6	6	6	6	6	6
Profiles										
	Oxygen	8	8	8	8	8	8	8	8	8
	pH		3	2	2	2	2	2	2	2
	Fe	2	2	2	2	2	2	2	2	2
	SO_4^{2-}	2	2	2	2	2	2	2	2	2
	NH_4	2	2	2	2	2	2	2	2	2
	NOx	2	2	2	2	2	2	2	2	2
	Density		2			2		2		
	Porosity		2			2		2		
	OM content		2			2		2		
	^{13}C		6			6			6	
	^{210}Pb								1	
Rates										
	SRR	3	3	3	3	3	3	3	3	3
	Denitrification	3	3	3	3	3	3	3	3	3
	Anammox	1	1	1	1	1	1	1	1	1
Bag Incubations										
	SRR			6			6		6	
	DIC			6			6		6	
	NH4+			6			6		6	
	Fe, Mn			6			6		6	
Number of cores		9	17	15	9	17	15	11	22	9

3.4 Primary production and Sediment traps

3.4.1 Primary Production

The content of the glass bottles used for primary production was filtered onto GF/C filters. The filters were placed in 20 ml scintillation vials and 100 µl of HCl (1 M) was added to each vial. The vials were then incubated in the fume hood for 24 hours, followed by the addition of 10 ml of scintillation liquid (Ultima Gold Tm, 2x5l, perkinElmer cat. no 6013329). The vials were then left for 24 hours, before counting them on the scintillation counter (Liquid Scintillation Analyzer, Tri-Carb 2800TR, PerkinElmer). Primary Production was calculated by using following formula:

[1] $$Production: \frac{DPM \cdot C_{DIC} \cdot 1.05 \cdot 1.06}{Act_{C14} \cdot T} \qquad (P1)$$

where DPM is the count from the scintillation counter, C_{DIC} is the concentration of DIC at the different depths in the water column, Act_{C14} is the activity of the added of $NaH^{14}CO_3$ in DPM/200µl and T is time in hours. The production was calculated for each of the depths. The production was subsequently corrected for the dark production:

[2] $$Production: \left(Mean\left([P1]_{light\,1} : [P1]_{Light\,2}\right) - [P1]_{Dark}\right) \cdot 12.01\ g/mol \cdot 24\,h/d \quad (P2)$$

where [P1] is the production calculation in formula 1 and Light 1 and 2 is the replicas of each depth. The unit was moreover converted from mmol c/m^3/h to mg C/m^3/d. The total production was calculated as:

[3] $$Depth\ integrated\ Production: [P2]_{5\,m} \cdot 5 + [P2]_{10\,m} \cdot 10 + [P2]_{20\,m} \cdot 10 + [P2]_{30\,m} \cdot 1 + [P2]_{40\,m} \cdot 10 \qquad (P3)$$

In this calculation the contributions of all depths are accounted for by multiplying the production at each depth ([P2]) with the depth difference. As light changes significantly during the year, the total production has to be corrected for the light. The ration between the total light (in Par) during the day and the light at the sampling time was used to correct the production. The data on light was obtained by ASIAQ (www.asiaq.gl). For each depth the light ratio was multiplied with the production and the total primary production was calculated as follows:

[4] $$Total\ Primary\ Production: Light\ Ratio \cdot [P2]_{5\,m} \cdot 5 + Light\ Ratio \cdot [P2]_{10\,m} \cdot 10 + Light\ Ratio \cdot [P2]_{20\,m} \cdot 10 + Light\ Ratio \cdot [P2]_{30\,m} \cdot 10 + Light\ Ratio \cdot [P2]_{40\,m} \cdot 10$$

The primary production was thus adjusted to annual variation in the light levels.

3.4.2 Sediment Traps

The contents of the sediment traps were filtered on pre-combusted filters (GF/C filters heated to 450°C) Particulate organic carbon (POC), Carbon content and C/N ratios were measured by weight and mass spectrometry (MS) (Mass Spectrometer: Isotope ratio Mass Spectrometer Hydra 20-20, SerCon; Autosampler: SerCon; Separation unit: Gas Solid Liquid Sample Prep Unit, ANCA GSL, SerCon). The total weight of the filtered material indicated the POC. The filters used for the carbon content and C/N ratio were packed into small tin capsules to be burned and analyzed using MS.

When MS is used to analyze the carbon and nitrogen content, the result are indicated as a peak on a mass-to-charge ratio scale as the ions are separated according to this. The peak area may be used as an indicator

of the amount of the specific ion; hence the relative content of a specific ion can be calculated from the peak area if the mass-to-charge of the specific ion is known. To calibrate the integrating peak area samples containing C and N (two different samples) were run through the MS and the specific ion was trapped in the detector to adjust the integrated peak area. By using a standard curve obtained from running specific masses of e.g. carbon the exact C-atom content could be calculated. The result from the MS analysis for both nitrogen and carbon is in percent of the element – in this case the sediment. From this the respective masses could be calculated by knowing the total mass of the analyzed sample:

[5] $$Mass_{N\ or\ C} = \frac{\%Element\ (N\ or\ C)\ \cdot Total\ Mass}{100}\ (mg)$$

When calculating the C/N ratio the molar mass is needed. The molar mass is calculated by multiplying the mass with the molecular mass (14.01 for N and 12.01 for C).

[6] $$n_{N\ or\ C} = m_{N\ or\ C}\ \cdot M_{N\ or\ C}$$

$$\Rightarrow C/N\ Ratio\ = \frac{n_C}{n_N}$$

The total sedimentation rate was calculated by using the total weight of the collected material in the traps (larger organisms were removed) (T. Juul-Pedersen et al 2006).

[7] $$Sedimentation\ rate = \frac{C_{Trap}\ \cdot\ V_{Trap}}{A_{Trap}\ \cdot T}\ (mg\ \ C\ m^{-2}d^{-1})$$

3.5 Exchange rates (O_2, DIC, NO_x and NH_4^+)

Sediment cores were placed in an incubation chamber containing bottom water collected at the sampling site and at in situ temperature. Magnets were used in the cores to ensure mixing of the overlying water column. A fiber optic oxygen transmitter unit (FIBOX) was used to measure oxygen saturation it the water. Patches of sensor coating formulation was attached on the inner side of the core lids. The sensor coating formula reacts to light at a certain wavelength and the formula is excited and becomes fluorescent. In the presence of oxygen, the energy is instead transferred to the oxygen and the fluorescent effect decreases. In this manner, the oxygen concentration can be calculated according to the fluorescence signal (Tengberg et al 2006). The FIBOX (Fibox 3, PreSens; program OxyView) was calibrated using the core lids. One lid was placed in the oxygen-saturated water (100% sat) and another lid was placed in a 100 percent dithionite solution (0% sat). In October and November a FireSting unit was used instead (FireSting O_2, Pyroscience, Germany).

Initial (start) samples were extracted using a glass syringe (50 ml) and transferred to exetainers and centrifuge tubes;

1. Dissolved inorganic carbon (DIC)	Exetainers containing a few drops of saturated $HgCl_2$ solution
2. Nitrate (NO_3^-) and Nitrite (NO_2^-)	Centrifuge tubes that were frozen at -18 degrees
3. Ammonium (NH_4^+)	Centrifuge tubes that were frozen at -18 degrees
4. Alkalinity	Exetainers containing a few drops of saturated $HgCl_2$ solution

The lids were attached to the cores and the oxygen concentration was measured using the optode. The Oxygen concentration was measured and logged once every hour until a drop of 20 percent in the oxygen satuation had occurred. Following the incubation, end samples for DIC, NO_3^-, NH_4^+ and alkalinity were taken. The exchange rates were calculated according to the following formula:

[8] $$Flux\ (J_x) = \frac{(C_E - C_S) \cdot h}{t}$$

where C_e and C_s are end and start concentration in µM (or µmol dm^{-3} = mmol m^{-3}), h is the height of the water column above the sediment in m (or cm/100) and t is the incubation time in days (or hours/24). For the oxygen calculation (TOU), the slope of the curve where concentration (mmol/m^3) was plotted against time (d), was used instead.

3.5.1 DIC

DIC was analyzed using a coulometer (CM 5012 CO_2 Coulometer, UIC $_{Inc}$ Coulometrics), an autosampler (Gilson sampling injector 232 XL) and a carbon extraction system (AKOTE carbon extraction system 2000W). The sample was injected into the carbon extraction system via the autosampler, where 0.3 ml of H_3PO_4 (8.5 %) was injected as well. CO_2 (gas) was hereby transferred to the cathode liquid in the coulometer cell, which contains proprietary solution with monoethanolamine and a pH-indicator. Acid was formed by the reaction of CO_2 and monoethanolamine. The color of the cathode liquid fades as acid was produced and a photodetector detected this color change. A current produced in the anode liquid counteracted the effect of the acid by an electrochemical production of OH^- in the cathode liquid, thus neutralizing the acid and stabilizing the color of the pH indicator. The current in this case acted as the titrant in the reaction and was

therefore used to calculate the CO_2 concentration in the sample (OPERATION MANUAL for the CM5012 CO_2 Coulometer; Betjeningsvejledning til CM5012 Coulometer).

The results from the coulometer was in counts and as 1 µg of carbon corresponds to 401.65 counts (OPERATION MANUAL for the CM5012 CO_2 Coulometer) and the concentration was calculated by the following formula:

$$[9] \qquad DIC\ Concentration\ (\mu M) = \frac{X\ Count}{401.65\ Counts/\mu g\ C \cdot 12.017\ g/mol\ \cdot V\ l}$$

Where x is the number of counts and v was the sample volume in l used in the analysis. To test the accuracy of the analysis, references from *Oceanic Carbon dioxide quality control* (Andrew G. Dickson, Scripps Institution of Oceanography), were used. The references were also used to calibrate data, as the concentration in the references is known (Batch No. 106 and 111 were used during the study - http://andrew.ucsd.edu/co2qc/batches.html#mostrecent).

3.5.2 NO_x (NO_3^- and NO_2^-)

Nitrate (NO_3^-) and Nitrite (NO_2^-) concentrations were measured according to the method described by Braman and Hendrix, 1989. This method does not differentiate between NO_3^- and NO_2^-, which is why the result is denoted as NO_x, however the contribution of NO_2^- to the total concentration was very small $^-$. Using an autosampler setup (Gilson sampling injector and syringe pump, Biolab, and a Gilson minpuls 3) the sample was pumped into a thermostat (KC Denmark) with a temperature of 90°C with a vanadium(III)chloride solution (100 percent saturation of vanadium(III)chloride in HCl 2M). When heated, the sample is reduced to NO by vanadium(III) and the NO gas is then passed through a trap with NaOH (2M) to cool down the sample and to neutralize it. The samples were then transferred to a detector (42C NO-NO_2-NO_x analyzer, Thermo Electron Corporation). As NO entered the detector it was exposed to O_3 and a flash occurs. The intensity of the flash was proportional to the concentration of NO. The flash intensity was recorded on a writer (Flatbed Recorder, Kipp & Zonen) and by using a standard curve the concentration of the samples was calculated. To check the standard curve, VKI standards with known concentrations were used.

3.5.3 NH_4^+

Ammonium (NH_4^+) was measured using the Bower and Holm-Hansen method (Bower and Holm-Hansen 1980). 2.5 ml of the sample/standards were transferred to tubes and 0.3 ml reagent I (110 g sodiumsalicylate, 0.07 g sodiumnitroprusside in 250 ml distilled water) was added followed by the addition of 0.5 ml of reagent II (1:9 solution of 1: 5% sodium hypochlorite and 2: 18.5 g sodium hydroxide, 100g

trisodiumcitrate in 1 l distilled water). Prior to the sample handling, a standard curve was made using a stock solution (0.6685 g ammonium chloride and a drop of chloroform in 500 ml distilled water) and artificial seawater (89.3 g sodium chloride, 28.6 g magnesium sulfate heptahydrate, 0.13 g sodiumhydrogencarbonate in 1 l distilled water) diluted to the same salinity as the samples. VKI standards were used to check the accuracy of the standard curve. Samples and standards were incubated in the dark for 2 hours and the measured spectrophotometric (UV mini 1240-UV-vis Spectrophotometer, SHIMADZU) at 640 nm. In the tubes ammonium reacted with salicylate and hypochlorite and when nitroprusside was present indophenols blue was formed. This change in color was proportional to the concentration of ammonium and the concentration of ammonium in the samples can thus be extrapolated from the standard curve (Bower and Holm-Hansen 1980).

3.5.4 Alkalinity

Alkalinity was measured using a Titrator (TIM840 Titration manager Titralab, Radiometer analytical) and the program titramaster to handle the results. The pH electrode was calibrated using pH buffer solutions (pH 4, 7 and 10) prior to every analysis. Sensitivity of the titrator and calibration of the results was done using references (Same references from *Oceanic Carbon dioxide quality control* as mentioned in section 3.5.1). The samples were weighed and placed on the titrator with a magnet stirring the sample while titrating with HCl (0.5M). Acid was added until pH 4.5 was reached and at this point electrical current (mV) was measured whenever a certain volume of HCl was added to the sample. The titration was continued until pH 3 was reached. Using the volume and the current the following is plotted in a graph:

$$[10] \qquad M_{HCl}\,(kg) = \frac{V_{HCl}\ \cdot 1.029}{1000}$$

$$[11] \qquad F1 = \left(m_{Sample}\,(kg) + \ [9]\right)e^{\left(\frac{Current\ mV}{1000\ \cdot (T \cdot R\ \cdot F)}\right)}$$

Where V_{HCl} is the volume of the added HCl (ml), 1.029 is the density of HCL (g/ml), m_{sample} is the weight of the sample (kg), the current is the current (mV) measured after the added acid, T is the temperature (kelvin), R is the gas constant and F is the Faraday constant. When plotting m_{HCl} on the X-axis and F1 on the Y-axis, the slope and interception from the linear regression can be used to calculate the alkalinity:

$$[12] \qquad TA = \frac{-1\ \cdot Intercept/Slope \cdot\ C_{HCl}}{m_{sample}} \cdot 10^6\ (\mu mol\ kg^{-1})$$

The total alkalinity calculated here indicated how much the sediment was able to buffer CO_2 in the water (Thomas et al 2009).

3.6 Oxygen and pH Profiles

Oxygen and pH profiles were measured using micro-electrodes (pH electrodes: prepared LIX electrodes or electrodes from UniSense, Oxygen electrodes: Prepared electrodes from SDU). The electrodes were attached to an automatic micromanipulator which was controlled using the program ProFix (Pyro Science). The electrodes were connected to an AD converter (ADC-216 USB) were the signal was transferred to the computer and logged in the ProFix program. For the pH profiles a voltmeter was used and a manual calibration was made prior to profiling. A picoamperemeter was used for the oxygen signal (Picoamperemeter PA2000, UniSense). Using the micromanipulator the electrodes were placed at the top of the sediment. The maximum and minimum depth, the interval depths and time intervals were set in the ProFix program (Max: -2000 µm, int. 100/50 µm, min. 8000 µm, time pr interval 4 sec for O_2 and Max: -2000 µm, int. 200 µm, min. 20000 µm, time pr interval 20 sec for pH). Three or four profiles were made in 2 to 3 different cores. In between the profiling the electrodes were moved slightly to avoid profiling in the same spot. Magnet stirring was continued while profiling and the lights were turned off. DOU values were calculated from the profiles according to formulas in Glud 2008 and oxygen consumption rates within the sediment was estimated using the program ***Profile,*** which is described in Berg et al 1998.

3.7 Denitrification

Denitrification was determined by $^{15}NO_3^-$ incubations in intact cores as described in Rysgaard et al. 2004. Three cores were used every month. Initial water samples were extracted to measure NO_3^- and background N_2. A volume of $^{15}NO_3^-$ was added to the cores to obtain a concentration of 50 µM and new water samples were extracted to measure the $^{14}N/^{15}N$ ratios. The cores were pre-incubated over night without lids, in the dark and with a magnet stirring the water. Water samples were then extracted to measure initial $^{15}NO_3^-$ and the cores were sealed off using lids. After two hours the first incubation (Core 1) was ended. A water sample was taken to measure $^{15}NO_3^-$ followed by mixing of the top 4 cm of the sediment with the water. Three exetainers were filled with the slurry. $ZnCl_2$ (100 µl) was added to two of the exetainers and formaldehyde (100 µl) to the last exetainer. The same procedure was applied to core 2 and 3 which were ended after 12 and 24 hours respectively.

All samples were measured using MS and the procedure is as explained in section 3.4.2 except that only the gas phase was measured in these samples. Approximately 5 ml of slurry in each exetainer was replaced by helium (He) and the exetainers were shaken to get the N_2 into the headspace above the slurry. At the same time exetainers with water were made to measure area/beam size according to the N_2 concentration. In the exetainers containing water, air was injected into the headspace in the volumes of; 0, 5, 10, 30 and 50 µl. From this the total concentration of N_2 in the injected air could be calculated as follows:

[13] $$n_{N_2} = \frac{V_{Air} \cdot 0.78 \cdot 1}{R \cdot T}$$

where n_{N2} is the total molar content in the exetainer, V_{Air} is the volume (µl) of the injected air in the exetainer, 0.78 is the ration of N_2 in the air, 1 is the atmospheric pressure, R is the gas constant and T is the temperature in Kelvin.

[14] $$C_{N_2} = \frac{n_{N_2}}{V_{Exetainer}}$$

The total concentration of N_2 in the exetainer was the molar amount divided by the volume of the water in the exetainer in litres. A part of the concentration was not factored in, wherefore the concentration was corrected according to the Bunsen factor, which factors in the contribution in the water phase:

[15] $$Total\ C_{N_2} = C_{N_2} + C_{N_2} \cdot 0.015633887 \cdot V_{water}$$

By plotting the concentration (x-axis) against the total beam area (y-axis) the linear correlation between the two could used to calculate the actual concentration of the different isotopes ($^{28}N_2$, $^{29}N_2$ and $^{30}N_2$) in each of the samples.

From the ratios $^{29}N_2$:$N_{2\ Total}$ and $^{30}N_2$:$N_{2\ Total}$, the excess production could be calculated by subtracting the background (from the references). The production of $^{29}N_2$ and $^{30}N_2$ could hereafter be calculated by following:

[16] $$Production = Excess\ Production \cdot Total\ N_2\ Concentration$$

The total N_2 concentration was calculated from the linear regression obtain through the standard curve mentioned above and the total beam/area of each sample. As the production was expressed in a concentration change, the height of the water and the sediment including the time was necessary to calculate the fluxes. The concentration difference was therefore multiplied by the height (m) and divided by the time (d) as in formula [7]. Throughout all the calculations the fluxes were found for both $^{29}N_2$ and $^{30}N_2$ and the contribution of both to denitrification were calculated as follows:

[17] $$D15 = {}^{29}N_2 + 2 \cdot {}^{30}N_2$$

[18] $$D14 = \frac{{}^{29}N_2}{2 \cdot {}^{30}N_2} \cdot D15$$

D_{total} indicated the total N_2 production within the sediment, but a part of the conversion of $^{29}N_2$ might have been caused by anammox. Calculations were based on personal comments from Søren Rysgaard at GCRC (2011).

3.8 Anammox

The N_2 Production by anammox was measured by the procedure described in Trimmer et al 2006. The top 4 cm in the cores were mixed and the slurry was transferred to exetainers (12.6 ml) in 4 time intervals. The cores were pre-incubated for approximately 24 hours, to ensure that available $^{14}NO_3^-$ and oxygen would be completely depleted from the slurry. Three different treatments were employed in the experiment; in the first series the concentration in the exetainers was adjusted to 50 µM of $^{15}NO_3^-$ (series A), in the second series the concentration was adjusted to 50 µM of $^{15}NH_4^+$ (series B) and in the last series the concentration was adjusted to 50 µM of $^{14}NO_3^-$ and $^{15}NH_4^+$ (series C). To stop the incubation 200 µl of $ZnCl_2$ was injected into the exetainer and the vial was vigorously shaken. The time series was: day 0, day 1, day 3 and day 7.

As with the denitrification samples, the volume equivalent to 5 ml was removed by the use of helium prior to MS analysis of the amounts of $^{28}N_2$ and $^{29}N_2$ (and $^{30}N_2$). To calculate the actual contribution to the N_2 production by anammox the percentage of the contribution was calculated by these experiments and then compared to the intact cores. In these experiments the processes were stimulated to a great extend by the mixing of the sediment and the rates were thus higher than the actual ones. Calculations of the contribution were made by following formula (Risgaard-Petersen et al. 2003):

Depending on the purity of the $^{15}NO_3$ used in the incubations, the amount of the available $^{14}NO_3^-$ was accounted for by assuming hardy-Weinberg equilibrium.

[19] $$Denitrification: \frac{P_{30}}{(0.99)^2}$$

[20] $$Anammox\ (\%) = \frac{P_{29} - Denitrification\ \cdot\ (2\ \cdot 0.01\ \cdot 0.99)}{0.99}\ (= ra)$$

The anammox contribution was calculated from series A, where $^{15}NO_3^-$ and $^{14}NH_4^+$ was available thus forming $^{29}N_2$. The excess production values were used in P_{30} and P_{29}. Series B acted as a control as only $^{15}NH_4^+$ was available as the $^{14}NO_3$ was presumed to be depleted. Series C contained both NO_3^- and NH_4^+ and $^{29}N_2$ should be produced and was therefore used as a control to confirm production of $29N_2$ by anammox. By using ra the theoretical ratio between $^{14}NO_3^-$ and $^{15}NO_3^-$ (r_{14}) could be calculated:

[21] $$r_{14} = \frac{(1 - ra) \cdot R^{29} - ra}{(2 - ra)}$$

Where, R^{29} is the ratio between $P^{29}N_2$ and $P^{30}N_2$. The r_{14} and ra value was thereafter used to calculate the N_2 production through anammox:

[22] $$A_{28} = \frac{P_{14} \cdot ra}{2}$$

Where, P_{14} is the actual N_2 production calculated in the intact cores incubation ($P_{14} = D_{14}$). The values of D_{14} and r_{14} could hereafter be used to calculate the NO_3^- contribution from the water column and nitrification to the denitrification, if the ratio between $^{14}NO_3^-$ and $^{15}NO_3^-$ in the water column was known. The ration between $^{14}NO_3^-$ and $^{15}NO_3^-$ was determined by the use of denitrifying bacteria (producing N_2 from the NO_3^-) prior to MS, to examine nitrification (Risgaard-Petersen et al 1993).

[23] $$P_{14}w = \frac{P_{14} \cdot r_{14}w}{r_{14}}$$

[24] $$P_{14}n = p_{14} - P_{14}\, w$$

The denitrification rates could thus be divided into denitrification supplied with NO_3^- from the water and denitrification supplied with NO_3^- from nitrification. Rates were calculated as in Risgaard-Petersen et al. 2003.

3.9 Porewater and solid phase profiles

3.9.1 Core sectioning and porewater extraction

The core was sliced under anoxic conditions using a glove bag filled with N_2. The sediment was sliced in the following depth intervals: 0-0.5, 0.5-1, 1-1.5, 1.5-2, 2-3, 3-4, 4-6, 6-8 cm. Directly after slicing the pH was measured after which the sediment slice was transferred to a centrifuge tube. Next the sliced sediment samples were centrifuged (C3i centrifugation centrifuge, Holm og Halby, Thermo Electron Corporation) at 3000 rpm for 5 min. The centrifuged samples were subsequently used for porewater extraction. The porewater samples were transferred to vials through disposable filters (Q-max CA-S syringe filters, Pore size 0.45 µm) in following volumes:

1. DIC 400 µl sample, 350 µl distilled water, 50 µl $HgCl_2$ and glass beads
2. Fe, Mn 800 µl sample and 10 µl HCl (6M)
3. NO_3^- 500 µl sample
4. NH_4^+ 200 µl sample and 3 ml distilled water
5. SO_4^- 400 µl sample
6. H_2S 400 µl sample and 10 µl Zink acetate (20%)
7. Alkalinity 500 µl sample and 50 µl $HgCl_2$

After the porewater extraction, approximately 200-300 mg of the centrifuged sediment was transferred to tubes containing 5 ml HCl (0.5 M). Samples for NO_x, NH_4^+, $SO_4^{2.}$ and H_2S analysis were frozen, while the remaining samples were kept cold until further analysis.

3.9.2 DIC

The small DIC samples were measured at SDU, Denmark. The procedure was as described in Hall and Aller 1992. Standards with the concentration of 1, 2, 3 and 5 mM were prepared (stock solution (100 mM): 2.1 g $NaHCO_3$ in 250 ml distilled water). A volume of approximately 150 µl of standards or samples was injected into the injection port (loop size 20 µl) where it was mixed with HCl (45 mM) and loaded onto the exchange cell. The total CO_2 (TCO2) in the standard or sample diffused across a Teflon membrane strip into the opposite stream of NaOH (10 mM). When the slightly acidic TCO_2 reacted with NaOH, a measurable drop in the conductivity was detected. The conductivity drop was proportional to the concentration of TCO_2 allowing quantification of the concentration in the samples by a standard curve.

3.9.3 Iron (Fe)

The particulate iron pools were determined by the Ferrozine method (Stookey 1970; Lovley and Phillips 1987) following extraction of the iron with HCl. The concentration was determined spectrophotometrically using mixtures of ferrozine (11.93 g Hepes and 0.2 g ferrozine in 1 l distilled water, pH adjusted to 7) and hydroxylamine (1 g per 100 ml ferrozine solution). Prior to sample handling a standard curve was made for a stock solution (stock solution made with $Fe(NH_4)_2(SO_4)_2$). For each sample two measurements were made; one with the ferrozine solution and the other with the hydroxylamine solution. 200 µl of the porewater samples was used whereas only 30 µl was used from the samples containing sediment. All cuvettes contained 2 ml of either the ferrozine solution or the ferrozine and hydroxylamine solution. Samples were subsequently measured at 562 nm. The ferrozine reacted with the reduced iron forming a complex with a magenta color (Stookey 1970). The concentration was proportional to the color change, thus the concentration could be calculated from the color change. Hydroxylamine acted as a reducing agent, which reduces the oxidized iron. Because of this, the oxidized iron could be calculated from the difference

between the reduced iron (the ferrozine solution) and the total iron (the hydroxylamine solution). For the porewater the linear regression of the standard curve was simply used to calculate the concentration, whereas the concentration in the sediment has to be corrected for the weight of the sediment, the density of the sediment:

$$[25] \qquad [Fe^{2+}] = \frac{\frac{(Abs_{562\,nm} - b)}{a} \cdot F \cdot (5 + m_{sed} \cdot \beta \cdot 10^{-2}) \cdot 10^{-3}}{m_{sed}} \qquad (Ferrozine)$$

$$[26] \qquad [Fe^{Total}] = \frac{\frac{(Abs_{562\,nm} - b)}{a} \cdot F \cdot (5 + m_{sed} \cdot \beta \cdot 10^{-2}) \cdot 10^{-3}}{m_{sed}} \qquad (Hydroxylamine)$$

Where Abs_{562} is the absorbance at 562 nm, a and b are the linear regression slope and interception values, F is the dilution factor of the measured volume, m_{sed} is the weight of the sediment and β is the water content of the centrifuged sediment.

3.9.4 Manganese (Mn)

The samples were diluted 10 times in nitric acid (HNO_3^- - 0.2%) and standards (0; 0.5; 1; 2; 4 mg/l) were prepared from a stock solution (1 g/l) and nitric acid. Both standards and samples were analyzed by standard atomic absorption (PerkinElmer A Analyst 100 – Atomic Absorption Spectrometer; FIAS 100 – PerkinElmer Flow injection system; PerkinElmer AS 90 plus – Autosampler) at 279.5 nm. As the samples or standard entered the standard atomic absorption analyzer, it was converted into a gas (burned). Light was absorbed by Mn to reach an excited state and the absorption of light could thus be measured. The absorption of light was proportional to the concentration of Mn (Atomic Absorption Spectroscopy – Analytical Method, PerkinElmer).

3.9.5 NO_3^- and NH_4^+ analysis

Procedure as explained in part 3.5.2 and 3.5.3.

3.9.6 SO_4^{2-} analysis

Samples were analyzed by the use of an Ion chromatography system (Dionex IC S-1500). In ion chromatography, ions were separated on a column according to charge and different ion were thus eluted (eluent: 4.5M Na_2CO_3 and 1.4 M $NaHCO_3$) at different time intervals. Sulfate was eluted from the column at a certain time and by using the integrated peak area in the spectrum the concentration was calculated. A standard curve was made prior to the sampling handling and in between the samples references were run to calibrate the data.

3.9.7 H_2S analysis

The sulfide (H_2S) samples were analyzed using the Cline method (Cline 1969). 125 µl of each sample was diluted once in 125 µl distilled water and 20 µl of cline reagent was added to each sample. The samples were closed, shaken and incubated for 20 min. The absorbance was hereafter measured at 650 nm and the concentration was calculated using a standard curve.

3.10 Sulfate reduction Rate (SRR)

Cores (2.6 cm in diameter and 20 cm in height) with silicon sealed injection ports were used for the incubations. The sediment from bigger cores was pushed to the top of the cores and overlaying water was removed. 5 µl of a $^{35}S\text{-}SO_4^{2-}$ solution was injected in every injection port down to 15 cm depth. The cores where then incubated for 6-8 hours in darkness at in situ temperature. During the incubation the labeled $^{35}S\text{-}SO_4^{2-}$ is reduced to $^{35}S\text{-}H_2S$ by sulfate reducing bacteria (Jørgensen 1978). At the end of the incubation the cores were sliced in the following depth interval: 0-1, 1-2, 2-4, 4-6, 6-8, 8-10 cm (from December the reduction rates were measured until 16 cm). The sediment was transferred to pre-labeled centrifuge tubes containing 5 ml zinc acetate (5%) per cm of sediment. The tubes were shaken and stored frozen until further processing.

The cold distillation method described by Kallmeyer et al (2004) was used. The samples were centrifuged at 3000 rpm for 10 min and 200 µl of the supernatant was transferred to scintillation vial containing 3 ml distilled water. These porewater samples were used for determination of $^{35}S\text{-}SO_4^{2-}$ activity. Approximately 2 to 3 g of sediment (m_{sub}) was transferred to the three necked distillation bottles. 20 ml dimethyl sulfoxide (DMSO) was added to the distillation bottled and the system was sealed off. N_2 was bobbled through the system for 15 min, whereafter 8 ml of HCl (6M) was added and 16 ml of reduced chromium solution (266 g $CrCl_3$ in 960 ml HCl 2M, reduced by 60 g Zink granulates and N_2 bobbling for 2 hours). Adding acid released the H_2S in solution. However to release the strongly bound sulfides in e.g. FeS and FeS_2, the addition of a stronger reducing agents such as the reduced chromium was essential. The H_2S was transferred to a citrate trap (19.3 g citric acid and 4 g NaOH in 1 l distilled water, pH adjusted to 4) and then to a Zink acetate (5%) trap. Distillation took 2 hours with N_2 flowing through. At the end of the destillation 5 ml of the zink acetate trap (containing the H_2S) was transferred to a 20-ml scintillation vial. The remaining trap material was transferred to 2 ml centrifuge tubes for later analysis of the total reduced inorganic sulfur (TRIS) content. The TRIS samples were analyzed according to section 3.9.7.

Scintillation liquid was added to each of the samples, both the porewater and the trap material (10 ml to the trap material and 6 ml to the porewater). The samples were then counted on the scintillation counter

(se specification for counter under section 3.4.1). In the presence of scintillation liquid, beta radiation was emitted from the reaction with the labeled ^{35}S. These beta waves in turn excite molecules that emitted light, which was then measured (Patterson and Green 1965).

[27] $$SRR = \frac{[SO_4^{2-}]_s \cdot a \cdot 24 \cdot 1.06}{(A + a) \cdot h}$$

[28] $$a = \frac{K \cdot (dpm_a \cdot dpm_b) \cdot m_{sed\ c} \cdot d}{m_{sub} \cdot m_{sed}}$$

[29] $$A = \frac{(V_{ZnAc} + m_{sed} \cdot \beta/100\ ) \cdot (dpm_a - dpm_b) \cdot d}{V_A \cdot m_{sed}}$$

Where $[SO_4^{2-}]_s$ is sulfate concentration in nmol cm^{-3} sediment = $[SO_4^{2-}]_s$ (mM) ⊕ ϕ ⊕ 1000; a is the total radioactivity in the traps; A is the total activity of $^{35}SO_4^{2-}$ (from the supernatant); h is incubation time in hours; 1.06 is a correction factor for bacterial isotopic fractionation; K is the correction factor to total trap volume; m_{sed} is the weight of sliced sediment prior to centrifugation (g); m_{sedc} is the weight of sediment after centrifugation and removal of ZnAc (g); m_{sub} is the weight of sediment subsample (g); dpm_a is the radioactivity of $H_2{}^{35}S$; dpm_b is the background radioactivity; d is the sediment density (g cm^{-3}); V_{ZnAc} is the volume of ZnAc (5.0 or 10.0 ml) and V_A is the volume of sampled supernatant (0.2 ml).

3.11 Sediment density, Porosity and Organic content

The sediment cores were sliced in chosen depth intervals; 0-1, 1-2, 2-3, 3-4, 4-5, 5-6, 6-8, 8-10 cm). The sediment slices were transferred to pre-weighed and -labeled aluminium trays. Part of the sediment was used to measure density by filling pre-weight centrifuge tubes. The remaining sediment was weight and heated to 105°C (Oven: Memmert model 600, D06062) for approximately 24 hours to estimate the water content.

Part of the dried sediment was grinded and used for estimation of the organic material content by burning the sediment in the Muffle Oven at 450°C (Muffeloven: Nabertherm (30-3000°C), Buch & Holm).

[30] $$Density\ (d) = \frac{m}{V}$$

[31] $$Water\ Content\ (\beta) = \frac{(ww - dw)}{ww} \cdot 100\ \%$$

[32] $$Porosity\ (\varphi) = \beta \cdot d\ 100^{-1}$$

[33] $$Organic\ Content\ (OC) = \frac{(dw - aw)}{dw} \cdot 100\ \%$$

Where m is the mass of the sediment, v is the volume of the sediment, ww is the weight of the wet sediment, dw is the weight of the dried sediment and aw is the weight of the burned sediment.

3.12 Bag incubation (DIC, NH_4^+, Fe^{2+}, Mn^{2+} and SRR)

In bagincubations sediment was placed in gas tight bag, so that both produced gases and nutrients were contained in the bags. By measuring concentrations of the gases and the nutrient, production/reduction rates were estimated. Furthermore, the contribution to the total carbon oxidation from the different processes was estimated. The method was modified from Hansen et al. 2000. 6 cores were used for these experiments. The cores were sliced in a glove bag to keep conditions anoxic. The bags were made from multilayered plastic film and welded into cone shaped bags. The sediment from the same depth of the 6 cores were mixed and the slurries were transferred to the bags following the removal of subsample to determine initial concentrations of DIC, NH_4^+, Fe, Mn, and SO_4^2. The bags were incubated and samples were taken at different time steps; 1: 0h, 2: 8h, 3: 20h, 4: 48h, 5: 80h. Each time centrifuge tubes were filled and centrifuged. Next the porewater was extracted in the glove box and used for analysis of DIC, NH_4^+, Fe, Mn, and SO_4^{2-} At the second sampling session 10 ml syringes were filled and used for SRR. $^{35}SO_4^{2-}$ was injected into the middle of the syringe and incubated. The analysis methods for DIC, NH_4^+, Fe and Mn are described in section 3.9.2; 3.5.3; 3.9.3; 3.9.5.

4. Results

Due to time constraints, this project only covers the pelagic and benthic variation from May 2011 to January 2012. The remaining measurements of the project are presently being carried out by Lorenz Meire (NIOO) and Thomas Juul-Pedersen (GCRC).

4.1 Seasonal variation in the pelagic system

4.1.2 Physical parameters and Oxygen

Prior to spring, the water column was well mixed. During spring temperature and light intensity increased. Temperature only varied slightly at the bottom of the water column, whereas the temperature variation in the upper layer of the water column was larger. The increase in temperature resulted in stratification of the water column during the spring and summer (Figure 23A). Between June and September, salinity was lower in the top of the water column further enhancing stratification. Salinity did not vary seasonally deeper in the water column, which is why the graph is not shown. The oxygen concentration in the water column varied slightly during the season. From June to November oxygen concentrations were elevated in approximately the upper 80 m, peaking in August (Figure 23B). Light intensities increased during the spring. The extinction coefficients decreased in June, whereafter in increase (Figure 24).

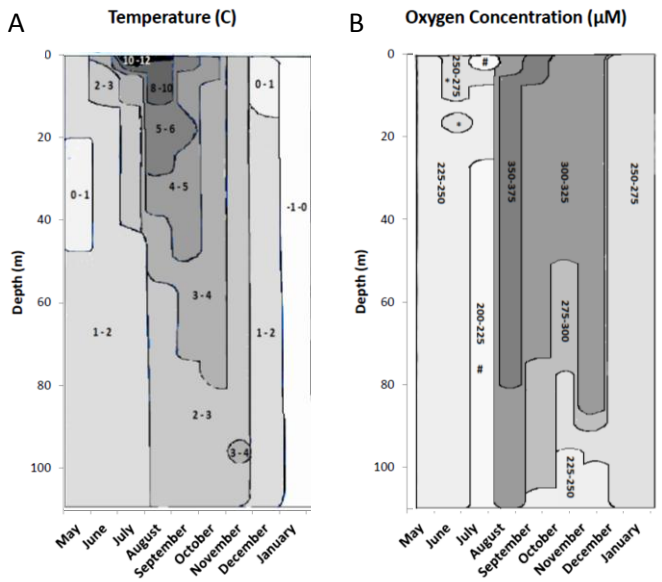

Figure 23. Seasonal changes in (A) temperature and (B) oxygen concentration according to water depth. Measurements were preformed from May 2011 to January 2012. During the spring/summer the water column was stratified due to the temperature (and salinity).

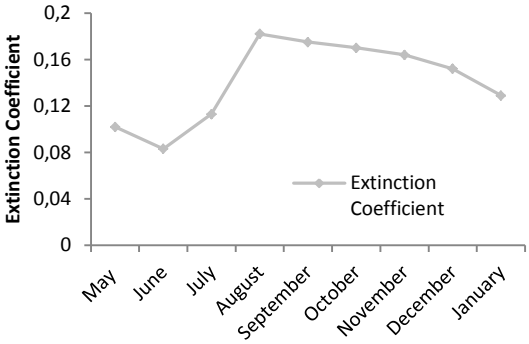

Figure 24. The seasonal variation in the light levels is indicated by the Extinction coefficient of the light penetration in the water column. Irradiance measurement where measured from May 2011 to January 2012)

4.1.2 Biological Parameters

The highest primary production rate of 72 mmol C m^{-2} d^{-1} was measured in May (Figure 24). Hereafter, primary production decreased with the exception of a small peak in August. Primary production values are corrected according to the daily light levels and not only the light at the sampling time. The daily light measurements are normally supplied by ASIAQ, but unfortunately, it was not possible to obtain light data from the year 2011. Data from year 2010 was used instead. However, levels do not vary significantly between previuous years and the calculated production rates were within limits of rates measured previously (NERO 1st, 2nd, 3rd and 4th annual report). Moreover, the primary production pattern resembles the patterns recorded in 2006 and 2009 (NERO 1st and 3rd annual report).

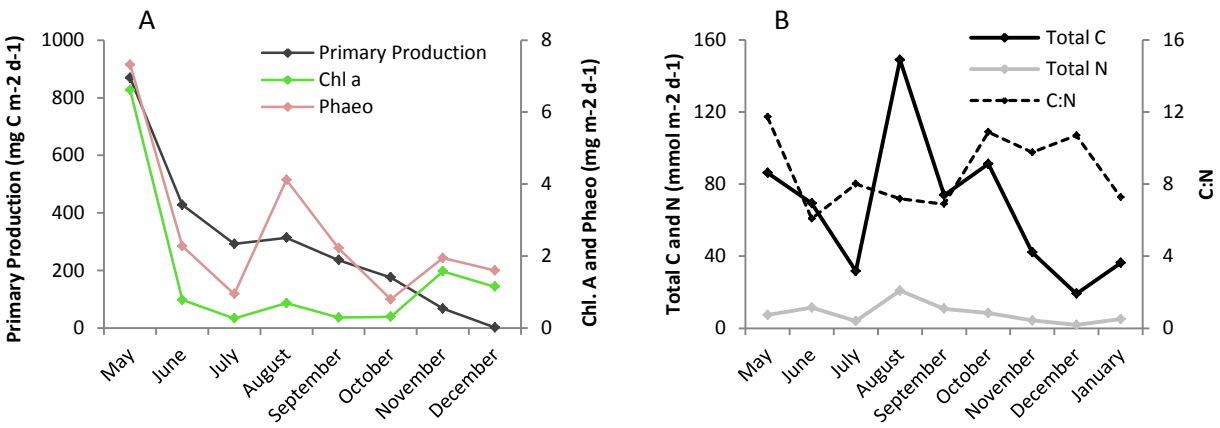

Figure 25. A. Concentrations of Chl. A and phaeopigments (Phaeo) were measured in sediment trap material. The concentrations were high during May and decreased hereafter. The concentration of the photosynthetic pigment (Chl. A) and it's degradation product (Phaeopigment) coincided with primary production. B. Sedimentating carbon and nitrogen content was measured in the sediment trap material. Carbon sedimentation ranged between 19 and 149 mmol m^{-2} d^{-1}, whereas nitrogen sedimentation ranged between 1.8 and 20.8 mmol m^{-2} d^{-1}. Peaks in sedimentating particles were observed in May, August and October. The C:N ratio in the sedimentation material was higher in May (~12), whereafter it decreased to approximately 8. Between October and December the ratio was around 11, followed by a decrease in January (~7).

The composition of sedimenting material was measured each month and converted to flux. The Chlorophyll *a* (chl. a) flux peaked as primary production peaked (Figure 25A). The degradation product of chl. a phaeopigment (pheao) likewise increased in May, but another peak in the flux was observed in August (Figure 25B). The carbon flux ranged between 19 and 149 mmol m^{-2} d^{-1}, whereas nitrogen content ranged between 1.8 and 20.8 mmol m^{-2} d^{-1}. Sedimentation of carbon peaked in May, August and October, as sedimentation increased. Towards the end of the year, content of Chl. a, phaeopigments, total C, and total N decreased in the sedimentating material, hence less organic material was transferred to the sediment. The C:N ratio was around 12 in May, October, November, and December, but was only around 8 between June and September. The average C/N value of the nine months was 8.22. Nevertheless, it is important to keep in mind that the sinking material was collected from a depth of 65 m (at the edge of the photic zone). The composition and amount of the organic material reaching the sediment may therefore have changes through the water column.

4.2 Seasonal Variation in the benthic system

4.2.1 Sediment Characteristics

The sediment was muddy and macro organisms were found by sieving the sediment. Sediment characteristics did not vary much during the season and averages were used further on (Figure 26). Porosity decreased from 0.86 to 0.70 with depth in the sediment, while density increased from 1.28 to 1.55. Organic content in the sediment was 5.87% at the top and decreased to 4.11% at 9 cm. The C/N ratio of the sediment was between 7.91 and 8.27 throughout the sediment. The average C/N ratio of the sedimentation material was 8.22, hence the C/N ratio in the sediment was lower.

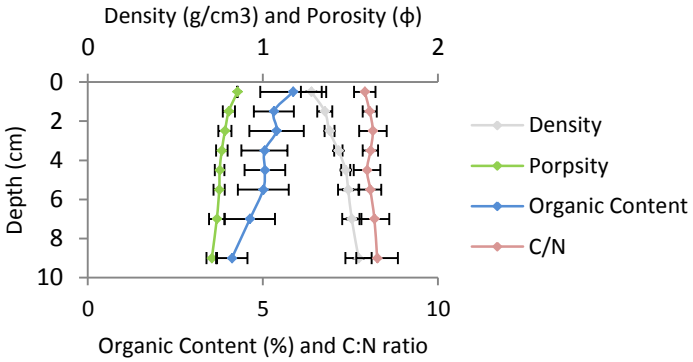

Figure 26. Depth distribution of averages of density, porosity, organic content in sediment and C/N ratio performed in June, September and November.

4.2.2 Porewater and solid phase profiles

Porewater nutrients were measured to a depth of 8 cm. Samples for each measurement were taken at every sampling session. Due to time limitation only some of the porewater profiles where analyzed, while the following await further processing: DIC (September 2011 – January 2012), SO_4^{2-} (November 2011 – January 2012), NO_x (July 2011 – January 2012), H_2S (October 2011 – January 2012), NH_4^+ (May 2011 – January 2012), Fe^{2-} (January 2012). Concentrations of DIC (n=4) and SO_4^{2-} (n=6) showed neither a distinctive variation throughout the sediment nor a seasonal variation. (Figure 27). NO_x is the combination of NO_3^- and NO_2^-, but NO_2^- concentrations tends to be low and most of the NO_x was attributed to NO_3^-. Only two profile of NO_x were measured, but both showed the same tendency with decreasing concentrations to a depth of 1.5 cm, whereafter concentrations remained constant at around 1 µM. I attribute this background level to an analytical artefact (Figure 27 - NO_x). Additional porewater profiles of iron, pH and alkalinity can be found in the appendix (section 8.1).

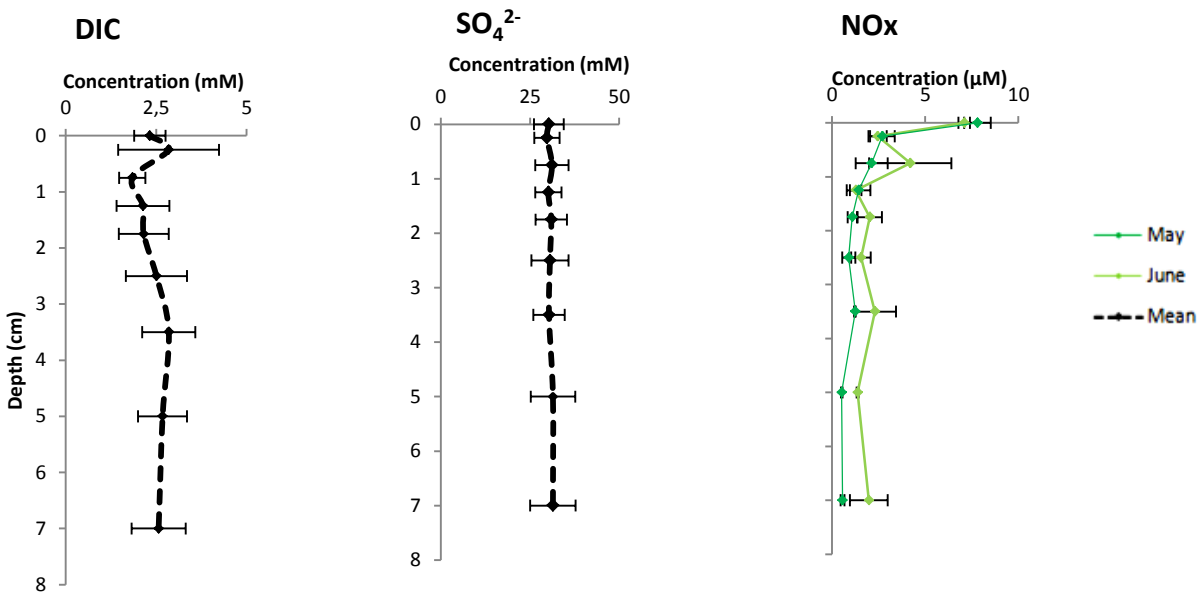

Figure 27. Porewater profiles of DIC, NO_x and SO_4^{2-}. Mean values are marked with a dotted line. Distribution of DIC (n=4) only varied slightly. SO_4^{2-} (n=6) concentrations did not vary according to depth and the concentration remained around 30 mM NO_x (n=2) decreased until approximately 1.5 cm, whereafter the concentration remained low.

With the exception of measurements from July all solid phase profiles of HCl-extractable iron resembled each other. Concentrations were around 25 µmol cm^{-3} and remained the same throughout the sediment. The majority of the iron was reduced (Fe(II); Figure 28). In the top of the sediment part of the iron was oxidized (Fe(III); from 0 to 1 cm). Below a depth of 2 cm ratios between total and reduced iron indicated that the majority of the iron was reduced. Concentrations measured in July were very high compared to the measurements from the remaining months. Porewater measurements of iron were also higher than the other months (appendix section 8.1). This is most likely due to an error in the measurements as both the porewater and sediment content was higher.

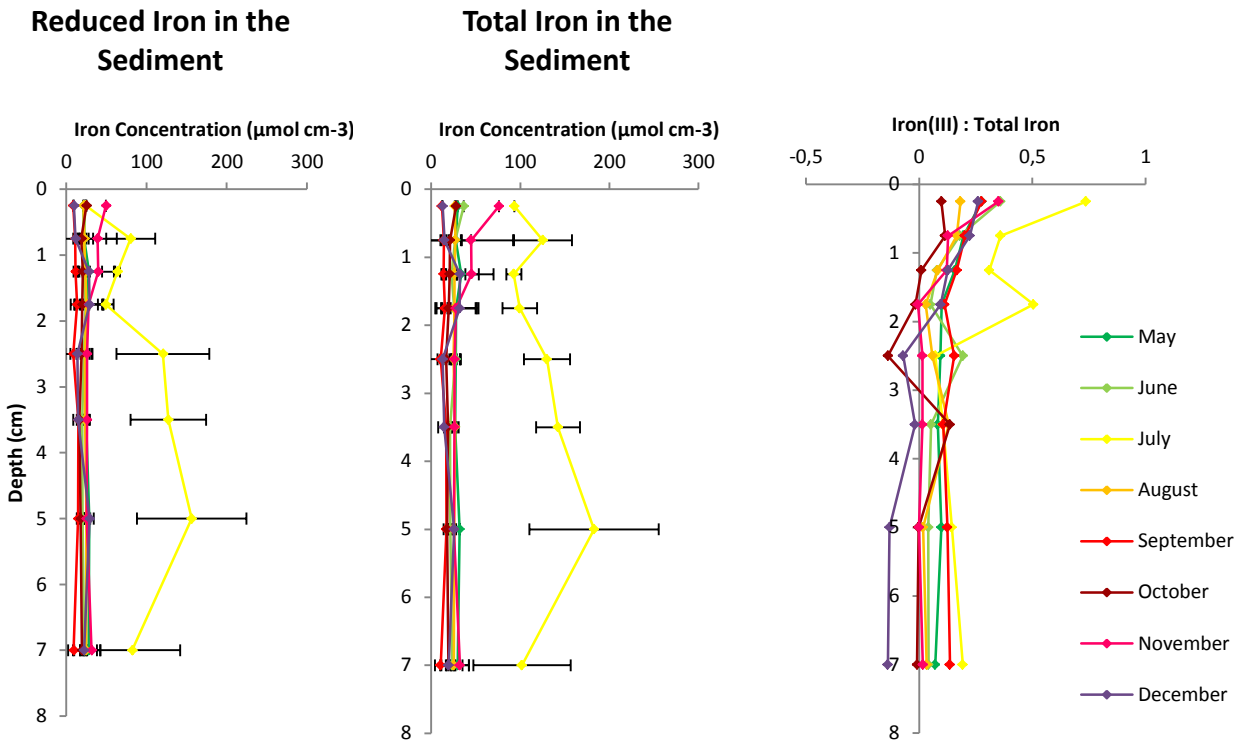

Figure 28. Profiles of solid phase iron (reduced and total iron). With the exception of measurements from July all measurements were similar. The concentration of iron was around 25 µmol cm^{-3} throughout the sediments and was mostly in the reduced form. Iron (III) to total Iron indicated that more iron was oxidized at the top of the sediment, while most of the iron was reduced below 2 cm.

4.2.3 Oxygen profiles and penetration depth

Oxygen profiles were made each month and the average of the profiles was found (n=8). Oxygen was depleted within the first centimetre in the sediment (Figure 29). From each of the profiles, the depth-integrated volume-specific oxygen uptake was calculated. In June, November, and December oxygen consumption rates were higher toward the bottom of the oxygen penetration depth. In the remaining months oxygen consumption rates were highest at the top of the oxic zone. In general, oxygen profiles only varied slightly. The diffusive oxygen uptake (DOU) was calculated from each of the profiles as explained in Glud 2008 (Figure 2). The sum of the depth integrated volume specific oxygen uptake in each profile was equal to the average diffusive oxygen uptake. Additional oxygen profiles for the remaining months are shown in appendix 8.2.

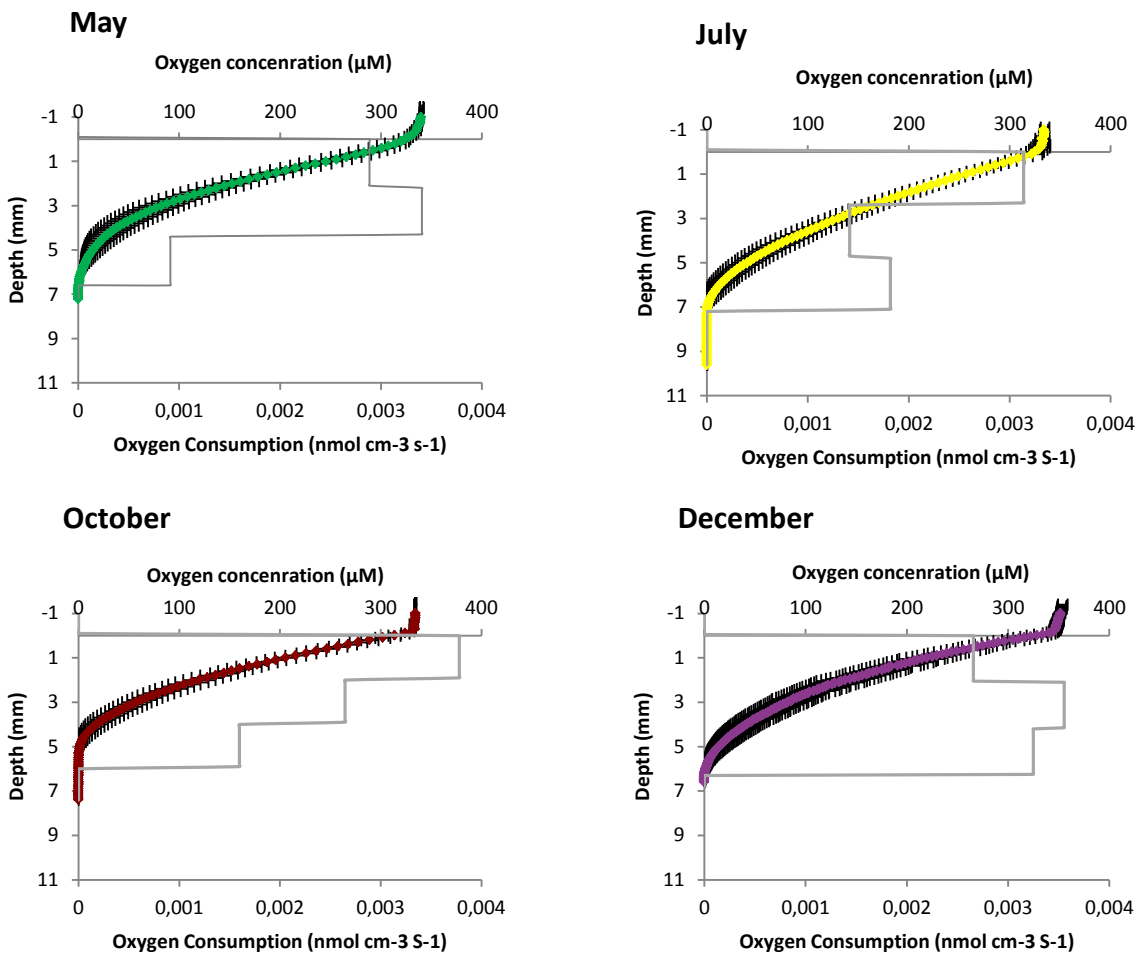

Figure 29. Oxygen profile with standard deviation from May, July, October, and December (additional profiles are in the appendix). Oxygen profiles are constructed from an average of single profiles from every month (n=8). Only a slight difference was observed between the months. Oxygen consumption rates according to the depth are indicated in each graph. The diffusive oxygen uptake (DOU) was calculated from each of the profiles used in the average profile.

Oxygen concentrations in the bottom water decreased from June until November, whereafter concentrations increased. The oxygen penetration depth varied between 5.3 and 8.4 mm. The high value in September was interpreted as an outlier. The oxygen penetration depth decreased along with decreasing oxygen concentration in the bottom water (Figure 30). The DOU values seemed to be inversely proportional to both the oxygen concentrations in the bottom water and the oxygen penetration depth, with the exception of the measured DOU value in November.

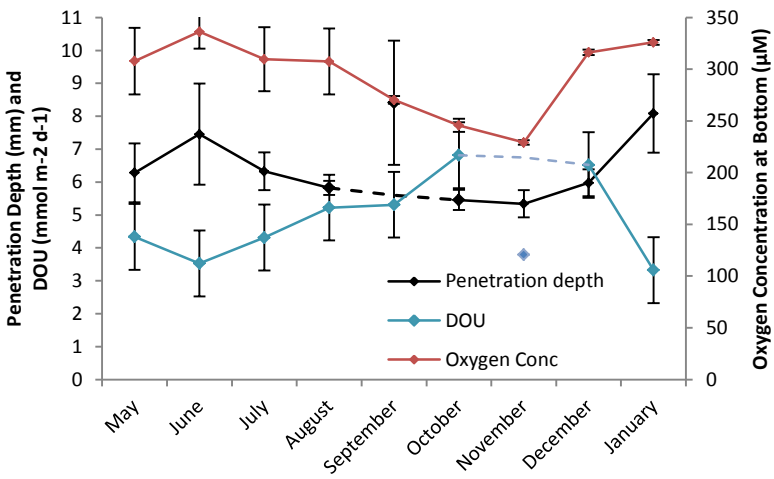

Figure 30. Oxygen concentrations in the bottom water decreased from August until November, whereafter the concentration increased again. Oxygen penetration depth decreased from 7.5 cm in June to 5.5 in November, whereafter the penetration depth increased again. With the exception of the measurement of DOU in November, DOU values were inversely proportional to both the oxygen concentration and the oxygen penetration depth.

4.2.4 Exchange rates

Exchange rates were measured using whole core incubations (n=6). The total uptake of oxygen ranged from 6.3 to 11.9 mmol m^{-2} d^{-1} (Figure 31A). Oxygen uptake peaked in June and September. After September uptake slowly decreased. The DOU comprised between 31 and 78% of the total uptake, with increasing

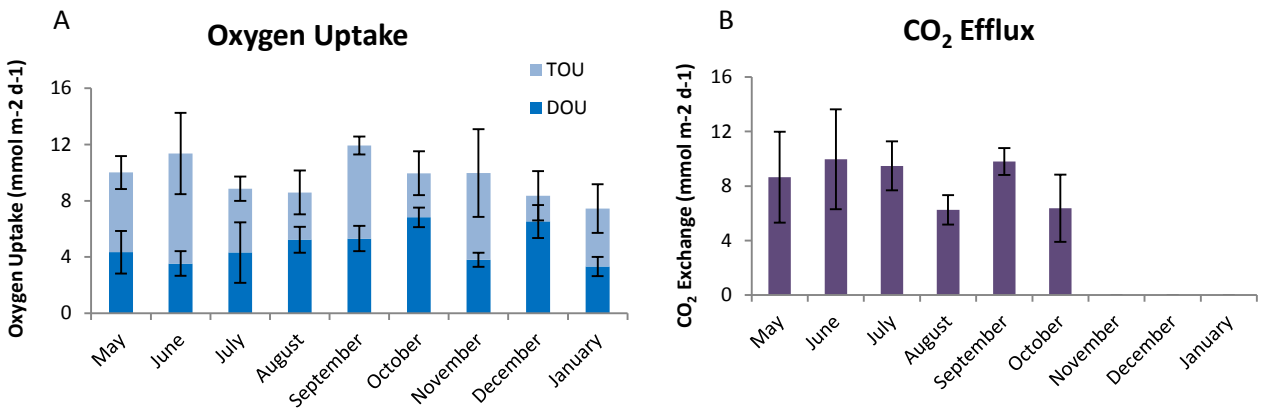

Figure 31. A. Total oxygen uptake (TOU) and diffusive oxygen uptake (DOU) rates from each month with corresponding standard deviations (n=6). Measurements were made by whole core incubations. Uptake seemed higher in June as well as September and seemed to decrease slightly from September. B. Flux of CO_2 out of the sediment with corresponding standard deviation (n=6). Measurements made by whole core incubations. Efflux rates seemed higher during the summer (May, June and July). Furthermore a peak in CO_2 efflux was observed in September corresponding to higher oxygen consumption.

values until October. The remainder of the oxygen uptake was expected to be mediated by benthic fauna and irrigation. Efflux of CO_2 from the sediment more or less corresponded to the oxygen uptake. Thus, the CO2 flux was between 6.3 and 10.0 mmol m-2 d-1 and increased uptake of oxygen rates matched the increased release of CO_2, corresponding to increased amounts of organic material at the sediments surface (Figure 31B). Due to problems with the coulometer, DIC samples from November 2011 to January 2012 remain to be analysed.

Oxygen consumption at times exceeded the CO_2 production in the sediment. The respiration quotient (RQ) is the ratio between oxygen consumption and CO_2 production. Except for July, RQ values were below 1 and ranged between 0.64 and 0.88 (Figure 32). The average RQ value was 0.83.

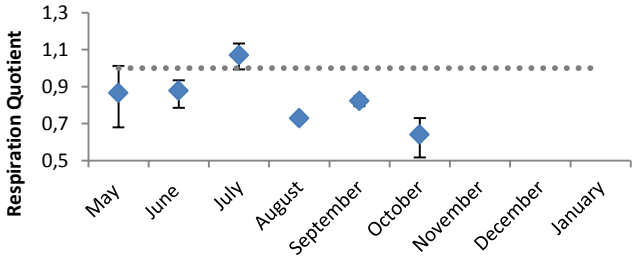

Figure 32. The respiration quotient (RQ) is the ratio between oxygen consumption and CO_2 production. The ratio was only above 1 in July, while oxygen consumption exceeded CO_2 production in the remaining months.

In May a small influx of NO_x was observed (-0.02 mmol $m^{-2}d^{-1}$). This was followed by production of NO_x within the sediment, where rates ranged between 0.19 and 0.87 mmol $m^{-2}d^{-1}$ with the exception of the measurement from August where rates reached 2.9 mmol $m^{-2}d^{-1}$. In general, the flux seemed to increase until August corresponding to organic material transfer, whereafter they decreased again (Figure 33). Water samples for NH_4^+ were taken, but have not yet been analyzed.

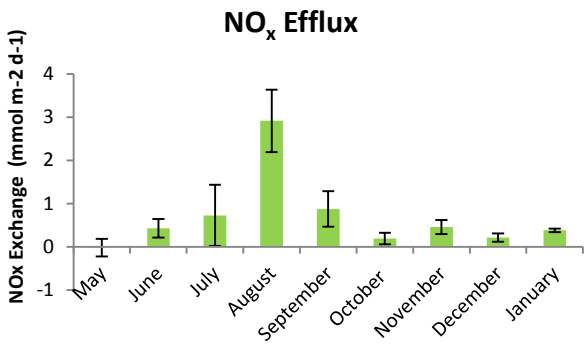

Figure 33. Fluxes of NO_x (NO_3^- and NO_2^-) out of the sediment measured from whole core incubation (n=6). Except for August rates were between -0.02 and 0.87 mmol m^{-2} d^{-1}.Negative fluxes correspond to uptake of NO_x. In August the rate was 2.9 mmol m^{-2} d^{-1}.

4.2.5 Denitrification and Anammox

Denitrification was measured using whole core incubations with labeled $^{15}NO_3^-$ (n=3). With the exception of rates measured in July and September, measurements of denitrification rates were between 0.16 and 0.56 mmol $m^{-2}d^{-1}$ (Figure 34). The relative contribution to N_2 production through anammox was measured using slurry incubations and corresponded to only 0 – 3.6% of the total. N2 production through anammox was not measurable in May and June. Applying these fractions to the whole-core data, rates of anammox ranged between 0.001 and 0.018 mmol $m^{-2}d^{-1}$.

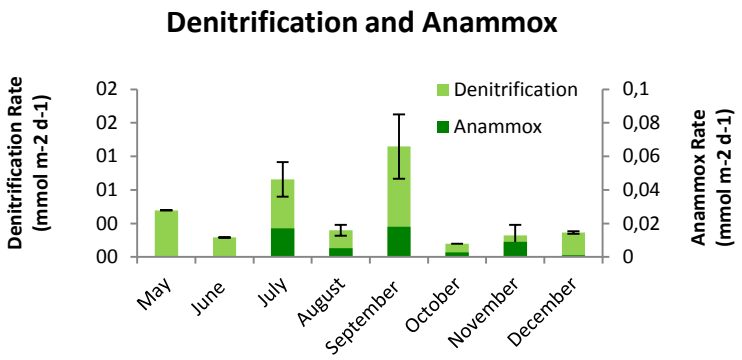

Figure 34. Denitrification rates was measured by whole cores incubation (n=3), while anammox contribution was measured through slurry incubation. Rates were high in July and September, but except for these, the rates were in general low. In May and June no production of N_2 through anammox was measured.

4.2.6 Sulfate Reduction Rates

Sulfate reduction was measured in intact cores each month. Rate measurements were performed until 10 cm and in December and January to a depth of 16 cm. As rates continued to decrease below 10 cm in December and January, it is presumed that the rates in general decrease below 10 cm. The highest sulfate reduction activity was measured at 1 - 2 cm depth every month (Figure 36), where the rates ranged between 13.3 and 44.3 nmol SO_4^{2-} cm^{-2} d^{-1}. The depth-integrated sulfate reduction rates to 10 cm ranged between 0.4 and 2.4 mmol SO_4^{2-} $m^{-2}d^{-1}$. In June and July rates were low, but from August rates increased. Rates were low again in November and January, whereas rates were high in December (Figure 35). To obtain the total rates from each month (including the SR below 10 cm) the relationship between the rates measured from 0 to 10 cm and the rates measured from 10 to 16 in December and January was used.

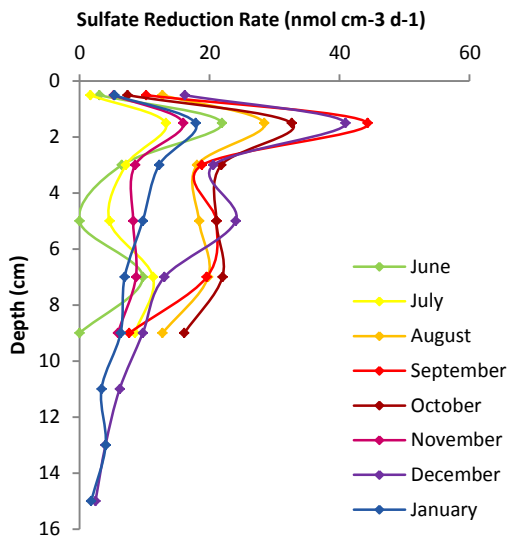

Figure 36. Sulfate reduction rates measured each month showed the same tendency, with the highest rate around at 2 cm followed by a decrease in the rates. In December and January rates were measured to a depth of 16 cm, showing a continued decrease in rates.

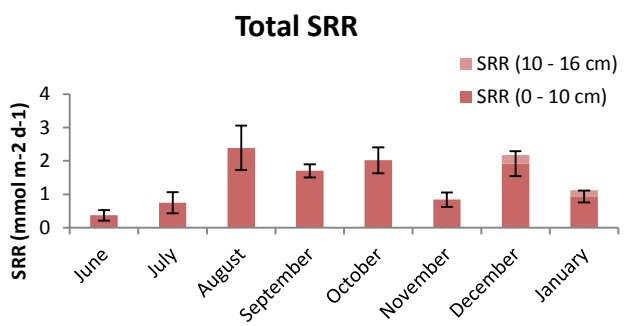

Figure 35. Total sulfate reduction rates according to the months with corresponding standard deviation (n=3). Reduction rates were measured in the top 10 cm, but rates were additionally measured from 10 – 16 cm in December and January (rates are shown in the graph with a lighter color). The rates increased in august and remained high except in November and January, where rates were lower.

4.2.7 Relative Iron and Manganese reduction contribution to carbon oxidation (Bag Incubations)

To obtain the relative contribution from iron and manganese reduction to total carbon oxidation, bag incubations were performed. Furthermore, to justify using the data from the bag incubations, the accumulation/reduction rates are described and compared to whole core rate measurements. All graphs can be found in the appendix section 8.3.

All CO_2 produced in the bags is presumed to be produced through anoxic processes. Hence, CO_2 is produced by iron, manganese, denitrification and sulfate reduction. In all bag incubation experiments, CO_2 and NH_4^+ accumulated linearly in the porewater at all depths. Fe^{2+} accumulated linearly in the porewater in the top 2 cm, whereas Mn^{2+} only accumulated in the porewater in the top layer (see graphs on accumulation in appendix section 8.3). CO_2 was not measured in the incubation from October, but an estimate of CO_2 production was derived from NH4+ production and the average of the ratios of CO2 to NH4+ production measured in June and December (see Canfield et al. 1993). The depth distribution of CO_2 and NH_4^+ accumulation more or less aligned throughout the sediments with highest accumulation in the top sediment and around 5-6 cm. In June and December accumulation also occurred at a depth of 9 cm.

The CO_2 production attributable to sulfate reduction was subtracted from the total CO_2 production. The remaining production could hereafter be attributed to iron and manganese reduction. As both Fe^{2+} and Mn^{2+} accumulated in the porewater, reduction of both compounds occured (se graphs in appendix section 8.3). In total, sulfate reduction accounted for 63 - 74% of the carbon oxidation, while iron and manganese reduction should hence account for 24 -28% (See graphs in appendix section 8.3).

The depth-integrated DIC accumulation rates were between 3 and 3.4 times higher than the exchange rates from the whole core incubations, while sulfate-reduction rates in the bag incubations were 1.5 -8.5 times higher than the whole-core rates. Stimulation of metabolic rates during bag incubations relative to whole cores is expected (e.g. Glud et al. 2000, Hansen et al. 2000).

4.2.8 Total Carbon Oxidation from whole core incubation and the relative iron and manganese contribution

When using oxygen as a proxy for the total benthic carbon oxidation, the contribution of the different electron acceptors could be calculated (Figure 37). The relative contribution from iron and manganese was calculated from the bag incubations according to the whole core incubations. Oxygen was the main electron acceptor in carbon oxidation, but the contribution from anoxic carbon oxidation increased from August as sulfate reduction was more prominent. Denitrification, iron and manganese reduction only contributed to a small fraction of the total carbon oxidation.

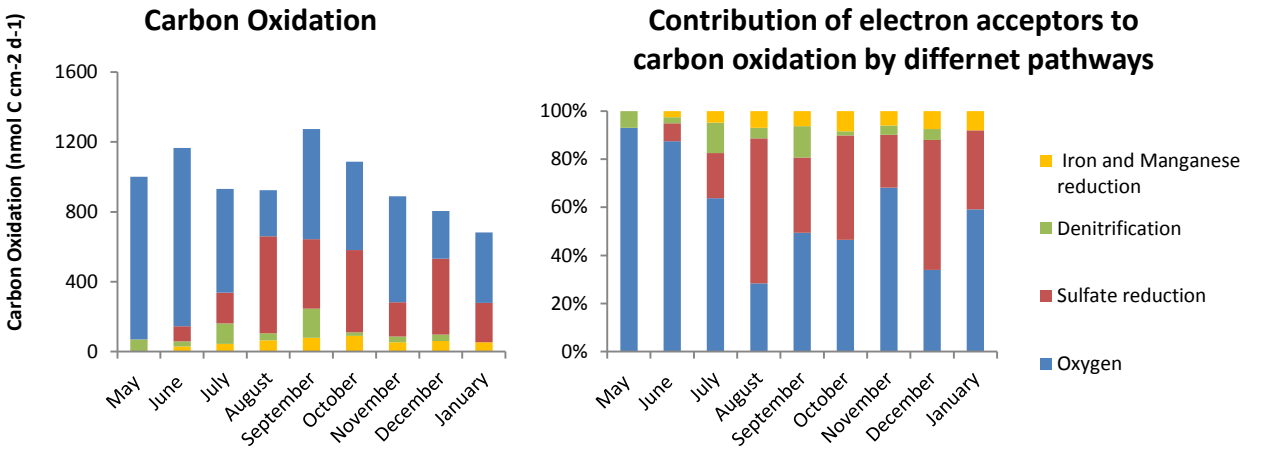

Figure 37. Oxygen consumption was used as a proxi for the total carbon oxidation. Total carbon oxidation rates varied between ~600 to 1200 nmol C m^{-2} d^{-1}, with the highest rates in June and September. Oxygen was the main electron acceptor in carbon oxidation, but from August anoxic respiration processes (sulfate reduction, denitrification and anammox) were more prominent. Iron and manganese only accounted for a minor part of the total carbon oxidation.

A total estimate of the relative electron acceptors during the nine months was made. Of the total carbon oxidation rate (2535 mmol C m^{-2} $month^{-1}$) 31% of the oxidation was through sulfate reduction based on the contribution from 10 to 16 cm. 6% was through denitrification. 6% was through iron and manganese reduction, while the remaining oxidation was mediated through oxygen (Figure 38). As pointed out these results only account for 9 months. The measurements from the remaining months (February, March and April) are needed to make an estimate of the annual distribution.

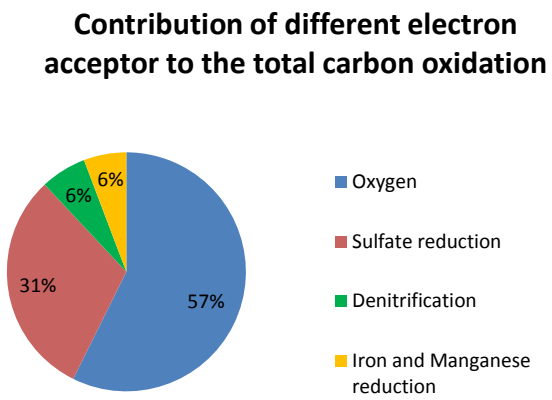

Figure 38. Total contribution to carbon oxidation calculated from May to December indicated that oxygen is the main electron acceptor in Kobbefjord and that denitrification and anammox only contribute to a smaller fraction.

5. Discussion

The main focus of the thesis was to describe the seasonal variation in the benthic metabolism in a Subarctic fjord. Throughout the discussion the seasonal variation in the present study and its resemblance with the temperate and Higharctic region is described.

5.1 Pelagic Variation

The measurements of primary production from this study were compatible to previous measurements preformed at the main pelagic station in the NERO annual reports located at the mouth of the Godthåbsfjord system (64°07'N, 51°53'W) (Table 2). The seasonal variation in this study (Figure 25A) resembled the variation in 2009 (NERO 3rd annual Report), where primary production peaked in May and August. The highest peak was measured in May compared to the peak in August. The seasonal variation measured during 2006, 2008 and 2010 likewise indicated two peaks in primary production, but showed a slightly different trend, with either higher primary production rates in August compared to May or the two peaks being closer together (NERO 1st, 2nd, and 4th annual report). In 2007 only a single peak in primary production was observed in July (NERO 1st annual report).

Table 2. Primary production rates from the present study (Figure 25A) and the NERO 1st, 2nd, 3rd, and 4th annual reports. Rates from the present study are represented as the rates measured in 2011 /12.

Year	Min. Primary Production ($mg\ C\ m^{-2}\ d^{-1}$)	Max. Primary Production ($mg\ C\ m^{-2}\ d^{-1}$)
2011/12	2	868
2010	>5	1350
2009	>5	400
2008	>5	1150
2007	>5	850
2006	10	700

As emphasised in the introduction (Figure 15), primary production in the Subarctic is lower compared to temperate regions, but higher than at the Higharctic region (Table 3). In fact, the peak in the primary production measured in Kobbefjord only corresponds to 54% of the production in Limfjorden (Krause-Jensen et al. 2012). In Young Sound the primary production peak (Rysgaard et al. 1999) only corresponded to 32% of the production in Kobbefjord. In Kobbefjord primary production peak earlier compared to both the temperate region and the Higharctic region (Table 3). In the typical Higharctic fjord system Young Sound, the seasonal variation in primary production is constrained to the open water period lasting only a

Table 3. Comparison of maximum primary production rates as well as the time of the first primary production peak in different regions. Data from the Kobbefjord is from the present study (Figure 25A), data from the Limfjord is from Krause-Jensen et al. (2012) and data from the Young Sound is from Rysgaard et al. (1999).

Site	Max. Primary Production Rate (mg C m^{-2} d^{-1})	First Peak in Primary Production (month)
Limfjord	1600	June
Kobbefjord	868	May
Young Sound	275	Mid July

few months. On the contrary, primary production in Kobbefjord is not nearly as constricted.

Sedimentation rates measured in the present study resemble most of the rates measured previous years ranging from 0.2 to 2.4 g C m^{-2} d^{-1} on an annual basis (NERO 1st, 2nd, and 4th Annual Reports). Sedimentation rates indicated by carbon content seemed to depend upon primary production. Sedimentation rates increased following a primary production bloom in both May and August (Figure 25A and B). In this study local primary production could maximally account for 35% of sedimenting material. This therefore indicates that organic material is transferred to the area from either the open sea or land. Kobbefjord is located close by Nuuk and Kobbefjord may therefore be affected by discharge from Nuuk. Compared to rates measured by Lund-Hansen et al. (2004) in Aarhus Bay the rates in Kobbefjord were only slightly lower (Table 4). At Young sound the sedimentation rates have been measured to increase from 1.6 g dw m^2 d^{-1} in June to 2.5 g dw m^2 d^{-1} in July, corresponding to 17.3 mmol C m^{-2} d^{-1} and 32.8 mmol C m^{-2} d^{-1}, respectively. This sedimentation rate only corresponds to 55% and 22%, of the sedimentation rate in Kobbefjord, when comparing the lowest and highest rate. Thus sedimentation rates at Kobbefjord by far exceeded the sedimentation rates at Young Sound.

Table 4. Sedimentation rates measured in the Aarhus Bay, Kobbefjord and Young Sound region. Values from the subarctic region are from the present study performed at Kobbefjord. Values from the temperate region are from Aarhus bay (Lund-Hansen et al 2004) and values from the higharctic region are from Young Sound (Rysgaard et el. 2004).

Site	Max Sedimentation Rate (mmol C m^{-2} d^{-1})	Min Sedimentation Rate (mmol C m^{-2} d^{-1})
Aarhus Bay	163.0	22.5
Kobbefjord	148.9	19.2
Young Sound	32.8	17.3

5.2 Benthic Variation

5.2.1 Exchange rates

In this study porewater and solid phase profiles (Figure 27, Figure 28, and Figure 29) indicated the expected benthic biogeochemical pattern (Konhauser 2007), but no distinctive changes among the months was observed. The benthic biogeochemistry pattern was comparable to both temperate and Higharctic regions (Canfield et al. 1993; Kostka et al. 1999; Rysgaard et al. 1998). The TOU seemed to increase following the primary production peaks. However, the measured rates of both DOU and TOU (Figure 31A) from the present study showed less seasonal variation than rates measured previous years in the NERO annual reports (the main sediment Station is located in Kobbefjord) (Figure 39).

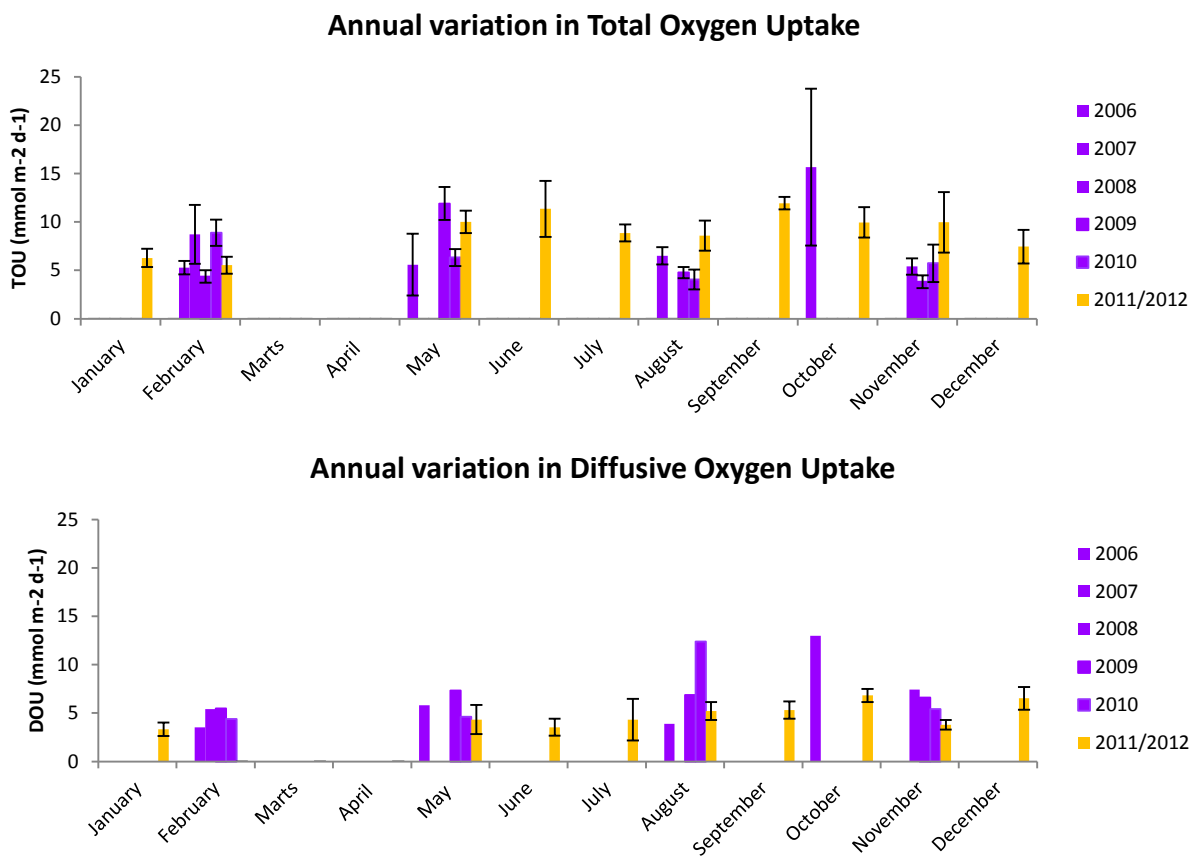

Figure 39. Rates of TOU and DOU measured from 2006 to 2011/2012. Rates reported in the NERO 1st, 2nd, 3rd, and 4th annual report and in the present study. Rates from the present varied only little compared to measurements from 2006, 2008, 2009 and 2010. All blue bars all measurements from the NERO reports and the yellow bars are from the present study.

This variation could however be the result of difference between the methods applied. In this study TOU rates was determined after a 20% drop in oxygen concentration (incubations lasted approximately 8-12h),

whereas rates measured in the NERO reports were based on 24h incubations, which would have led to stronger oxygen depletion and a potential underestimation of TOU (Glud 2008). Furthermore, in the NERO 2nd, 3rd, and 4th annual report DOU rates have been reported to exceed the TOU values, which should not be possible, as the DOU is included in the TOU. Thus, rate measurements in the present study seem more reliable. Comparing average values ± SD from the NERO (TOU 6.23 ± 3.35, DOU 6.58 ± 2.85) with the present study (TOU 8.99 ± 2.08, DOU 4.32 ± 1.93) rates varied slightly. Throughout the study the DOU variation affected both the oxygen penetration depth and the oxygen concentration in the bottom water. As DOU increased, oxygen was consumed rapidly in the sediment, wherefore the oxygen penetration depth decreased (Figure 30).

The oxygen uptake and CO_2 production throughout the study yielded an average RQ value of 8.3. The fact that the RQ value was lower than 1 could either be explained by $CaCO_3$ formation (Therkildsen and Lomstein 1993), re-oxidation of reduced equivalents (Therkildsen and Lomstein 1993) or benthic faunal mediated oxygen uptake. However, it is important to keep in mind that the RQ value in this study only represents nine months. Hence, the annual average may be different.

Formation of $CaCO_3$ could be expected, although this was not measured. During a potential oxygen debt, additional oxygen would be necessary to oxidize reduced compounds in the sediment. However, unexpectedly the CO_2 production in the sediment did not support this in the present study, as CO_2 production likewise seemed constant. CO_2 production may exceed oxygen consumption from November to April, but this has not been analyzed yet.

As indicated by the big difference between the TOU and the DOU values, the enhanced oxygen uptake is explained by the regulation by benthic fauna. Blicher et al (2009) estimated that the two macrozoobenthic species *Strongylocentrotus droebachiensis* and *Chlamys islandica* had an annual carbon demand of 30.6 g C m^{-2} (corresponding to 2547 mmol C m^{-2} y^{-1}) in Kobbefjord. Thus, oxygen uptake of these or other macrozoobenthic species may therefore account for a significant fraction of the total oxygen uptake. However, these particular organisms were not found at the site. Both carbon demand and oxygen consumption of benthic macroorganisms differ between organisms, but nevertheless an influence was expected from the unidentified worms in the sediment.

Comparing the seasonal oxygen uptake in Kobbefjord with the temperate and higharctic region, oxygen uptake was lower than in the temperate region, but higher than in the higharctic region (Figure 40). The rates in Kobbefjord only corresponded to 30-60% of the uptake measured in the temperate region (Glud et al. 2003) with the exception of the measurement in October. The oxygen uptake rates in Kobbefjord

resembled the rates measured in Young Sound (Thamdrup et al. 2007). On the other hand, the seasonal variation varied between regions. In the temperate region the seasonal oxygen uptake did not vary distinctively. However, in both the Subarctic and the Higharctic region a more distinctive seasonal variation has been observed (Figure 40). The variation in the uptake at all sites is most likely due to the sedimentation of organic material. The high and fluctuating uptake in the temperate region could thus be due to increased amounts of sedimenting material. At the Subarctic and the Higharctic region a "baseline" in oxygen consumption seems to be formed during winter. This "baseline" in the Subarctic and the Higharctic were similar, with values of 6-7 mmol m^{-2} d^{-1}. This baseline is probably fuelled by organic material that has accumulated over the past years (Thamdrup et al. 2007). In all regions, the biomass of benthic macrofauna has been reported to increases during spring and summer (Sejr and Christensen 2007; Therkildsen and Lomstein 1993; Blicher et al 2010). These are therefore expected to affect the oxygen uptake to a greater extend in this period. The site examples used in this section to compare the difference between regions may of course differ in many ways, making it difficult to compare them. For instance, the water depths of the fjord systems vary between the sites. This clearly affects the oxygen uptake as more organic material is deposited and the oxygen demand is higher at larger water depths.

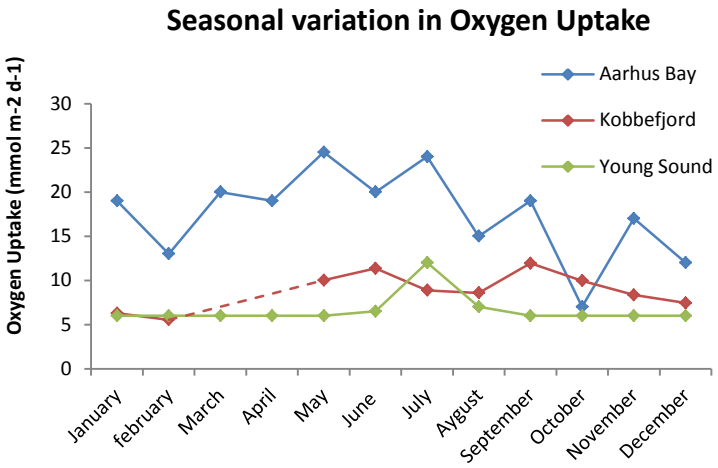

Figure 40. The seasonal variation in oxygen uptake at different sites. Values from Aarhus Bay and Young Sound are approximate values from shown graphs. All units are displayed in mmol $m^{-2}d^{-1}$. Data from Aarhus Bay is from Glud et al. 2003 and data from Young Sound is from Thamdrup et al (2007), while data from Kobbefjord is from the present study (Figure 31A).

5.2.2 Denitrification and Anammox

The seasonal variation in the N_2 production in Kobbefjord was less clear than in the seasonal study performed by Rysgaard et al (1998). Even though the denitrification rates did increase following increased sedimentation of organic material at Kobbefjord (Figure 34 and Figure 25B), the coupling was more distinctive at Young Sound (increasing from approximately 0.15 to 0.63 mmol m^{-2} d^{-1}).

In general, maximum denitrification rates (July: 0.94 mmol m^{-2} d^{-1} and September: 1.34 mmol m^{-2} d^{-1}) were higher in the Subarctic region than the rates measured in the arctic region (Rysgaard et al. 2004). Other than the maximum rate, the remaining rate measurements resembled rates measured along the west and

east coast of Greenland (Rysgaard et al. 2004). Rysgaard et al. (1993) measured denitrification rates in Nordsminde Fjord, ranging between 0.62 and 0.72 mmol m^{-2} d^{-1}. Only the measurements from July and September in the present study where higher than these rates. From this it could be extrapolated that total denitrification rates in a Subarctic fjord system are higher than in a Higharctic fjord system, but lower than in a temperate fjord system (Rysgaard et al 1993; Rysgaard et al 2004; Present study). Nevertheless, other studies on the temperate region has measured different rate (Canfield et al. 2005/Jørgensen 1996). At Aarhus Bay rates were much lower, but this site has been exposed to extensive eutrofication, which may have affected the mineralisation patterns.

In the present study, the measured anammox rates were very low accounting for maximum 3.6% of the total N_2 production. Rates measured in the Disco Bay indicated a higher contribution to the total N_2 production through anammox ranging between 18.5 and 26.7%, whereas this contribution decreased at higher longitudes (Rysgaard et al. 2004). It was therefore expected that the contribution from anammox would be higher at Kobbefjord, which was not the case. In the temperate region, anammox contribution has been shown to differ to a great extend. Thamdrup and Dalsgaard (2002) measured the relative contribution at both Skagerrak and Aarhus Bay, where contribution was 20-80% and ~5%, respectively. This could indicate that anammox is mainly affected by the water depth high rather than the geographical location. The importance of anammox seems increase as the water depth increase, which is further supported by the fact that the water depth at the sample site in Kobbefjord was larger (110 m), than at the other sites in Aarhus Bay (16 m) and Young Sound (36 m)(Rysgaard et al. 2004; Thamdrup and Dalsgaard 2002; Present study).

5.2.3 Sulfate Reduction

The sulfate reduction rates indicated a delayed increase in the rates following increased sedimentation (Figure 36 and Figure 25B). This trend has likewise been observed at Young Sound (Rysgaard et al 1998). Total rates were however higher in Kobbefjord compared to Young Sound. In the study by Thode-Andersen and Jørgensen (1989), the sulfate reduction rates measured in Aarhus Bay showed similar seasonal variation trends (April: 1.07 mmol m^{-2} d^{-1}, June: 3.84 mmol m^{-2} d^{-1}). This indicated that rates are higher in the temperate region compared to the Subarctic region. As increased sedimentation rates are expected to enhance the relative importance of sulfate reduction, the difference in total sulfate reductions rates between the regions could therefore be explained by the difference in the sedimenting material. Thus, in this instance, sulfate reduction rates measured at Kobbefjord seem to be an intermediate between temperate and Higharctic sites.

5.2.4 Carbon Oxidation

By comparing rates of TOU, sulfate reduction and denitrification rates from Aarhus Bay, Kobbefjord and Young Sound, the trend indicated that Kobbefjord has rates between the other locations (Figure 41). Oxygen respiration and sulfate reduction seem to increase moving from Young Sound to Aarhus Bay, whereas the opposite seemed to happen for denitrification.

Oxygen was used as a proxy for the total carbon oxidation and on this basis the relative contribution from the different electron acceptors was estimated (Table 5).

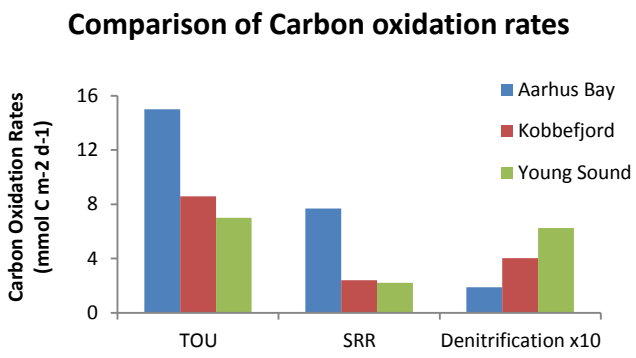

Figure 41. Comparison of the carbon oxidation rates from Oxygen, Sulfate reduction and denitrification from Aarhus Bay, Kobbefjord and Young Sound. All rates are from August and are corrected for the stoichiometry. Rates from Kobbefjord are from the present study and rates from Young Sound are from Rysgaard et al (1998). TOU rates from Aarhus Bay are from Glud et al. (2003), sulfate reduction rates from Aarhus Bay are from Thode-Andersen and Jørgensen (1989) and denitrification rates are from Jensen et al (1988).

Table 5. The relative importance of the different electron acceptors in carbon oxidation at Kobbefjord Aarhus Bay and Young sound. Values from Young Sound are from Rysgaard et al. (1998) and values from Aarhus Bay is from Jørgensen (1996). Values from Kobbefjord are from the present study (Figure 38).

Electron Acceptor	Aarhus Bay (Denmark)	Kobbefjord (SW Greenland)	Young Sound (NE Greenland)
O_2	43%	57%	38%
NO_3^-	2%	6%	4%
Mn^{4+}/Fe^{3+}	5%/5%	6%	0%/25%
SO_4^{2-}	45%	31%	33%

In the subarctic and higharctic regions oxygen was the main electron acceptor and in the Subarctic region this accounted for more than half of the total carbon oxidation. Denitrification seemed more prominent in the subarctic region compared to both of the other regions. However, as mentioned earlier values may vary significantly in the temperate region, as the coastal areas are more exposed to terrestrial factors such as enhanced nutrient discharge. The contribution to the total carbon oxidation from iron reduction was

however expected to be higher at Kobbefjord as most measurements of Iron contribution at sites located in the Arctic have been higher that the rates measured in this study (Thamdrup 2012). Sulfate reduction was, as expected, higher in the temperate region as the organic material loading is much higher in this region. Sulfate reduction contribution in the subarctic was unexpectedly lower than in the Higharctic region, as sedimentation is higher in the Subarctic region. However, water depth plays a significant role in benthic metabolism. The water depth at the compared sites differed; Aarhus Bay (16m), Young Sound (36m) and Kobbefjord (110m) (Jørgensen 1996; Rysgaard 1998; Present study), therefore the result of a comparison is relatively constrainted due to water depth differences. Thamdrup et al. (2007) showed that both CO_2 release from the sediment and the relative importance of the electron acceptors changed according to water depth. The relative importance of the anoxic processes increased with water depth, while the total exchange rates decreased (Thamdrup et al. 2007). The exponential decrease in CO_2 production according to water depth, can be estimated through the following formula from Thamdrup et al. (2007):

[34] $$DIC_{Release} = 2.26 + 18.2\, e^{1.05-\,(0.0525\,\cdot Z)}$$

Where Z is the water depth.

By applying this formula to the compared sites, the CO_2 release from Aarhus Bay (16m), Kobbefjord (110m) and Young Sound (36m) corresponded to 24.7, 2.4, and 10.0 mmol m^{-2} d^{-1}, respectively.

5.3 Carbon Budget for Kobbefjord (May 2011 – January 2012)

In this study an estimate of the carbon cycle could be made from both the pelagic and the benthic processes (Figure 42), with the reservation that measurements were made only at a single station and neither data from sedimentation nor from carbon oxidations rates at shallow areas were incorporated.

From May to December 2011, primary production was 6092 mmol C m^{-2} yr^{-1}. The sedimentation rate of carbon was estimated to be 17246 mmol C m^{-2} yr^{-1}. The sedimentation carbon was expected mainly to be fecal material and dead organisms. However, a part may have been of terrestrial origin. By assuming that the amount of sedimenting material is constant throughout the water column, this material is either mineralized or buried in the sediment. In total 2340 mmol C m^{-2} yr^{-1} was oxidized leaving approximately 15677 mmol C m^{-2} yr^{-1} to be buried in the sediment. However, part of the organic material may be resuspended to the water column. All rates mentioned in this section are assumed to be an underestimate of the actual annual rates as the contribution from February, March, and April has not been included.

The retention of carbon in Kobbefjord corresponded to approximately 91% of the sedimentating carbon pool not accounting for resuspension of parts of the organic material. Hence, retention in Kobbefjord is very efficient. Comparing this to measurements from a higharctic system, a lower retention has been estimated. Rysgaard et al. (1989) estimated retention of carbon in Young Sound to be 48%. Thus, retention of carbon is higher in Kobbefjord.

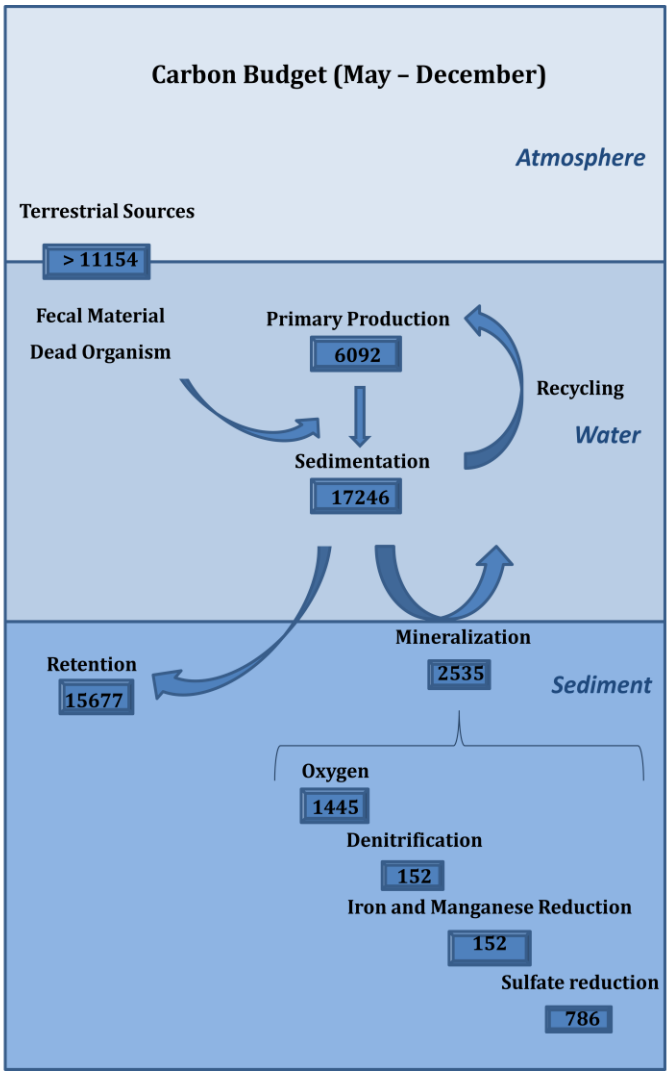

Figure 42. A carbon budget from was constructed for Kobbefjord from May 2011 to January 2012. All units in the figure are in mmol m^{-2} yr^{-1}.

6. Conclusion and Future Perspectives

Comparing the pelagic seasonal variation, Kobbefjord seemed to be an intermediate between a temperate and a Higharctic site. Both primary production and sedimentations rates measured at Kobbefjord ranged between the rates measured at a temperate and a higharctic location. This was the case for both total rates and the seasonal variation. Comparing the benthic variation, Kobbefjord seemed to function as an intermediate when looking at exchange, denitrification and sulfate reduction rates. However, it is still important to keep in mind the variation may be due to the water depth differences. At present, anoxic pathways of carbon oxidation were more dominating in Young Sound compared to Kobbefjord.

Provided that climate changes would increase sedimentation rates at Higharctic sites, anoxic processes are expected to become more important (Rysgaard and Glud 2007). Using the natural climate gradient along the Greenlandic coastline it has been hypothesized the Young sound in time will Kobbefjord. As Kobbefjord resembled an intermediate between temperate and higharctic fjord system, one can assume that the seasonal variation in both the pelagic and the benthic system at the higharctic region in time would change begin to resemble those in Kobbefjord. In general rates in both the pelagic and the benthic systems could be expected to increase. However, unexpectedly a dominant importance of the anoxic pathways was not observed at Kobbefjord despite the fact that Kobbefjord receive more organic material compare to Young Sound.

Overall the project provided a thorough overview of the benthic metabolism interaction. During the project many parameters were measured, wherefore the work load was extensive. Due to this, time was very limited and in the future prioritising only few parameters could improve the end result significantly. By collaborating with other scientists/students throughout the entire project additional parameters could be included. Generally, a thorough investigation of the seasonal variation in; (1) the pelagic and benthic coupling, (2) the benthic fauna and (3) both pelagic and benthic variation at shallow sites would improve the understanding of the fjord system significantly.

Overall this study provides a good basis for continuing future work with benthic metabolism and through this gain further knowledge on how climate changes may in fact affect the arctic systems.

7. References

Andersen F.Ø. and Kristensen E. (1992).

The importance of benthic macrofauna in decomposition of microalgae in a coastal marine sediment. Limnol. Oceanogr. Vol. 37, No. 7, 1392 - 1403

Arnosti C. and Holmer M. (1999). Carbohydrate dynamics and contribution to the carbon budget of an organic-rich coastal sediment. Geochem. Cosmochem. Acta. Vol. 63 No. 3/4, 393 - 403

Arrigo, K.R., G. van Dijken and S. Pabi (2008). Impact of a shrinking Arctic ice cover on marine primary production. Geophys. Res. Lett. Vol. 35, L19603

Baeyens W., Panutrakul S., Elskens M., Leermakers M., Navez J. and Monteny F. (1991). Geochemical Processes in Muddy and Sandy Tidal Flat Sediments. Geo-Mar Lett. Vol. 11, 188 - 193

Bendtsen J., Gustafsson K.E., Rysgaard S. and Vang T. (2007). Physical conditions, dynamics and model simulations during the ice-free periode of Young Sound/Tyrolerfjord system. In: Rysgaard S. and Glud R.N. (Eds). Carbon cycling in Arctic marine ecosystems: Case study Young Sound. Meddr. Grønland, Bioscience 58: 46 - 59

Berg P., Risgaard-Petersen N. and Rysgaard S. (1998). Interpretation of measured concentration profiles in sediment pore water. Limnol. Oceanogr. Vol. 43 No. 7, 1500 – 1510

Blicher M.E., Sejr M.K. and Rysgaard S. (2009). High carbon demand of dominant macrozoobenthic species indicated their central role in ecosystem carbon flow in a sub-arctic fjord. Mar. Ecol. Prog. Ser. Vol 383, 127 - 250

Blicher M.E., Rysgaard S. and Sejr M.K. (2010). Seasonal growth variation in *Clamys iskandica* (Bivalvia) from sub-Arctic Greenland in linked to food availability and temperature. Mar. Ecol. Prog. Ser. Vol. 407, 71 - 86

Bower C.E. and Holm-Hansen T. (1980). A salicylate-Hypochlorite Method for Determining Ammonia in Seawater. Can. J. Fish. Aquat. Sci. Vol. No. 37, 794 – 798

Braman R.S. and Hendrix S.A. (1989). Nanogram Nitrite and Nitrate Determination in Environmental and Biological Materials by Vanadium(I I I) Reduction with Chemiluminescence Detection. Anal. Chem. Vol. No. 61, 2715-2718.

Buch E. (2007). Physical oceanography of the Greenland Sea. In: Rysgaard S. and Glud R.N. (Eds). Carbon Cycling in Arctic marine ecosystems: Case study Young Sound. Meddr. Grønland, Bioscience 58, 14 - 21

Bury S.J., Zeldis J.R., Nodder S.D. and Gall M. (2012). Regenerated Primary Production dominates in the Periodically upwelling shelf Ecosystem, northeast New Zealand. Cont. Shelf Res. Vol. 32, 1 - 21

Canfield D.E, Thamdrup B. and Hansen J.W. (1993). The anaerobic degradation of organic matter in Danish coastal sediment: Iron Reduction, manganese reduction, and sulfate reduction. Geochem. CosmoChem. Acta. Vol. 57, 3867 - 3882

Canfield D.E., Thamdrup B. and Kristensen E. (2005). Aquatic Geomicrobiology – Advances in Marine Biology Vol. 48 Elsevier Academic Press.

Carmack E. and McLaughlin F. (2011). Towards recognition of physical geochemical change in subarctic and Arctic Seas. Prog. Oceanogr. Vol. 90, 90 - 104

Cline J.D. (1968). Spectrophotometric Determination of hydrogen sulfide in Natural waters. Limnol .Oceanogr. Vol. 14, 454–458

Domine L.M. Vanni M.J. and Renwick W.H. (2010). New and regenerated primary production in a productive reservoir ecosystem. Can. J. Fish Aquat. Sci. Vol. 67, 278 - 287

Doney S.C., Fabry V.J., Feely R.A and Klypas J.A. (2009). Ocean Acidification: The Other CO_2 Problem. Annu. Rev. Mar. Sci. Vol. 1, 169 - 192

Dugdale R.C. and Goering J.J. (1967). Uptake of new and regenerated forms of Nitrogen in Primary Productivity. Limnol. Oceanogr. Vol. 12, 196.

Eppley R.W. and Peterson B.J. (1979). Particulate Organic Matter Flux and Planktonic new Production in the deep Ocean. Nature Vol. 282, 677 – 680.

Glud R.N. (2008). Oxygen dynamics of marine sediments. Mar. Biol. Res. Vol. 4, 243 – 289.

Glud R.N., Berg P., Hume A., Batty P., Blicher M.E., Lennert K. and Rysgaard S. (2010). Benthic O_2 exchange across hard-bottom substrates quantified by eddy correlation in a sub-Arctic fjord. Mar. Ecol. Prog. Ser. Vol. 417, 1 - 12

Glud R.N., Gundersen J.K., Røy H. and Jørgensen B.B. (2003). Seasonal dynamics of benthic O_2 uptake in a semienclosed bay: Importance of diffusion and faunal activity. Limnol. Oceanogr. Vol. 48, No. 3, 1265 – 1276

Glud R.N., Holby O., Hoffmann F. and Canfield D.E. (1998). Benthic mineralization and exchange in Arctic sediments (Svalbard, Norway). Mar. Ecol. Prog. Ser. Vol. 173, 237 - 251

Glud R.N., Risgaard-Petersen N., Thamdrup B., Fossing H. and Rysgaard S. (2000). Benthic Carbon mineralization in a high-Arctic Sound (Young Sound, NE Greenland). Mar. Ecol. Prog. Ser. Vol. 206, 59 - 71

Giorgio P.A D., Cole J.J. and Cimbleris A. (1997). Respiration rates in bacteria exceed phytoplankton production in unproductive aquatic systems. Nature, Vol. 385, 148 - 151

Hall P.O.J. and Aller R.C. (1992). Rapid, small-volume, flow injection analysis for $\sum CO_2$ and NH_4^+ in marine and freshwater. Limnol. Oceanogr. Vol. 37 No. 5, 1113 – 1119

Hansen J.W., Thamdrup B., Jørgensen B.B. (2000). Anoxic incubation of sediment in gas-tight plastic bags: a method for biogeochemical process studies. Mar Ecol Prog. Ser Vol. 208, 273–282.

Howarth R.W. (1988). Nutrient limitation of net Primary Production in marine ecosystems. Ann. Rev. Ecol. Vol. 19, 89 – 110.

Iversen N. and Jørgensen B.B. (1985). Anaerobic methane oxidation rates at the sulfate-methane transition in marine sediments from Kattegat and Skagerrak (Denmark). Limnol. Oceanogr. Vol. 30, No. 5, 944 – 955.

Jensen M.H., Andersen T.K. and Sørensen J. (1988). Denitrification in coastal bay sediment: Regional and seasonal variation in Aarhus Bright, Denmark. Mar. Ecol. Prog. Ser. Vol. 48, 155 – 162

Jensen, L. M. and Rasch, M. (Eds.) 2008. Nuuk Ecological Research Operations, 1st Annual Report, 2007. – Copenhagen, Danish Polar Centre, Danish Agency for Science, Technology and Innovation, Ministry of Science, Technology and Innovation, 2008.

Jensen, L.M. & Rasch, M. (eds.) 2009. Nuuk Ecological Research Operations, 2nd Annual Report, 2008. National Environmental Research Institute, Aarhus University, Denmark. 80 pp.

Jensen, L.M. and Rasch, M. (eds.) 2010. Nuuk Ecological Research Operations, 3rd Annual Report, 2009. National Environmental Research Institute, Aarhus University, Denmark. 80 pp.

Jensen, L.M. and Rasch, M. (eds.) 2011. Nuuk Ecological Research Operations, 4th Annual Report, 2010. Aarhus University, DCE – Danish Centre for Environment and Energy. 84 pp.

Juul-Pedersen T., Nielsen T.G., Michel C., Møller E.F., Tiselius P., Thor P., Olesen M., Selander E. and Gooding S. (2006). Sedimentation following the spring bloom in Disco Bay, West Greenland, with special emphasis on the role of copepods. Mar. Ecol. Prog. Ser. Vol. No. 314, 239 – 255.

Jørgensen B.B. (1978). A comparison of methods for the quantification of bacterial sulfate reduction in coastal marine sediments. Geomicrob. Jour. Vol. 1 No. 1, 29 - 47

Jørgensen B.B. (1996). Case study – Aarhus Bay. In: Jørgensen B.B. and Richardson K. (Eds.), Eutrophication in Coastal Marine Ecosystems. American Geophysical Union, Washington DC.137 – 154

Kallmeyer J., Ferdelmann T.G., Weber A., Fossing H. and Jørgensen B.B. (2004). A cold chromium distillation procedure for radiolabeled sulfide applied to sulfate reduction measurements. Limnol. Oceanogr. Methods 2, 171 – 180

Klimant I., Kühl M., Glud R.N. and Holst G. (1997). Optical measurements of oxygen and temperature in microscale: Stratagies and biological applications. Sensors and Actuators B 38 – 39. 29 – 37

Konhauser K. (2007). Introduction to geomicrobiology. Blackwell Science Ltd. – Blackwell Publishing Company UK.

Kostka J.E., Thamdrup B., Glud R.N. and Canfield D.E. (1999). Rates and Pathways of carbon oxidation in permanently cold Arctic sediments. Mar. Ecol. Prog. Ser. Vol. 180, 7 - 21

Krause-Jensen D., Markager S. and Dalsgaard T. (2012). Benthic and Pelagic Primary Production in Different Nutrient Regims. Estua. Coast. Vol. 35, 527 - 545

Kristensen E., Ahmed S.I. and Devol A.H. (1995). Aerobic and anaerobic decomposition of organic matter in marine sediments: Which is fastest? Limnol. Oceanogr. Vol. 40 No. 8, 1430 - 1437

Lovley D.R. and Phillips E.J.P. (1987). Rapid Assay for Microbial Reducible Ferric Iron in Aquatic Sediments. Appl. Environ. Microbiol. Vol. 53, No. 7, 1536 – 1540

Lund-Hansen L.C., Pejrup M. and Floderus S. (2004). Pelagic and seabed fluxes of particulate matter and Carbon, and C:N ratios resolved by sediment traps during a spring bloom, Southwest Kattegat. Jour. Sea Res. Vo. 52, 87 – 98

Luther G.W., Sundby B., Lewis B.L., Brendel P.J and Silverberg N. (1997). Interactions of manganese with the nitrogen cycle: Alternative Pathway to denitrogen. Geochim. Cosmochim. Acta. Vol 61, No. 19, 4043 - 4052

Mackin J.E. and Aller R.C. (1984). Ammonium adsorption in marine sediments. Limnol. Pceanogr. Vol. 29, No. 2, 360 - 257

Martens C.S. and Berner R.A. (1974). Methane production in Interstitial Waters of Sulfate-Depleted Marine Sediments. Science, New Series, Vol. 185, No. 4157, 185, 1167 - 1169

Mernild S.H., Sigsgaard C., Rasch M., Hasholt B., Hansen B.U., Stjernholm, M. and Petersen D. (2007). Climate, river discharge and suspended sediment transport in the Zackenberg River drainage basin and Young Sound/Tyrolerfjord, Northeast Greenland, 1995 – 2003. In: Rysgaard S. and Glud R.N. (Eds). Carbon cycling in Arctic marine ecosystems: Case study Young Sound. Meddr. Grønland, Bioscience 58: 24 - 43

Middelboe M., Glud R.N. and Sejr M.K. (2012). Bacteroplankton – Key players in sub-arctic carbon cycling: A seasonal study on microbial activity and virus-induced mortality in Kobbefjord, Greenland.

Mikkelsen D.M., Rysgaard S., Glud R.N. (2008). Microalgal composition and primary production in Arctic sea ice: a seasonal study from Kobbefjord (Kangerluarsunnguaq), West Greenland. Mar. Ecol. Prog. Ser.Vol. 368, 65 – 74.

Nielsen T.G., Ottosen L.D. and Hansen B.W. (2007). Structure and function of the pelagic ecosystem in Young Sound, NE Greenland. In: Rysgaard S. and Glud R.N. (Eds). Carbon cycling in Arctic marine ecosystems: Case study Young Sound. Meddr. Grønland, Bioscience 58: 88 - 107

Risgaard-Petersen N., Nielsen L.P., Rysgaard S., Dalsgaard T. and Meyer R.L. (2003). Application of the isotope pairing technique in sediments where anammox and denitrification coexist. Limnol. Oceanogr.: Methods vol. 1, 63–73

Risgaard-Petersen N., Rysgaard S. and Revsbech N.P. (1993). A sensitive assay for determination of $^{14}N/^{15}N$ isotope in NO_3^-. Jour. Microbiol. Method Vol.. 17, 155 – 164

Rysgaard S. and Glud R.N. (2007). Carbon cycling and climate change: Predictions for a Higharctic marine ecosystems (Young Sound, NE Greenland). In: Rysgaard S. and Glud R.N. (Eds). Carbon cycling in Arctic marine ecosystems: Case study Young Sound. Meddr. Grønland, Bioscience 58: 206 – 214.

Rysgaard S., Glud R.N., Risgaard-Petersen N. and Dalsgaard T. (2004). Denitrification and Anammox activity in Arctic marine sediments. Limnol. Oceanogr. Vol. 49 No. 5, 1493 – 1502

Rysgaard S., Nielsen T.G. and Hansen B.W. (1999). Seasonal variation in nutrients, pelagic primary production and grazing in a high-Arctic coastal marine ecosystem, Young Sound, Northeast Greenland. Marine Ecology Progress series Vol. 179, 12 – 25

Rysgaard S., Risgaard-Petersen N., Nielsen L.P. and Revsbech N.P (1993). Nitrification and Denitrification in Lake and Estuarine Sediments Measured by ^{15}N Dilution and Isotope Pairing. Appl. and Environ. Microbiol.Vol. 59, No. 7, 2093 – 2098.

Rysgaard S. and Sejr M.K. (2007). Vertical flux of particulate organic matter in a Higharctic fjord: Relative importance of terrestrial and marine sources. In: Rysgaard S. and Glud R.N. (Eds). Carbon cycling in Arctic marine ecosystems: Case study Young Sound. Meddr. Grønland, Bioscience 58: 110 - 119

Rysgaard S., Thamdrup. B., Risgaard-Petersen N., Fossing H., Berg P., Christensen P.B. and Dalsgaard T. (1998). Seasonal carbon and nutrient mineralization in a high-Arctic coastal marine sediment, Young Sound, Northeast Greenland. Mar. Ecol. Prog. Ser. Vol. 175, 261 - 276

Sagemann J., Jørgensen B.B. and Greeff O. (1998). Temperature dependence and Rates of Sulfate Reduction in Cold Sediments of Svarlbard, Arctic Ocean. Geomicrobiol. J. Vol. 15, 85 - 100

Schulz H.D. and Zabel M. (2006). Marine Geochemistry 2nd ed. Springer-Verlag Berlin Heideberg, Germany.

Sejr M.K. and Christensen P.B. (2007). Growth, production and carbon demand of macrofauna in Young Sound, with special emphasis on the bivalves *Hiatella arctica* and *Mya truncate*. In: Rysgaard S. and Glud R.N. (Eds). Carbon cycling in Arctic marine ecosystems: Case study Young Sound. Meddr. Grønland, Bioscience 58: 110 - 119

Semiletov I., Makshtas A. and Syun.Ichi A. (2004). Atmospheric CO_2balance: The role of Arctic Sea Ice. Geophys. Res. Lett. Vol. 31, 1 - 4

Siem-Jørgensen M., Glud R.N. and Middelboe M. (2008). Viral dynamics in a coastal sediment: seasonal pattern, controlling factors and relations to the pelagic benthic coupling. Mar. Biol. Res. Vol. 4, 165 – 179

Stein R. (ed.) (2008). Arctic Ocean Sediments: Processes, Proxies, and Paleoenvironment. Developments in Marine Geology Vol. 2, 1 - 592

Stookey L. (1970). Ferrozine – A New Spectrophotometric Reagent for Iron. Anal. Chem. Vol.42, No. 7, 779 – 781

Subbar Rao D.V. and Platt T. (1984). Primary Production of Arctic Waters. Polar Biol. Vol. 3, 191 - 201

Sumich J.L. and Morrissey J.F. (2004). Introduction to the Biology of Marine Life 8th ed. Jones and Bartlett Publishers, Inc. UK

Søgaard D.H., Kristensen M., Rysgaard S., Glud R.N., Hansen P.J. and Hilligsøe K.M. (2010). Autotrophic and Heterotrophic activity in Arctic first-year sea ice: Seasonal study from Marlene Bright, SW Greenland. Mar. Ecol. Prog. Ser. Vol. 419, 31 - 45

Tengberg A., Hovdenes J., Andersson H.J., Brocandel O., Diaz R., Hebert D., Arnerich T., Huber C., Körtzinger A., Khripounoff A., Rey F., Rönning C., Schimanski J., Sommer S. and Stangelmayer A. (2006). Evaluation of a lifetime-based optode to measure oxygen in aquatic systems. Limnol. Oceanogr.: Methods 4, 7–17

Thamdrup B. (In press). Rates and regulation of Dissimilatory Iron reduction in Marine sediments – A review. In: Iron in the natural Environment (Coates J.D. and Zhang C. Eds). Biogeochemistry, Microbial Diversity, and Bioremediation, Kluwer, Dordrecht

Thamdrup B. (2000). Bacterial Manganese and Iron reduction in Aquatic Sediments. In: Schrink B. (Ed.) Advances in Microbial Ecology. Vol. 16, 41 - 84

Thamdrup B. and canfield D.E. (1996). Pathways of carbon oxidation in coastal margin sediments off central Chile. Limnol. Oceanogr. Vol. 41, No. 8, 1629 – 1650

Thamdrup B. And Dalsgaard T. (2002). Production of N_2 through Anaerobic Ammonium Oxidation Coupled to Nitrate Reduction in Marina Sediments. Appl. Environ. Microbiol. Vol. 68, No. 3, 1312 - 1318

Thamdrup B. and Fleisher S. (1998). Temperature dependence of oxygen respiration, nitrogen mineralization, and nitrification in Arctic sediments. Aquat. Microb. Ecol. Vol. 15, 191 - 199

Thamdrup B., Glud R.N. and Hansen J.W. (2007). Benthic carbon cycling in Young Sound, Northeast Greenland. – In: Rysgaard S. and Glud. R.N. (2007). Carbon cycling in Arctic marine ecosystems: Case study Young Sound. Meddr. Grønland, Bioscience 58, 138 - 157

Therkildsen M.S. and Lomstein B.A. (1993). Seasonal variation in net benthic C-mineralization in a shallow estuary. FEMS Microbiol. Ecol. Vol. 12, 131 – 142

Thode-Andersen S. And Jørgensen B.B. (1989). Sulfate reduction and the formation of ^{35}S-labled FeS, FeS_2, and S^0in coastal marine sediments. Limnol. Oceanogr. Vol. 34 No. 5, 793 – 806.

Thomas H., Schiettecatte L.S., Suykens K., Kon´e Y. J. M., Shadwick E. H., Prowe1 A. E. F., Bozec Y., De Baar H. J. W. and Borges A. V. (2009). Enhanced ocean carbon storage from anaerobic alkalinity generation in coastal sediments. Biogeosciences, Vol. No. 6, 267–274

Trimmer M., Risgaard-Pedersen N., Nicholls J.C. and Engström P (2006). Direct measurement of anaerobic ammonium oxidation (anammox) and denitrification in intact sediment cores. Mar. Ecol. Pro. Ser. Vol. 326, 37 – 47.

Turner J.T. (2002). Zooplankton fecal pellets, marine snow and sinking phytoplankton blooms. Aquat. Microb. Ecol. Vol. 27, 57 - 102

Wakeham S.G. and Lee C. (1989). Organic geochemistry of particulate matter in the Ocean: The role of Particles in Oceanic Sedimentary Cycles. Org. Geochem. Vol. 14, No., 83 - 96

Westrich J.T. and Berner R.A. (1984). The role of sedimentary organic matter in bacterial sulfate seduction: The G model tested. Limnol. Oceanogr. Vol. 29, No. 2, 236 – 249

Wolanski E. (2007). Estuarine Ecohydrology. Elsevier. ISBN 10: 0-4444-53066-5

Manuals

Atomic Absorption Spectroscopy – Analytical Method, PerkinElmer. The Perkin-Elmer Corporation, 761 Main Ave. Norwark, USA.

Coulometer 5012; Betjeningsvejledning til apparatur der benyttes i forbindelse med måling af CO_2 på coulometer. Danmarks Miljøundersgelser, Afdeling for Sø- og Fjordøkologi, Vejlsøvej 25, 8600 Silkeborg, Dk.

OPERATION MANUAL for the CM5012 CO_2 Coulometer, Revision B – 5/96, UIC $_{Inc.}$ Coulometrics P.O. Box 863, Joliet, IL 60434-0863 U.S.A.

Websites

http://www.ipcc.ch/

http://www.nuuk-basik.dk/

WWW.ASIAQ.Gl

http://earthobservatory.nasa.gov/Features/Sea ice/page3.php (Picture retrieved 21.03.12)

http://www2.dmu.dk/gem/

http://nsidc.org/cryosphere/sea ice/characteristics/formation.html

8. Appendix

8.1 Porewater Profiles

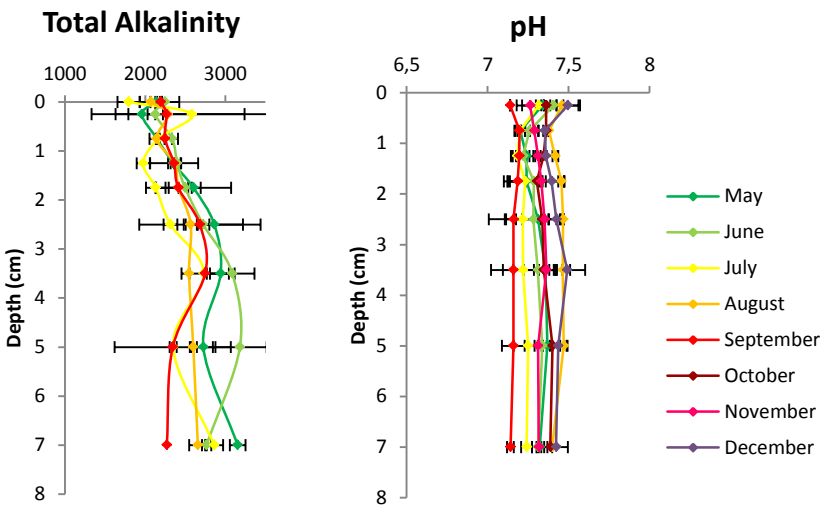

Figure 43. Alkalinity was measured in the porewater. The same trend was observed every month with increasing alkalinity throughout the sediment to a depth of approximately 4 cm, whereafter alkalinity seemed stable. PH was measured in the sediment prior to porewater extraction. The values varied slightly in the top 0-1.5 cm, whereafter pH values stabilized.

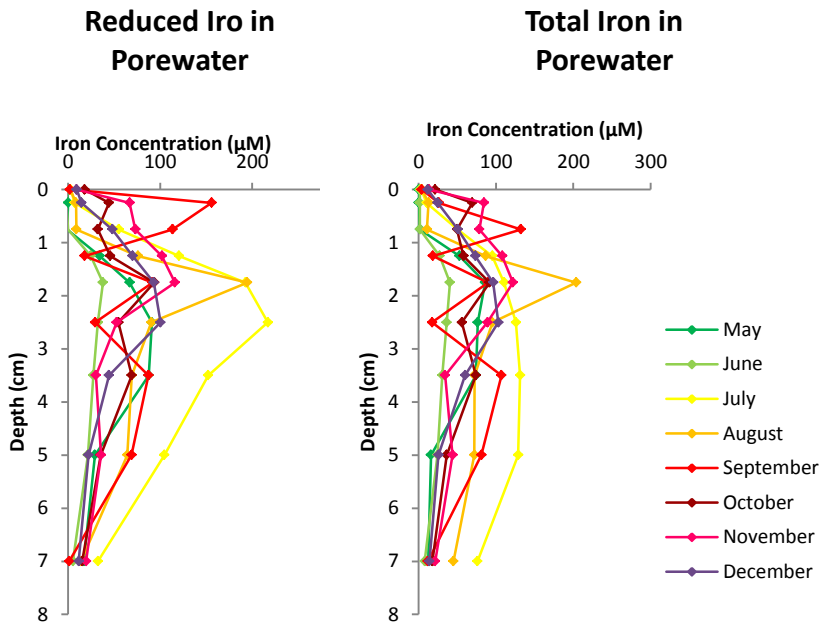

Figure 44. Both reduced and total iron was measured in the porewater. The iron in the porewater was generally reduced. Iron was absent in the water, but increase to concentrations between 50 and 100 µM with the exception of measurements from July, where concentrations were even higher. From a depth of 3 cm concentrations decreased again.

8.2 Oxygen Profiles

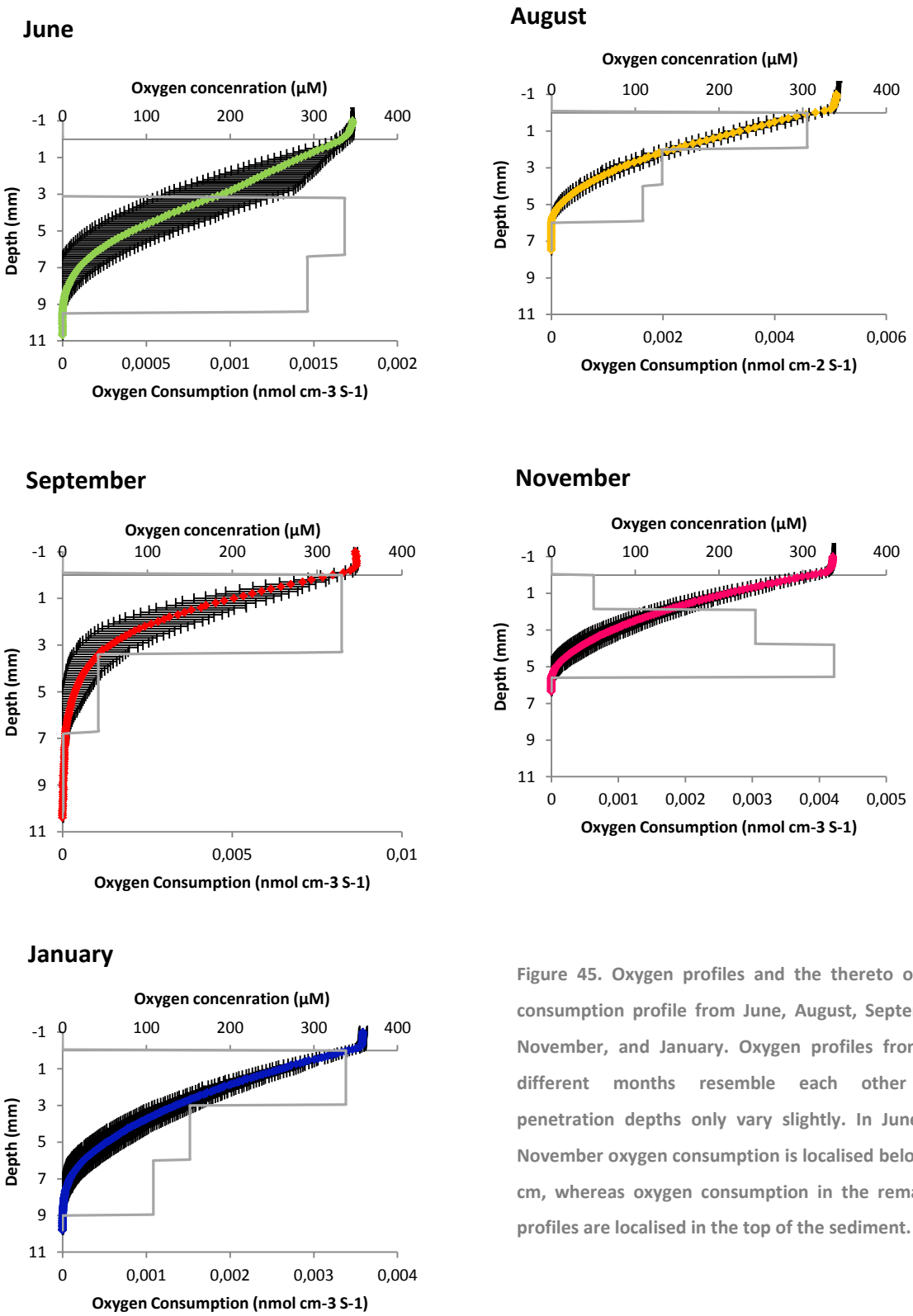

Figure 45. Oxygen profiles and the thereto oxygen consumption profile from June, August, September, November, and January. Oxygen profiles from the different months resemble each other and penetration depths only vary slightly. In June and November oxygen consumption is localised below 2-3 cm, whereas oxygen consumption in the remaining profiles are localised in the top of the sediment.

8.3 Incubation Experiments (bagincubations)

Accumulation of CO_2, NH_4^+, Fe^{2+}, and Mn^{2+} in June

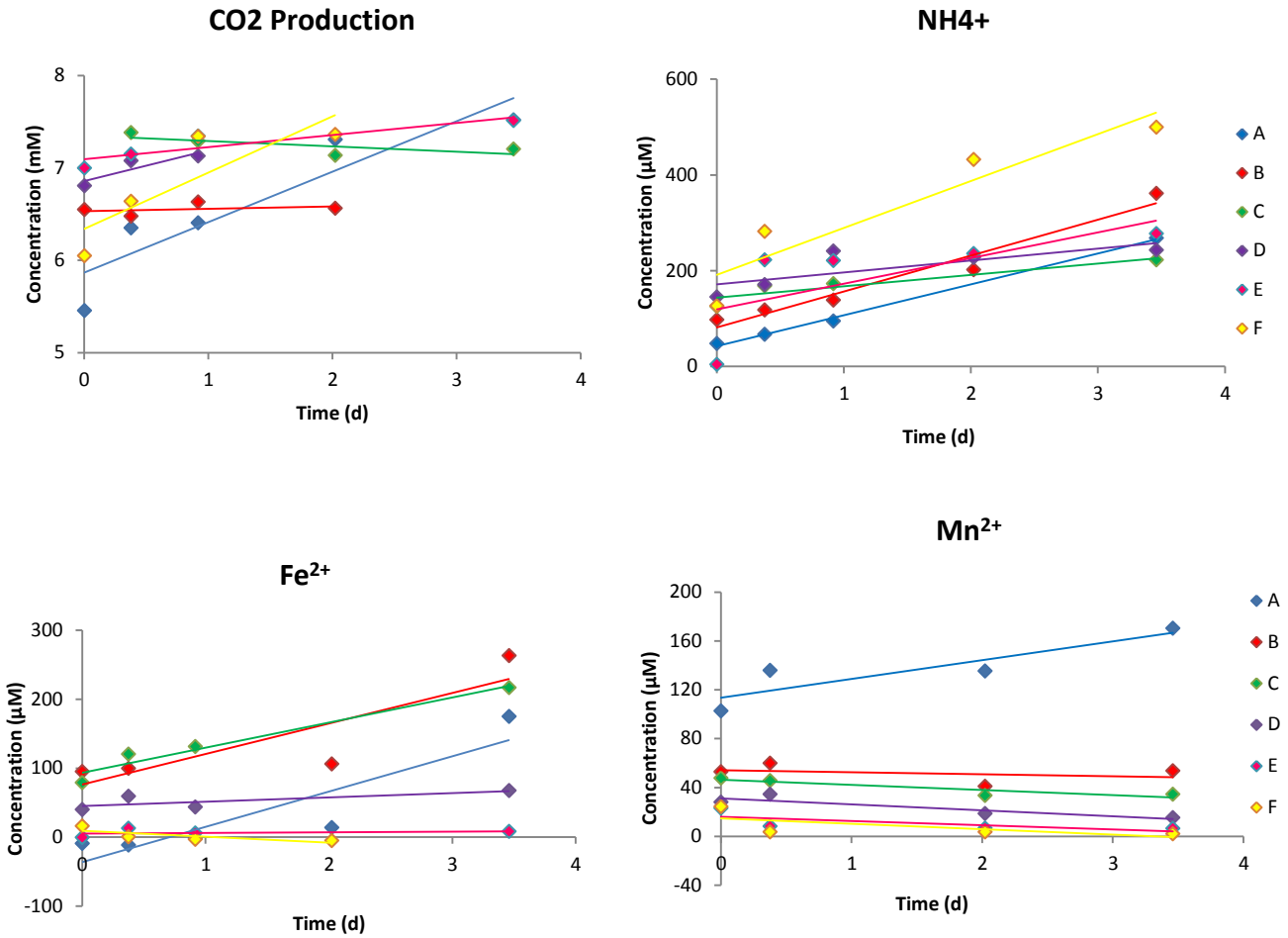

Figure 46. Accumulation of CO_2, NH_4^+, Fe^{2+}, and Mn^{2+} measured in bagincubations In June. A-F indicates the depth intervals in the bags; A: 0-1 cm, B: 1-2 cm, C: 2-4 cm, D: 4-6 cm, E: 6-8 cm, F: 8-10 cm. With the exception of depth B and C in CO_2 accumulation, CO_2 and NH_4^+ accumulated linear at all depths, while Fe^{2+} accumulated to a depth of 4 cm and Mn^{2+} only accumulated in 0-1 cm.

Accumulation of CO_2, NH_4^+, Fe^{2+}, and Mn^{2+} in October

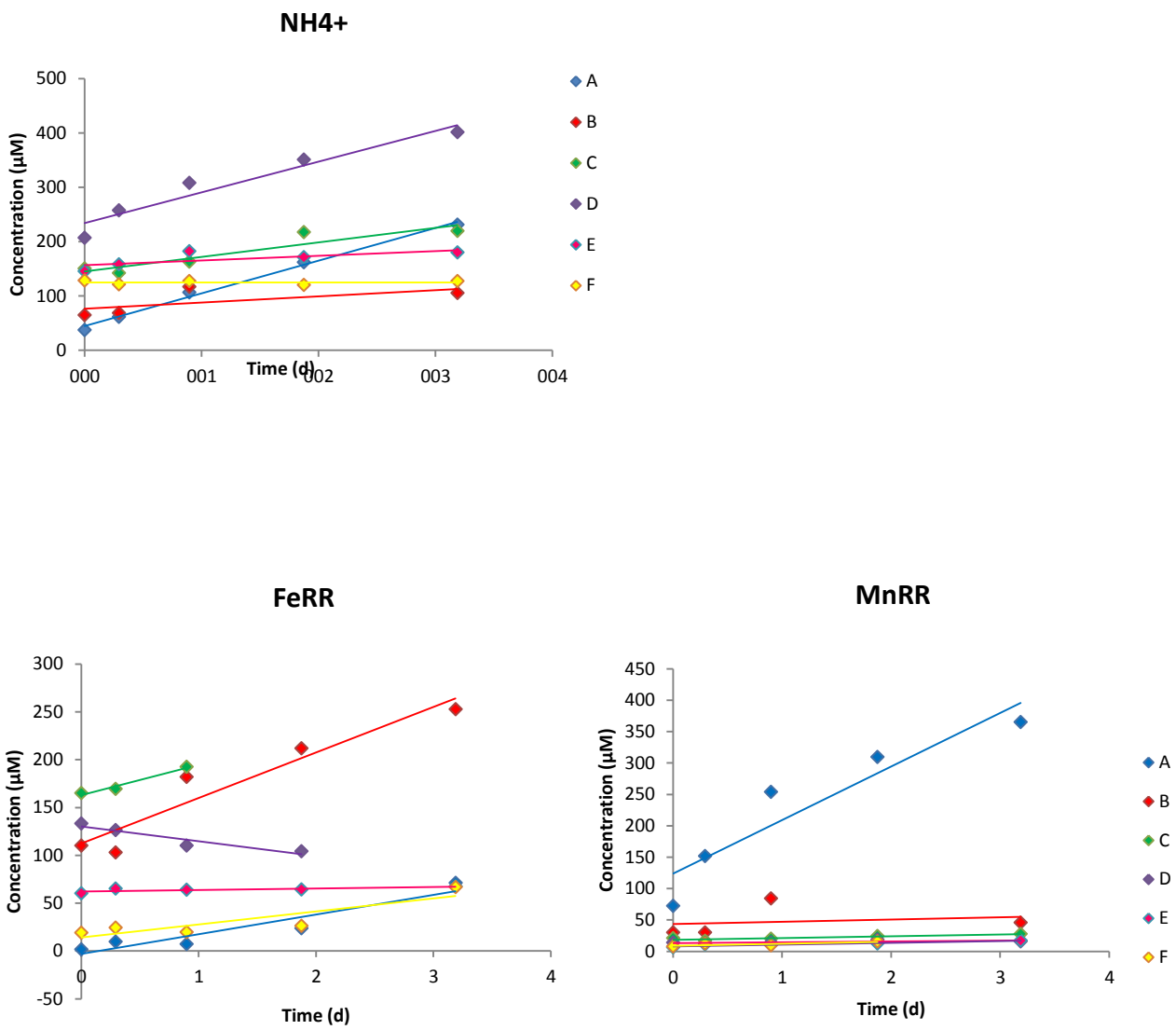

Figure 47. Accumulation of NH_4^+, Fe^{2+}, and Mn^{2+} measured in bagincubations In October. Accumulation of CO_2 was based on the relation between NH_4+ and CO_2, where measured ratio was within limits stated in Canfield et al (1993). A-F indicates the depth intervals in the bags; A: 0-1 cm, B: 1-2 cm, C: 2-4 cm, D: 4-6 cm, E: 6-8 cm, F: 8-10 cm. NH_4^+ accumulated linear at all depths, while Fe^{2+} seemed to accumulated to a depth of 4 cm and again between 8 -10 cm. Mn^{2+} only accumulated in 0-1 cm.

Accumulation of CO_2, NH_4^+, Fe^{2+}, and Mn^{2+} in December

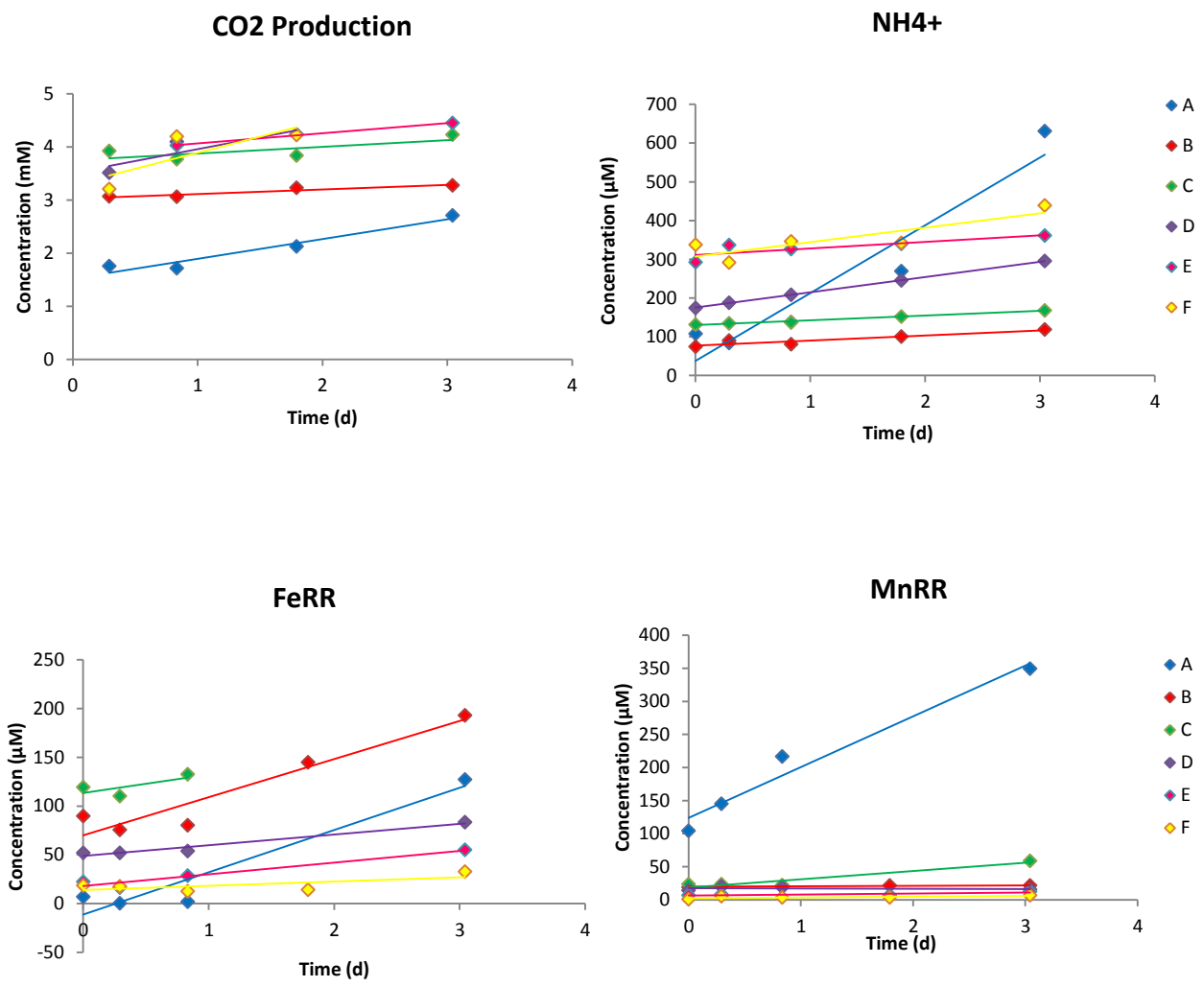

Figure 48. Accumulation of NH_4^+, Fe^{2+}, and Mn^{2+} measured in bagincubations In December. A-F indicates the depth intervals in the bags; A: 0-1 cm, B: 1-2 cm, C: 2-4 cm, D: 4-6 cm, E: 6-8 cm, F: 8-10 cm. CO_2 and NH_4^+ accumulated linear at all depths, while Fe^{2+} seemed to accumulated to a depth of 4 cm and Mn^{2+} only accumulated in 0-1 cm.

Accumulation Rates of CO_2, NH_4^+, Fe^{2+}, Mn^{2+} and sulfate reduction rates (June, October, and December)

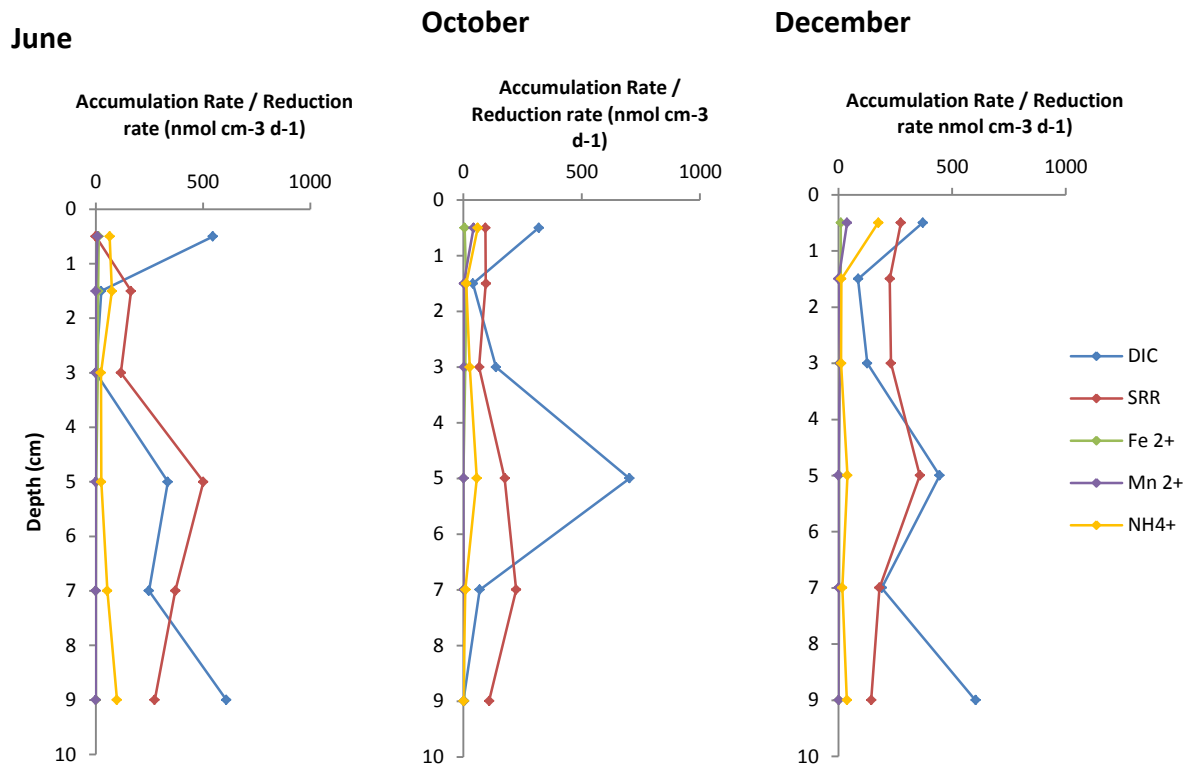

Figure 49. Accumulation rates of CO_2, NH_4^+, Fe^{2+}, Mn^{2+} and sulfate reduction rates measured in bagincubation in June, October, and December. The unit of all rates are in nmol C cm^{-3} d^{-1}.

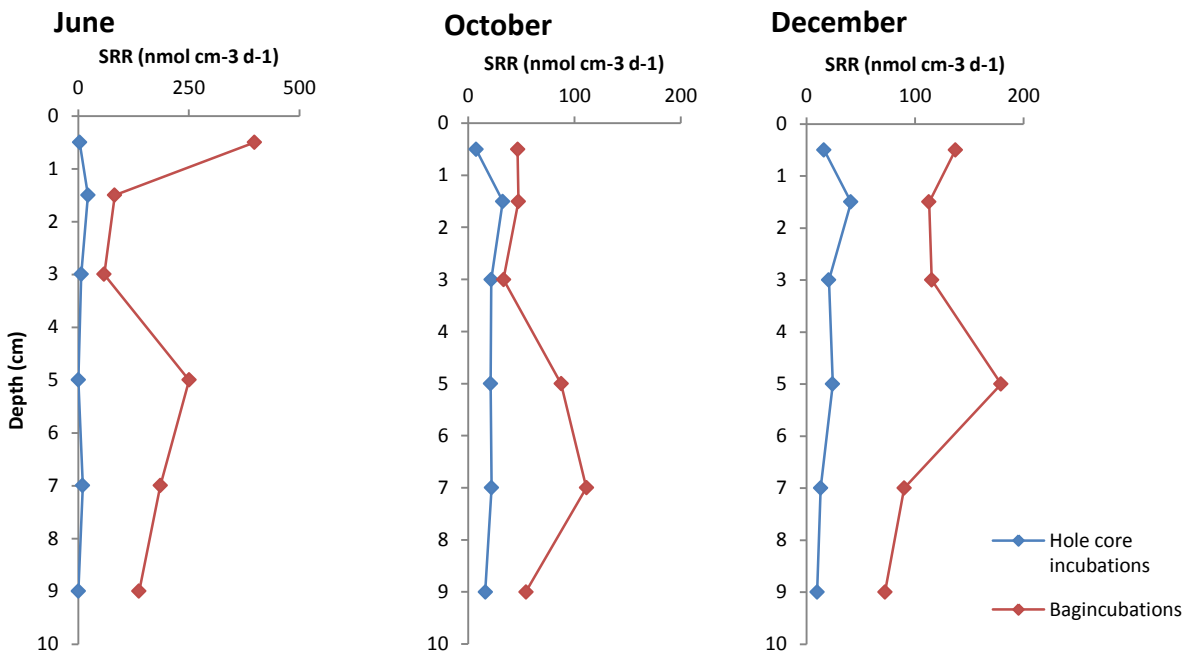

Figure 50. Comparison between measured sulfate reduction rates in bagincubations and intact cores. Rates in bagincubations were higher than the rates measured in the intact cores. In October and December rates were between 1.5 to 8.5 times higher. In June the variation was even higher.

Relative contribution to carbon oxidation measured June, September, and December

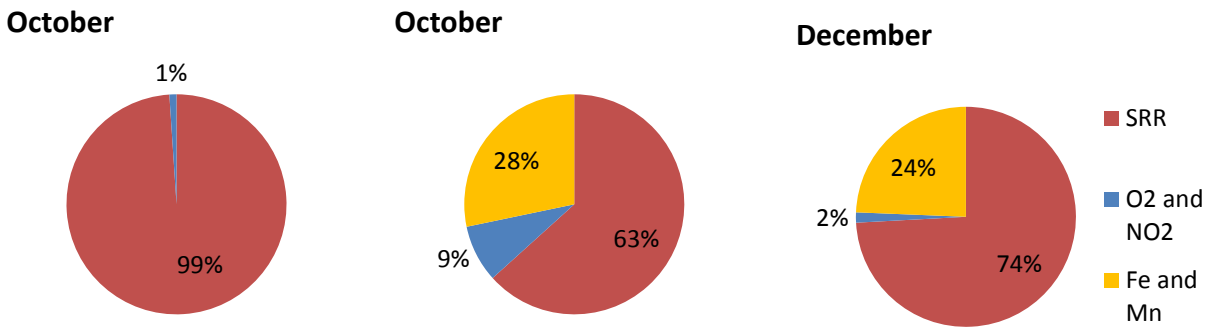

Figure 51. Bagincubation experiments were performed in June, October and December. In October as well as December sulfate reduction corresponded to 63-74% of the carbon oxidation, while it corresponded to 99% in June. Iron and manganese reduction corresponding to 28 and 24%,